Ryan P. North

Diss. ETH No. 20802

2012

The Influence of Climate Change on the Occurrence of Hypoxia in Swiss Lakes

Ryan P. North

eawag
aquatic research

ETH
Eidgenössische Technische Hochschule Zürich
Swiss Federal Institute of Technology Zurich

Diss. ETH No. 20802

2012

Diss. ETH No. 20802

The influence of climate change on the occurrence of hypoxia in Swiss lakes

---

A dissertation submitted to
ETH ZURICH

for the degree of
DOCTOR OF SCIENCES

presented by
RYAN PETER NORTH
MASc in Civil Engineering, The University of British Columbia
born 16.09.1979
citizen of Canada

accepted on the recommendation of
Prof. Dr. Rolf Kipfer, examiner
Dr. David M. Livingstone, co-examiner
Prof. Dr. Bernhard Wehrli , co-examiner
Prof. Dr. Frank Peeters, co-examiner

2012

Acknowledgments

I would like to start by thanking my supervisors, David Livingstone and Rolf Kipfer. Both David's and RoKi's enthusiasm, thoroughness, and support, made my experience, and the thesis itself, far better than I ever expected. I also thank them both for never refusing a request: meetings, conferences, workshops, or fieldwork, they were always willing to find a way to make it happen. Thanks also go to the rest of my dissertation committee, Bernhard Wehrli and Frank Peeters.

A big thank you to past and present members of the Environmental Isotopes Group at Eawag (Evelin, Lars, Lina, Matthias, Nadia, Ola, Simon, Stephan, Yama, and Yvonne), my office-mates Sämy and Sabine, and my project-mate Sebastian. While you all contributed in some way to my work, most importantly, all of you made my time at Eawag thoroughly enjoyable.

There are too many friends who deserve thanking to list here, but I trust you know who you are. Finally, I would like to thank my family. In particular, I owe a lot of thanks to my brother, Travis, and my sister Becky, who was involved from the start (introducing me to limnology) right through to the end (as my co-author). And most certainly, to Sonja, supportive and understanding through it all. Last but certainly not least, I would like to thank my parents, Donna and Peter. While maybe not immediately apparent, there is no doubt that their contribution to my thesis is immense, from instilling in me a love of nature, to supporting me in whatever I chose to pursue, even if it meant moving across an ocean.

Contents

Summary

The focus of this thesis was climate-lake coupling in the context of ongoing and future impacts of climate change on oxygen concentrations in the hypolimnion of lakes. Time-series analysis of historical data sets was used to investigate the effect of a climate regime shift (CRS) in the late 1980s on lake temperatures, lake mixing patterns and hypolimnetic oxygen concentrations. In addition, a hypolimnetic oxygen depletion model was modified and tested for use as a water resource management tool. The study sites included five perialpine lakes in Switzerland that were regularly monitored over 29 to 85 years.

The first study addressed an important issue when working with historical data sets: gap-filling. Because of the long time-span covered by historical data sets, missing data points are common. However, in many forms of data analysis a continuous data set with consistent measurement intervals is required. Two common gap-filling methods – cubic spline and linear interpolation – were compared using profiles of temperature, oxygen, phosphorus and chloride, which were considered representative of a variety of profile shapes. The simpler method, linear interpolation, was found to be more consistent than cubic spline interpolation, which was more susceptible to the creation of large errors. The results highlighted the potential for both methods to produce large errors when profile gradients were high, even at relatively small gap sizes.

The impact of climate variability on aquatic systems was assessed for river and lake temperatures across Switzerland. An abrupt increase in air temperature, linked to the late 1980s CRS, was reflected in the surface water temperatures of 18 rivers and streams (using an aggregated mean time-series) and four lakes (the Upper Lake of Zurich, the Lower Lake of Zurich, the Lake of Walenstadt and Greifensee). A month-by-month comparison of water temperatures before and after the late 1980s CRS showed seasonal differences in the magnitude of the warming, which was stronger in winter, spring and summer than in autumn. The abruptness of the shift and its magnitude diminished with increasing lake depth. The difference in warming rates between the surface and bottom water resulted in an increase in lake thermal stability. The study showed that the abrupt warming in the late 1980s contributed substantially to the overall increase in temperature that has occurred in inland waters in Switzerland.

The increase in thermal stability in the Lower Lake of Zurich reduced the frequency of occurrence and/or intensity of annual deep-water renewal and resulted in an increase in the duration and spatial extent of hypoxia. The increase in hypoxia was most likely the cause of a concurrent increase in the re-dissolution of phosphorus from the sediment, which may in turn have contributed to an observed increase in the potentially toxic cyanobacterium *Planktothrix rubescens*.

While historical data sets can help to determine past lake conditions and responses, water resource managers require more up-to-date results in order to properly manage lake resources. To address these needs, an existing oxygen depletion model was modified to predict oxygen concentrations at the end of the upcoming stratification period. The model was configured and tested using data from four Swiss lakes (the Upper Lake of Zurich, the Lower Lake of Zurich, the Lake of Walenstadt and Aegerisee). The model accurately predicted oxygen concentrations in the hypolimnion, as well as the occurrence of hypoxia at the end of the summer stratification period.

The major conclusion of the thesis is that climate change can negatively affect hypolimnetic oxygen concentrations in lakes. Considering the observed global increase in lake surface temperature over the past few decades, the ongoing global rise in air temperatures could result in a global rise in the extent and duration of lake hypoxia.

Résumé

Cette thèse porte sur l'interaction entre le climat et les lacs, dans le contexte des impacts, actuels et futurs, des changements climatiques sur la teneur en oxygène des lacs. Des méthodes de traitement de série temporelle sont appliquées à des données historiques pour étudier l'effet d'un changement de régime climatique (CRS), dans les années 1980, sur les températures des lacs, les modes de mélange et la concentration d'oxygène dans l'hypolimnion. De plus, un modèle de déplétion en oxygène de l'hypolimnion est modifié et testé pour être utilisé comme outil de gestion intégrée des ressources en eau. Les sites d'étude comprennent cinq lacs périalpins, situés en Suisse, dans lesquels une gamme de paramètres physico-chimiques a été régulièrement mesurée, durant des périodes de 29 à 85 ans.

La première étude aborde une question importante, associée aux données historiques: comment combler les lacunes? En raison de la longue durée des séries temporelles, les valeurs manquantes sont relativement nombreuses, ce qui limite l'emploi de méthodes statistiques nécessitant des données continues, c'est-à-dire définies par un intervalle de mesure constant. Deux méthodes d'interpolation – spline cubique et linéaire – sont comparées, sur la base d'une sélection représentative de profils de température, d'oxygène, de phosphore et de chlorure. La méthode la plus simple, l'interpolation linéaire, est jugée plus cohérente que l'interpolation spline cubique, qui est plus susceptible d'engendrer des erreurs importantes. Les résultats montrent, néanmoins, que les deux méthodes peuvent potentiellement produire des grandes erreurs lorsque les gradients de profil sont élevés.

L'impact de la variabilité climatique sur les systèmes aquatiques est évalué dans les lacs et cours d'eau de Suisse. L'augmentation abrupte de la température de l'air, liée aux CRS, est reflétée dans les températures de l'eau de 18 cours d'eau et quatre lacs (le haut-lac de Zurich, le bas-lac de Zurich, le lac de Walenstadt et celui de Greifensee). Dans les lacs, la soudaineté de la transition et son ampleur diminue avec la profondeur. Cette différence d'augmentation entre les couches d'eau superficielle et profonde a entraîné une augmentation de la stabilité thermique du lac. L'étude montre que le réchauffement abrupt des années 1980 a largement contribué à l'augmentation de la température qui s'est produite dans les lacs et cours d'eau de Suisse.

L'augmentation de la stabilité thermique dans le bas-lac de Zurich a réduit la fréquence ou la force des grands événements de mélange, qui à son tour a conduit à une augmentation de la durée et de l'étendue spatiale de l'hypoxie. Cette croissance d'hypoxie est probablement la cause d'une augmentation de la remise en solution du phosphore à partir des sédiments, ce qui peut, en son tour avoir contribué à une augmentation observée de la cyanobactérie *Planktothrix rubescens*, qui est potentiellement toxique.

Alors que les données historiques sont très utiles pour déterminer les conditions et les réactions des lacs dans le passé, les gestionnaires des ressources en eau ont besoin de résultats plus immédiat. Pour répondre à ces besoins, un modèle existant est modifié pour prévoir les concentrations d'oxygène à la fin de la prochaine période de stratification. Le modèle est configuré et testé en utilisant des données provenant de quatre lacs Suisses (le haut-lac de Zurich, le bas-lac de Zurich, le lac de Walenstadt et Aegerisee). Le modèle prédit avec précision les concentrations d'oxygène dans l'hypolimnion, et fournit des estimations relativement précises de la présence d'hypoxie en fin de la période de stratification.

La principale conclusion de cette thèse est que le changement climatique peut réduire les concentrations d'oxygène dans les lacs. Etant donné l'augmentation globale des températures observées dans les lacs au cours des dernières décennies, on peut s'attendre à ce que le réchauffement atmosphérique entraîne une hausse généralisée de l'étendue et de la durée de zones hypoxiques en milieu lacustre.

1

Introduction

1.1 Introduction and scope of work

In the environmental sciences historical data sets of physical, chemical and biological variables can be used to identify long-term trends and variability. Recent studies have used historical data sets and proxies to investigate long-term changes in global air temperatures and the implications of these changes for terrestrial and aquatic ecosystems (IPCC, 2007a,b). Analysis of historical lake data has shown that lakes are particularly susceptible to changes in global climate (Adrian et al., 2009; Schindler, 2009; Shimoda et al., 2011) and that lake surface water temperatures are currently increasing throughout most of the world (Schneider and Hook, 2010). A recent review of the state of research on climate-induced changes in lake ecosystems has called for further study of lake processes that may be affected by climate change, and of the coherence in the way lakes respond to climate change (Shimoda et al., 2011). The overarching aim of this thesis was to determine the impact of climate change on oxygen concentrations in lakes through the use of historical data sets. More specifically, the thesis attempted to determine whether the frequency of occurrence, duration and extent of hypoxia has been affected by ongoing climate change. In doing so, the heterogeneity of the physical response (temperature and thermal stability) to climate change for several Swiss lakes was assessed. Having considered ongoing climate change impacts, requirements for climate change adaptation were considered with the development of a modelling tool that predicts oxygen concentrations in lake hypolimnia.

The impact of climate change and climate variability on oxygen in Swiss lakes has been addressed in several previous studies (e.g., Livingstone, 1997; Jankowski et al., 2006; Rempfer et al., 2009, 2010; Posch et al., 2012). However, these studies have for the most part, focused on a particular event (e.g., Jankowski et al., 2006; Rempfer et al., 2010) and have not considered long-term trends and variabilities in lake oxygen concentration. This thesis used long-term data from several Swiss lakes to investigate the heterogeneity in the response of water temperature and thermal stability to a climate regime shift (Chapter 4), and to determine long-term changes in the duration and extent of hypoxia in response to the same climate regime shift (Chapter 5). Finally, a tool was developed to allow water resource managers to predict annual variability in hypolimnetic oxygen concentrations (Chapter 6). In order to conduct both types of analysis, the historical water column data must first be converted to a standard set of depths and any gaps in the data must be filled.

Therefore, the first step in the research was to determine the best method to fill data gaps in profiles of measured lake variables (Chapter 3). The next section provides a brief description of each chapter of the thesis.

1.2 Outline

Chapter 2: Scientific background General concepts used in the study are described, including the oxygen cycle in lakes, hypoxia and lake-climate coupling.

Chapter 3: Comparison of linear and cubic spline methods of interpolating lake profiles Two methods of interpolating lake water column profiles – linear interpolation and cubic spline interpolation – were compared and their relative performance assessed using "leave-k-out" cross-validation. Four representative variables (temperature and concentration of oxygen, total phosphorus, and chloride) from the Lower Lake of Zurich were used to assess the performance of each interpolation method. This chapter has been submitted for publication in the journal *Limnology and Oceanography: Methods*, and is under review.

Chapter 4: The physical impact of the late 1980s climate regime shift on Swiss rivers and lakes The impact of the late 1980s climate regime shift on rivers and lakes in Switzerland was investigated. River temperatures and lake surface temperatures reacted coherently with a nearly simultaneous abrupt increase. However, there were seasonal and spatial differences (with depth) between the four study lakes. In general, the abrupt warming in the late 1980s contributed substantially to the overall increase in temperature that has occurred in water bodies in Switzerland over the last few decades. This chapter has been accepted for publication in the journal *Inland Waters*.

Chapter 5: Long-term changes in hypoxia in a large temperate lake: consequences of a climate regime shift An extensive data set of measured lake variables from the Lower Lake of Zurich (including temperature, oxygen concentration and total phosphorus concentration) was used to study the impact of climate variability on the duration and extent of hypoxia. The study links lake warming with changes in mixing patterns that eventually led to an increase in the duration and extent of seasonal hypoxia. The increase in hypoxia may in turn have contributed to an increase in the internal loading of dissolved phosphorus from the sediment. This chapter is in preparation for submission for publication.

Chapter 6: Annual prediction of hypolimnetic oxygen depletion in lakes An existing dissolved oxygen model was modified to predict upcoming end-of-summer hypolimnetic oxygen concentrations. The model was tested using measured oxygen water column profiles from four Swiss lakes of varying depth and trophic state. In combination with a lake monitoring program, the model allows lake managers to estimate oxygen concentrations just prior to fall mixing, based on a profile of oxygen concentrations measured just before the onset of summer stratification. This chapter is in preparation for submission for publication.

Chapter 7: Conclusions and outlook The key findings of the thesis work are summarized and recommendations for future related work are discussed.

2

Scientific background

The following paragraphs provide background information about the oxygen cycle, the occurrence of hypoxia, the influence of climate change, and the implications of increasing hypoxia in temperate lakes. It is assumed that the reader has some background knowledge of lake processes so that the discussion can focus on oxygen-related processes. For more general lake process information see Wetzel (2001) and Imboden and Wüest (1995).

2.1 The oxygen cycle in temperate lakes

The oxygen cycle (Figure 2.1) in a temperate lake can be described by its sources, sinks and dominant transport mechanisms (Peña et al., 2010). The major source of oxygen is across the air-water interface. The diffusion rate across the air-water interface is controlled by the partial pressure of oxygen in the atmosphere, and the temperature and salinity of the water body (Wetzel, 2001). For many freshwater systems, it can be assumed that the salinity of the water body and the partial pressure of oxygen in the atmosphere will remain relatively constant. However, lake water temperatures vary on daily, seasonal and long-term (e.g., decadal) time scales. As water temperatures increase, the oxygen saturation concentration decreases (Hutchinson, 1957). Therefore, a long-term rise in water temperatures will result in a decrease in maximum lake oxygen concentrations.

Photosynthesis in the photic zone of the water column is another important oxygen source. Oxygen production from photosynthesis is mainly a function of the phytoplankton biomass and the length of the growing season (Wetzel, 2001). Other factors that affect primary productivity include light and nutrient availability, mixing patterns, stratification, and water temperature (Wetzel, 2001). As a result, oxygen produced from primary productivity varies on daily, seasonal and long-term time scales. For example, phytoplankton biomass in temperate lakes typically follows a bimodal pattern, with peaks in spring and summer. Due to the influence of climate on primary production (e.g., through mixing patterns and water temperature), changing climatic conditions can affect oxygen production rates (e.g., Straile, 2002; Anneville et al., 2004, 2005).

Turbulent mixing is the major transport mechanism by which oxygen is distributed throughout a lake (Wetzel, 2001). When a lake is stratified, the transport of oxygen into the hypolimnion is restricted. Typically, a lake is stratified during the summer when epilimnetic water is warmer, and therefore lighter than hypolimnetic water. In winter, if the water temperature in the epilimnion

drops below the temperature of maximum density (≈ 4 °C), the epilimnetic water becomes lighter than the hypolimnetic water, which typically remains near the temperature of maximum density. This is referred to as inverse stratification, and often occurs when a lake is ice covered. When the surface water cools in fall and winter (or warms in spring after inverse stratification) and lake stratification weakens, it becomes easier for turbulent mixing to penetrate into the hypolimnion. Mixing is often initiated by wind blowing across the lake's surface or by density differences (convective mixing). Convective mixing occurs when a layer of water is heavier than the layer below it (e.g., when the surface water cools), and mixing is initiated to stabilize the water column. When the mixed layer reaches the lake bottom, the entire lake has mixed; this is often referred to as lake turnover or deep-water renewal. Whether driven by a wind event or by density differences, deep-water renewal is the major source of oxygen replenishment to the hypolimnion. Because both forms of deep-water renewal are directly linked to climatic conditions, the transport of oxygen in lakes is highly affected by climate variability (e.g., Livingstone, 1997; Holzner et al., 2009).

The major oxygen sink in lakes is biological oxidation in the water column and at the sediment-water interface. Chemical oxidation can also act as a sink, but is generally less significant than biological oxidation (Wetzel, 2001). The epilimnion is typically rich in oxygen throughout the year because of primary production and diffusion of oxygen across the air-water interface. During summer and during periods of ice-cover, transport of oxygen to the hypolimnion is inhibited because of the lack of intense mixing between the upper layers of the lake and the lake bottom water. As long as the supply of organic matter to the hypolimnion is sufficient, and the lake is stratified, the oxygen content of the hypolimnion will decline (Wetzel, 2001). Within the hypolimnion, biological oxidation proceeds faster in the benthic zone – due to a larger supply of organic matter – than in the water column (Wetzel, 2001). A shortage of organic matter, and a replenishment of oxygen to the hypolimnion through mixing are therefore the two major factors that can inhibit continued depletion of the hypolimnetic oxygen content. Both of these factors can be indirectly affected by changes in climate through a change in mixing patterns, in the length of the stratification period and in phytoplankton growth rates (e.g., Straile et al., 2003; Foley et al., 2012).

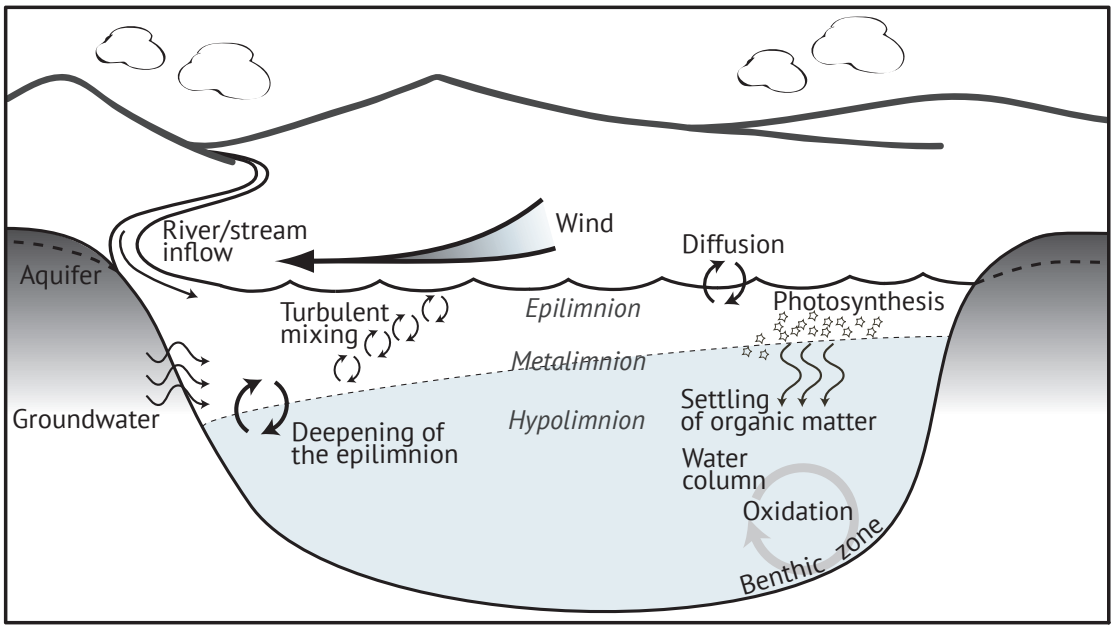

Figure 2.1: Conceptualization of the oxygen cycle in a lake, depicting major sources, sinks, and transport mechanisms.

2.2 Hypoxia in lakes

Oxygen depletion by biological oxidation at the sediment-water interface can result in hypoxia and eventually anoxia in lake bottom waters. Anoxia refers to a complete lack of oxygen, and hypoxia refers to dissolved oxygen concentrations below the threshold at which animal life can be sustained (Diaz and Rosenberg, 2008). The location of this threshold differs between organisms (Vaquer-Sunyer and Duarte, 2008), although 2 mg O_2 L^{-1} is often used in the literature. Hypoxia may occur intermittently, seasonally, or permanently, and aquatic systems may progressively experience all three stages (Diaz and Rosenberg, 2008). In the past few decades the combined effect of eutrophication and climate change has led to an observed increase in the extent, duration, and frequency of occurrence of hypoxia in oceans, seas, and lakes (Diaz, 2001; Diaz and Rosenberg, 2008). In a eutrophic lake a large amount of organic matter is supplied to the benthic zone, resulting in the rapid consumption of bottom-water oxygen through biological oxidation. If the supply of organic matter is large enough, oxygen is consumed so quickly that permanent anoxia develops. Climate change may also cause or intensify hypoxia in aquatic systems (e.g., Keeling et al., 2010; Deutsch et al., 2011; Foley et al., 2012). Lakes have a long history of hypoxia caused by anthropogenic eutrophication, and are particularly susceptible to variations in climate (Carpenter et al., 1998; Adrian et al., 2009; Schindler, 2009; Shimoda et al., 2011). As a result, lakes are experiencing an increase in the frequency of occurrence, duration and extent of hypoxia due to increasing thermal stability resulting from climate change (Livingstone, 1997; Foley et al., 2012; Rösner et al., 2012). Despite a growing awareness of increasing global hypoxia, research has tended to focus on coastal zones and estuaries. The shortage of research on hypoxia in lakes has been attributed to a lack of long-term data sets of sufficient quality to properly assess oxygen depletion in the hypolimnion (Foley et al., 2012). Those studies which did focus on lakes have consistently found a link between climate warming and a decline in hypolimnetic oxygen concentrations (e.g., Livingstone, 1997; Verburg et al., 2003; Foley et al., 2012; Rösner et al., 2012).

2.3 Climate change and lakes

The strong influence of climate on lakes means that changes in global and regional climate patterns will often be reflected in lakes (Blenckner and Chen, 2003). Changes in climate patterns may be the result of a change in a climate mode, natural events (e.g., volcanic eruptions), or anthropogenic forcing (e.g., increased emission of greenhouse gases leading to rising global air temperatures). In any case, the lag between a change in climate and the resulting change in a lake is often small, particularly for physical lake processes. The example discussed in this thesis is the impact of the late 1980s CRS on lakes in Switzerland. The CRS resulted from a shift in the Arctic Oscillation (AO; Figure 2.2a) and in related climate modes such as the North Atlantic Oscillation (NAO; Figure 2.2b), to more positive values (Hurrell, 1995; Hurrell et al., 2001; Yasunaka and Hanawa, 2002; Alheit et al., 2005; Rodionov and Overland, 2005). When discussing the influence of the AO and the NAO on aquatic systems, the indexes are typically restricted to their winter values (December to March) when their influence on regional climate is at its strongest (Hurrell, 1995; Alheit et al., 2005); for example a positive winter NAO index corresponds to milder, wetter winters with increased westerly winds over northern Europe (Hurrell, 1995). The winter AO and NAO indices are clearly highly correlated, and their variability is reflected in water temperatures in the upper mixed layer of the Baltic Sea and the North Sea (Hurrell, 1995; Alheit et al., 2005), and in winter lake surface temperatures from the Lower Lake of Zurich, Switzerland (Figure 2.2c). Variability in the climate modes has been linked to changes in rivers (e.g., Hari et al., 2006),

groundwater (Figura et al., 2011), oceans (e.g., Alheit et al., 2005; Conversi et al., 2010), and lakes (e.g., Gerten and Adrian, 2000; Anneville et al., 2005).

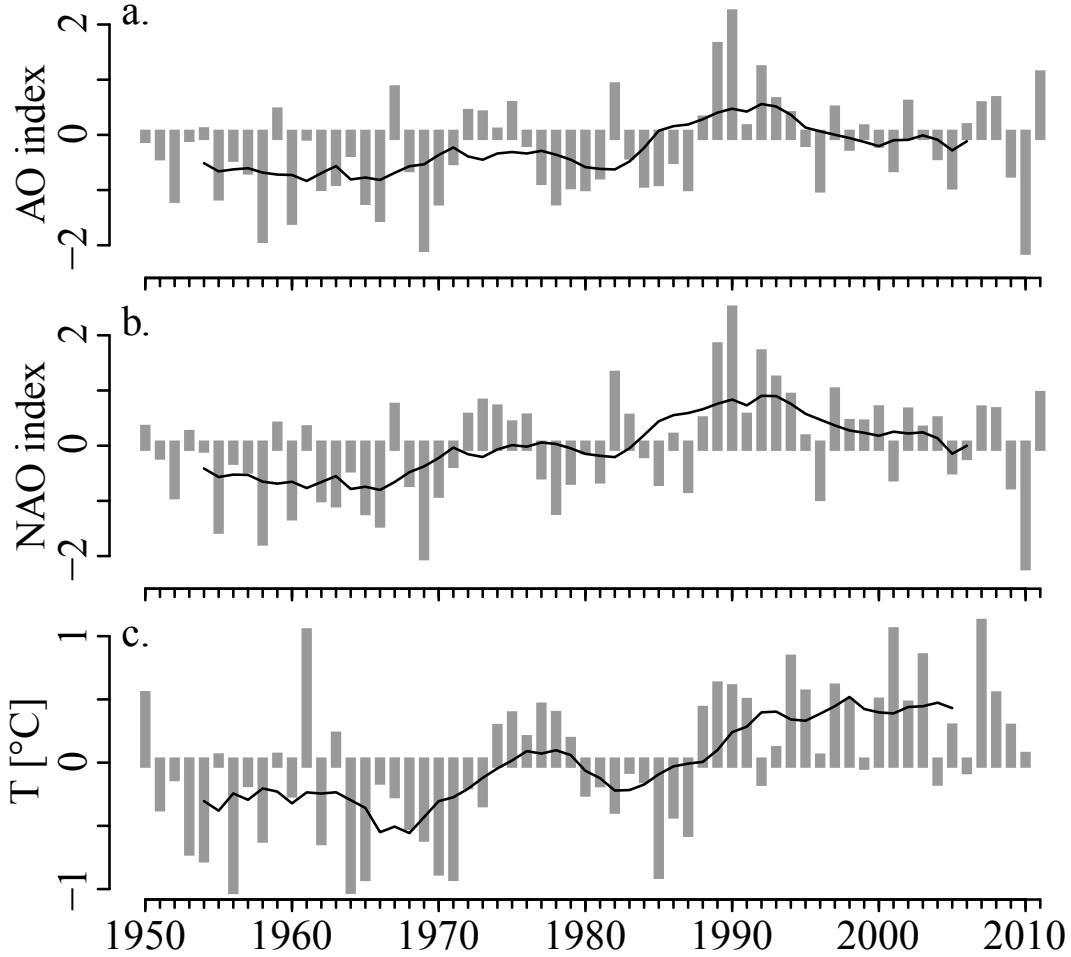

Figure 2.2: Time-series of the winter (December to March) a) Arctic Oscillation (AO) index, b) North Atlantic Oscillation (NAO) index, and c) lake surface temperature (T) in the Lower Lake of Zurich (plotted as the offset from the mean). The grey vertical lines show annual winter values and the solid black line is the 10-year running mean.

Previous studies have shown that an increase in air temperature will result in an increase in lake water temperature and thermal stability (e.g., Livingstone, 1997, 2003; Foley et al., 2012; Rösner et al., 2012). The increase in stability results from greater warming in the epilimnion than in the hypolimnion, increasing the density difference between the two layers. An increase in the thermal stability of the lake during the mixing season, or an extension of the stratification period, reduces the ability of a lake to undergo deep-water renewal. As discussed above, in a lake deep-water renewal is the major mechanism that transports oxygen into the lake hypolimnion. Deep-water renewal is not strictly determined by the strength of the stratification, but can also be influenced by wind, inflow (e.g., water temperature and suspended solids), and the occurrence of convective mixing. Increased stability in fall and winter may inhibit deep-water renewal, or at least reduce the intensity of mixing. In either case, a less-than-normal amount of oxygen is mixed into the hypolimnion and the lake begins the summer stratification period with a deficit in hypolimnetic oxygen content. In this case, hypoxic or anoxic conditions will likely be reached earlier because the rate of hypolimnetic oxygen consumption is fairly constant throughout the stratification period (Livingstone and Imboden, 1996). As a result, the lake bottom waters will be hypoxic or anoxic for longer periods and across a larger sediment area. Consecutive years of weak or absent deep-water

renewal will exacerbate this condition, leading to a further increase in both the spatial and temporal extent of hypoxia or anoxia.

Separating the effects of eutrophication from those of climate change or climate variability is a difficult task. For example, during eutrophication phosphorus may become buried in the sediment of a lake. If the lake experiences a small increase in hypoxia due to climate change, the buried phosphorus may return to the water column through re-dissolution – i.e., internal loading (Nürnberg, 1995). The increased phosphorus loading may intensify eutrophication in the lake, leading to permanent hypoxia. If the lake had not undergone the initial period of eutrophication, it may not have been affected very severely by a small increase in hypoxia. In this case, eutrophication reduced the lake's ability to adapt to changing oxygen concentrations. The ability of a system to adapt to change is referred to as its resilience (Folke et al., 2004). Both climate and nutrient loading can affect a lake's resilience, making it difficult to determine if there is a dominant driver of lake hypoxia.

2.4 Impacts of hypoxia on lake ecosystems

An increase in the frequency of occurrence, extent and duration of hypoxia can negatively affect aquatic ecosystems, leading to a loss of habitat and biodiversity (Diaz and Rosenberg, 2008; Foley et al., 2012). The majority of the relevant literature focuses on the impact of hypoxia on coastal marine regions, mobile species (e.g., fish) and benthic organisms (Gray et al., 2002; Diaz and Rosenberg, 2008; Levin et al., 2009). In lakes, hypoxic conditions can reduce fish habitat quality (Arend et al., 2010) and the maximum power output of juvenile lake trout (Evans, 2007), change fish distributions and foraging habits (Roberts et al., 2009), and, when combined with increasing water temperature, result in "thermal-dissolved oxygen squeeze" – constraining fish between a region of detrimentally high temperatures and a region of detrimentally low oxygen concentrations (Coutant, 1985; Arend et al., 2010). Hypoxic and anoxic conditions at the sediment-water interface may result in the re-dissolution of iron (Davison, 1981), ammonia (Beutel et al., 2001), and phosphorus (Nürnberg, 2009) from the sediment. Hypoxia and anoxia may also contribute to an increase in phytoplankton biomass (Carpenter et al., 1998), a shift in the dominant phytoplankton species (Posch et al., 2012), fish kills (Carpenter et al., 1998; Lamont et al., 2004), and a reduction in drinking water quality (Beutel, 2003). Through these and other impacts, human populations that depend on lakes as a recreational, drinking water and food resource will also be adversely affected.

3

Comparison of linear and cubic spline methods of interpolating lake profiles

North, R. P.[1,2] and Livingstone, D. M.[1]

1. Eawag, Swiss Federal Institute of Aquatic Science and Technology, Department of Water Resources and Drinking Water, Überlandstrasse 133, CH-8600 Dübendorf, Switzerland.

2. ETH Zurich, Department of Environmental Systems Science, Institute of Biogeochemistry and Pollution Dynamics, Universitätsstrasse 16, CH-8092 Zürich, Switzerland

Submitted to *Limnology & Oceanography:Methods*

Abstract Two commonly used methods of interpolating lake water column profiles – two-point linear interpolation and cubic spline interpolation – were compared and their relative performance assessed using "leave-k-out" cross-validation. Artificial "pseudo-gaps" of various sizes were created in measured water column profiles of four representative variables (water temperature, oxygen concentration, total phosphorus concentration, and chloride concentration) from the Lake of Zurich by removing measured data from the profiles and filling them using each of the two interpolation methods. The performance of each interpolation method was assessed based on the root mean square error, mean bias error, and maximum absolute bias error of the interpolated values in relation to the original measured values. The performance of the interpolation methods varied with depth, season, and profile shape. When the profiles were homogeneous both methods performed well, but when the profiles were heterogeneous, linear interpolation generally performed better than cubic spline interpolation. Although the data generated by cubic spline interpolation

Acknowledgements We would like to thank all who contributed to the collection of the lake data used in this study. The data were kindly provided by: Wasserversorgung Zürich, Switzerland; Amt für Abfall, Wasser, Energie und Luft, Canton of Zürich, Switzerland; Amt für Umweltschutz, Canton of Zug, Switzerland; Istituto Scienze della Terra, Scuola Universitaria della Svizzera Italiana, Switzerland; and Fondazione Mach - Istituto Agrario di S. Michele all'Adige, Italy. We also thank the entire Environmental Isotopes Group at Eawag for discussions that improved the manuscript greatly. This research forms part of project "HYPOX", funded under the European Commission's Seventh Framework Programme (grant no. 226213).

were less biased than those generated by linear interpolation, there were more instances of extreme errors. The results of this study suggest that linear interpolation is generally preferable to cubic spline interpolation for filling data gaps in measured lake profiles.

3.1 Introduction

Studies of long-term changes in lake ecosystems often require the analysis of historical water column data that were originally measured at inconsistent sampling depths. To facilitate the comparison of such data, some form of interpolation is usually employed to yield estimates of the data at standard depths (e.g., Livingstone, 2003; Coats et al., 2006; Rempfer et al., 2010) before going on to produce time-series based on these data. Because of their simplicity and ease of use, two-point linear interpolation (between the two measured values on either side of a gap) and cubic spline interpolation (which incorporates information from several measurements on each side of a gap) are both commonly used for this purpose. However, despite the importance of interpolation accuracy when standardizing profile sampling depths, very little published information is available on this topic. In the interest of consistency between studies, it would be advantageous to formalize the selection of an interpolation method for lake water column profiles.

In other contexts, comparisons have been conducted of various interpolation methods. Most of these comparisons have focused on temporal interpolation (Amritkar and Kumar, 1995; Baltazar and Claridge, 2002; Claridge and Chen, 2006) or spatial interpolation in two dimensions (Holdaway, 1996; Eischeid et al., 2000; Skaugen and Andersen, 2010). These studies applied a multitude of different interpolation methods, and found that each one performed differently depending on the data set being considered. There is therefore no "one-size-fits-all" interpolation method that is best for all data sets. However, the simplest form of interpolation often proves to be the optimal choice (Chen and Claridge, 2000; Baltazar and Claridge, 2002; Claridge and Chen, 2006). With this in mind, this study is confined to the two comparatively simple interpolation methods mentioned above – two-point linear interpolation and cubic spline interpolation – for regularizing spatial sampling intervals and filling data gaps in lake profiles. The study aims to obtain greater assurance of compatibility, quality, and reliability when analyzing lake profiles with inconsistent sampling intervals or missing data.

3.2 Materials and procedures

3.2.1 Data

The study compared the two interpolation methods by creating artificial data gaps, referred to henceforth as "pseudo-gaps", in measured water column profiles. The pseudo-gaps were then filled using each of the two interpolation methods. The relative ability of each interpolation method to reconstruct missing profile data was assessed based on the accuracy with which it was able to fill the pseudo-gaps.

This procedure requires many lake profiles that have been measured at standard sampling depths with no data gaps. Multi-annual data sets from five lakes in Switzerland (Lower Lake of Zurich, Greifensee, Lake of Lugano, Aegerisee, Lake of Walenstadt) and one in northern Italy (Lake of Garda) were examined to find the longest, most complete data set in which the profiles were sampled consistently at the same standard depths. The most suitable data set was found to be that from the (Lower) Lake of Zurich from 1976 to 2010. During this period, the lake was sampled at approximately monthly intervals a total of 420 times at its deepest point. Sampling depths were

consistent at 0.3, 1, 2.5, 5, 7.5, 10, 12.5, 15, 20, 30, 40, 60, 80, 90, 100, 110, 120, 130, and 135 m. All profiles with data missing from any of these 19 standard depths were excluded from the study from the outset. However, there were only few such profiles. For total phosphorus concentration, for example, 19 profiles had to be excluded based on this criterion; for other variables used in this study, even fewer profiles needed to be excluded. Further details on the Lake of Zurich data set are given by Zimmermann et al. (1991), Livingstone (2003), and Jankowski et al. (2006).

To assess the representativeness of the Lake of Zurich profiles, we qualitatively compared the profiles of physical (e.g., temperature), chemical (e.g., oxygen), and biological (e.g., chlorophyll a) variables from the Lake of Zurich (1976-2010) with corresponding profiles from the other five lakes listed above. The profiles from all six lakes were found to be similar in shape and seasonal variation, and we therefore concluded that the Lake of Zurich profiles were broadly representative of lakes in the European Alpine region. However, as this comparison only considered lakes from this particular region, caution should be exercised when applying the results of this paper beyond temperate climate lakes.

To provide a range of profile shapes, four representative lake variables were included in the analysis: water temperature, oxygen concentration ($[O_2]$), total phosphorus concentration (TP), and chloride concentration ($[Cl^-]$). Measured profiles of all four variables in the Lake of Zurich during a typical year (1993) are shown in Figure 3.1. These particular lake variables were selected as together they cover the majority of lake profile types; e.g., orthograde (temperature), positive clinograde (temperature, $[O_2]$), negative clinograde (TP, $[Cl^-]$), positive heterograde ($[O_2]$), negative heterograde ($[Cl^-]$), and positive-negative heterograde ($[O_2]$). It should be stressed here that this analysis is not concerned with explaining the behavior of these variables themselves, but with the methodology necessary to cope with interpolating the range of profile shapes represented by these variables at different times of the year.

Based on their shapes, the profiles can be roughly divided into three depth zones. Within the first depth zone, comprising the epilimnion and metalimnion (0 - 20 m), profile shapes vary the most, both spatially and temporally. In this depth zone in summer and fall, temperatures are constant within the mixed surface layer but decrease uniformly through the stratified thermocline. $[O_2]$ and $[Cl^-]$ show a great degree of variability with depth, in contrast to TP, which remains approximately constant. In the upper depth zone in winter and spring, profiles of all four variables vary little with depth. Temperature, $[O_2]$, and $[Cl^-]$ show a marked seasonal variability in profile shape, but seasonal variability in TP is much less pronounced. In the second depth zone, the upper hypolimnion (20 - 80 m), all variables have approximately uniform profiles regardless of season. In the third depth zone, the lower hypolimnion (80 - 136 m), temperature and $[Cl^-]$ profiles are approximately constant with depth, while $[O_2]$ decreases with depth and TP increases with depth.

3.2.2 Procedure

In the following, the term "spatial sampling interval" refers to the vertical distance between adjacent measurements in the same sampling profile. The term "spatial data gap" refers to one or more consecutively missing measurements from the standard set of depths, and the "spatial data gap size" is the number of missing measurements. Note that because spatial sampling intervals are not uniform, the length in meters of a spatial data gap of a given size is also not uniform.

All available temperature data from all six lakes mentioned above were analysed to determine typical spatial data gap sizes. We found that less than 3% of spatial data gaps contained more than three consecutively missed measurements (Figure 3.2). Interpolation is thus most often needed to fill spatial gaps of between one and three measurements. This range was therefore chosen as the range of spatial pseudo-gap sizes to be used in the comparison.

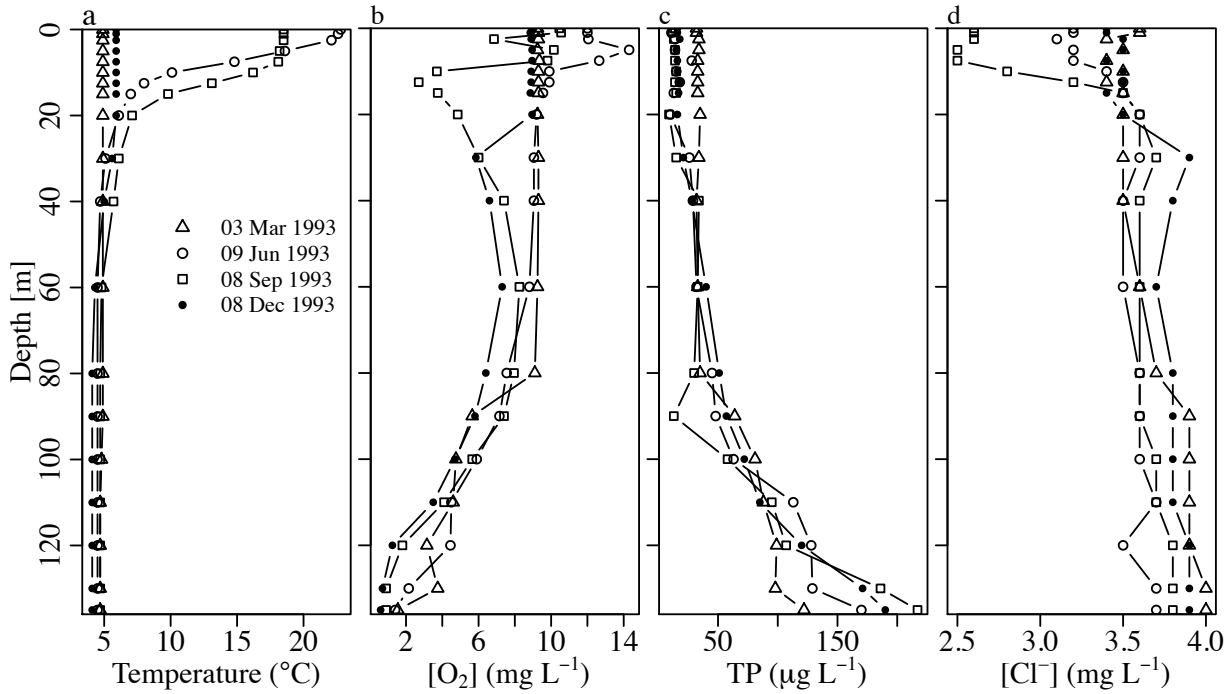

Figure 3.1: Water column profiles of a) temperature, b) oxygen concentration ($[O_2]$), c) total phosphorus concentration (TP), and d) chloride concentration ($[Cl^-]$), measured in the Lake of Zurich in 1993.

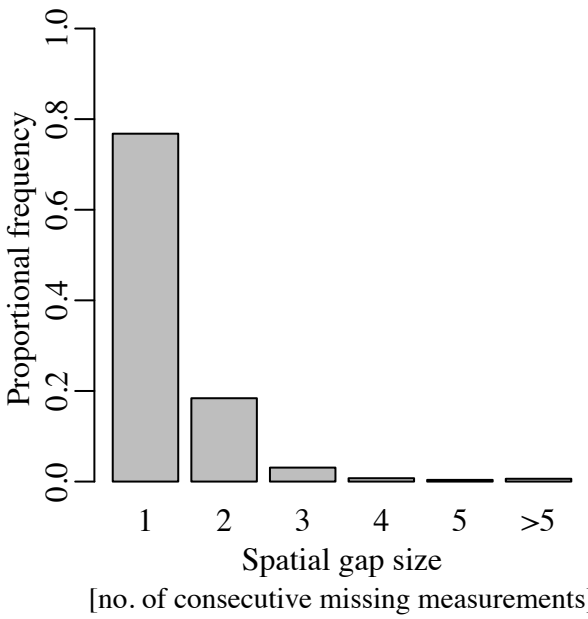

Figure 3.2: Proportional frequency of occurrence of spatial data gaps of a given size (expressed as the number of consecutive missing measurements) within temperature profiles normally measured at a set of standard depths from which at least one measurement was missing. The plot is based on profiles from the Lake of Zurich (1972 - 2010; 470 profiles), Greifensee (1942 - 2002; 609 profiles), Lake of Lugano (1987 - 2008; 416 profiles), Aegerisee (1950 - 1994; 278 profiles), Lake of Walenstadt (1972 - 2010; 391 profiles), and Lake of Garda (1991 - 2008; 219 profiles). Of the 2383 profiles, 354 contained at least one missing measurement and there were a total of 810 spatial data gaps of varying size.

The comparison of spatial interpolation methods used a leave-k-out cross-validation, where k = 1,2,3 is the pseudo-gap size (method derived from Baltazar and Claridge 2002; see Arlot and Celisse 2010, for a full review of cross-validation). Given a complete profile y_i (i = 1...n) of n observations (where n = 19 in the specific case of the Lake of Zurich data set), the procedure for creating and filling 1-point pseudo-gaps was as follows. First, observation y_2 was removed to create a new profile with one 1-point pseudo-gap between observations y_1 and y_3. This gap was then filled by interpolating across it (either by two-point linear interpolation or by cubic spline interpolation), creating a new value, x_2. The interpolation error for this pseudo-gap was calculated as $e_2 = x_2$-y_2. Starting from the original profile each time, and going down the profile from j = 2 to $j = n$-1, the process was conducted n-2 times, yielding n-2 new profiles, each with one interpolated pseudo-gap at a unique depth. The first and last points of the measured profile, y_1 and y_n, were always retained to avoid endpoint effects. For a pseudo-gap size of k = 2, the same procedure was used, except that observations y_j and y_{j+1} were removed each time for $j = 2 \ldots n$-2. For a pseudo-gap size of k = 3, observations y_j, y_{j+1}, and y_{j+2} were removed each time for $j = 2 \ldots n$-3. An interpolation error was calculated for every point within each interpolated pseudo-gap; e.g., for every pseudo-gap of size 2, interpolation errors $e_j = x_j$-y_j and $e_{j+1} = x_{j+1}$-y_{j+1} were calculated.

Linear interpolation across a pseudo-gap was conducted solely based on the two measured values bounding the pseudo-gap – i.e., on the two values y_{j-1} and y_{j+1} adjacent to the removed value y_j – and is therefore extremely local. Because of the nature of the spline function, cubic spline interpolation yields a value that is influenced not only by the measured values directly bounding the pseudo-gap, but also by several measured values on either side. However, because the effect of a constraint on a spline diminishes rapidly with increasing distance (Emery, 2001), spline-interpolated values are still influenced predominantly by values measured in the vicinity of the pseudo-gap.

Prior to analysis, the calculated interpolation errors for each variable were sorted in three different ways: (i) by pseudo-gap size only; (ii) by pseudo-gap size and then by the month in which the measurement was made; and (iii) by pseudo-gap size, by month and then by measurement depth. The three resulting groups of interpolation errors provided a varied assessment of the performance of the interpolation methods as well as insight into how sampling practices (which affect, for example, the density of measurements as a function of depth) influence interpolation accuracy.

3.3 Assessment

The statistical measures chosen to assess quantitatively the accuracy of each interpolation method were the root mean square error (RMSE), the mean bias error (MBE), and the maximum absolute bias error (MABE). The RMSE, defined as:

$$\text{RMSE} = \sqrt{\frac{\sum e_j^2}{n_e}}, \tag{3.1}$$

where n_e is the total number of interpolated data points within a given range of depths and profiles, gives an overall measure of the accuracy of the interpolation within this range. The MBE is defined as:

$$\text{MBE} = \frac{\sum e_j}{n_e}. \tag{3.2}$$

A negative MBE represents a consistent underestimate of the observed value by the interpolated value, and a positive MBE represents a consistent overestimate. Both RMSE and MBE are well

accepted and commonly used statistical measures that have been employed for the same purpose in similar studies (e.g., Amritkar and Kumar, 1995; Baltazar and Claridge, 2002; Neilsen et al., 2010). The MABE, defined as:

$$\text{MABE} = max(|e_j|), \tag{3.3}$$

was included additionally to provide insight into the magnitude of error each interpolation method could potentially create. Since both RMSE and MBE are averages, they do not provide an indication of the range of error associated with each of the interpolation methods. To assess the significance of the results, the RMSE, MBE, and MABE were compared with the measurement uncertainty (MU), on the assumption that any error less than the MU is not significant. Not all MUs were known, nor were they necessarily consistent throughout all measurement years. Therefore, as a conservative approach, the largest known MU for a given variable was chosen for comparison purposes (3.1). The relative performance of the two interpolation methods was assessed in terms of the difference of the RMSE (or MBE, or MABE) associated with two-point linear interpolation and the RMSE (or MBE, or MABE) associated with cubic spline interpolation. This difference will be referred to henceforth as the "RMSE difference" (or "MBE difference", or "MABE difference").

3.3.1 Pseudo-gap size

Interpolation errors were grouped by variable and by pseudo-gap size to calculate RMSE values (Table 3.1). For temperature, $[O_2]$, and TP, the RMSE exceeded the corresponding MU for all pseudo-gap sizes, but for $[Cl^-]$ the RMSE exceeded the MU only for the cubic spline interpolation of a 3-point pseudo-gap. For all variables and pseudo-gap sizes, the RMSE associated with two-point linear interpolation was always less than or equal to that associated with cubic spline interpolation. Using a pseudo-gap size of 3 as an example, temperature RMSEs were 1.1°C for linear interpolation and 1.4°C for cubic spline interpolation; $[O_2]$ RMSEs were 1.2 mg L^{-1} for linear interpolation and 2.2 mg L^{-1} for cubic spline interpolation; TP RMSEs were 11.6 μg L^{-1} for linear interpolation and 15.4 μg L^{-1} for cubic spline interpolation; and $[Cl^-]$ RMSEs were 0.2 mg L^{-1} for linear interpolation and 0.3 mg L^{-1} for cubic spline interpolation.

For all four variables the difference of the RMSE associated with linear interpolation and the RMSE associated with cubic spline interpolation increased rapidly with pseudo-gap size (Table 3.1). For a pseudo-gap size of 1, there was little difference between the two interpolation methods, but as the pseudo-gap size grew larger, cubic spline interpolation became increasingly less accurate than linear interpolation. For $[Cl^-]$ the RMSE differences were however very small at all pseudo-gap sizes, implying that for this variable the choice of interpolation method is not critical.

The MABEs associated with linear interpolation were consistently less than those associated with cubic spline interpolation, except for TP (pseudo-gap size of 1 and 2). The MABEs tended to increase with pseudo-gap size, as did the MABE differences, which were generally much larger for a pseudo-gap size of 3 than for a pseudo-gap size of 1 or 2. This means that the increase in MABE with increasing pseudo-gap size was less in the case of linear interpolation than in the case of cubic spline interpolation. For all variables and pseudo-gap sizes, the MABEs exceeded the corresponding MUs by at least an order of magnitude.

3.3.2 Season and month

When grouped by pseudo-gap size and month, the RMSE values for both methods showed a strong seasonal cycle in all cases, with values being lowest in winter and spring, increasing during summer, and peaking in fall (Figure 3.3). For temperature, the RMSEs associated with both methods exceeded the MU from April through December. For $[O_2]$ and TP the same was true throughout the entire year. For $[Cl^-]$ the RMSEs associated with linear interpolation were below the MU for 1-point and 2-point pseudo-gaps, and only exceeded the MU during August and September for a 3-point pseudo-gap. The RMSEs associated with the cubic spline interpolation of $[Cl^-]$ exceeded the MU from August through November for a 2-point pseudo-gap, and from June through November for a 3-point pseudo-gap.

Table 3.1: The root mean square errors (RMSEs) and maximum absolute bias errors (MABEs) associated with the linear interpolation and cubic spline interpolation of lake profiles over pseudo-gaps of various sizes, and the corresponding differences (cubic spline minus linear). The variables are temperature (T), oxygen concentration ($[O_2]$), total phosphorus concentration (TP), and chloride concentration ($[Cl^-]$). Pseudo-gap sizes vary from 1 to 3, where the size of a pseudo-gap is the number of missing data points within the gap. For comparison purposes, the measurement uncertainty (MU) for each variable is also listed. The profiles employed were measured in the Lake of Zurich during 1976-2010.

Variable [units]	Pseudo-	Linear		Cubic spline		Difference	
(± MU)	gap Size	RMSE	MABE	RMSE	MABE	RMSE	MABE
T [°C]	1	0.5	5.3	0.5	7.5	0.0	2.2
(± 0.1°C)	2	0.8	7.0	0.8	11.8	0.1	4.8
	3	1.1	8.7	1.4	27.8	0.3	19.2
$[O_2]$ [mg L^{-1}]	1	0.8	7.1	1.0	9.9	0.2	2.8
(± 0.3 mg L^{-1})	2	1.0	8.2	1.5	14.4	0.5	6.2
	3	1.2	8.7	2.2	32.8	1.0	24.1
TP [μg L^{-1}]	1	8.3	131.0	9.6	123.9	1.3	-7.1
(± 1.8 μg L^{-1})	2	9.7	152.4	11.8	149.6	2.1	-2.8
	3	11.6	165.1	15.4	238.9	3.9	73.7
$[Cl^-]$ [mg L^{-1}]	1	0.1	2.3	0.2	2.3	0.0	0.1
(± 0.27 mg L^{-1})	2	0.2	2.2	0.2	2.6	0.1	0.4
	3	0.2	2.2	0.3	4.2	0.2	2.0

In general, in all months the RMSEs for both methods increased with increasing pseudo-gap size, but as the rate of increase was higher for cubic-spline interpolation than for linear interpolation, the RMSE differences (Figure 3.3, shaded areas), and therefore the improvement of linear interpolation over cubic spline interpolation, also increased with pseudo-gap size. For a pseudo-gap size of 1, the RMSE differences for all four variables were small throughout most of the year (Figure 3.3a-d). As the pseudo-gap size was increased to 2 and 3, the RMSE differences became progressively larger, particularly from approximately July to November (Figure 3.33e-l). There was a strong seasonality in the RMSE differences (Figure 3.3, shaded areas), which were smallest in winter and spring but underwent an increase in summer to reach a maximum in fall.

3.3.3 Measurement depth

The influence of measurement depth on interpolation accuracy was investigated by successively grouping the interpolation errors by variable, pseudo-gap size, depth, and month, before calculating the RMSEs. As general patterns were similar for all pseudo-gap sizes, only the results for a pseudo-gap size of 2 are shown (Figure 3.4). For all three pseudo-gap sizes, the previously discussed seasonality in the RMSE (i.e., minimum in winter and spring, maximum in fall) and

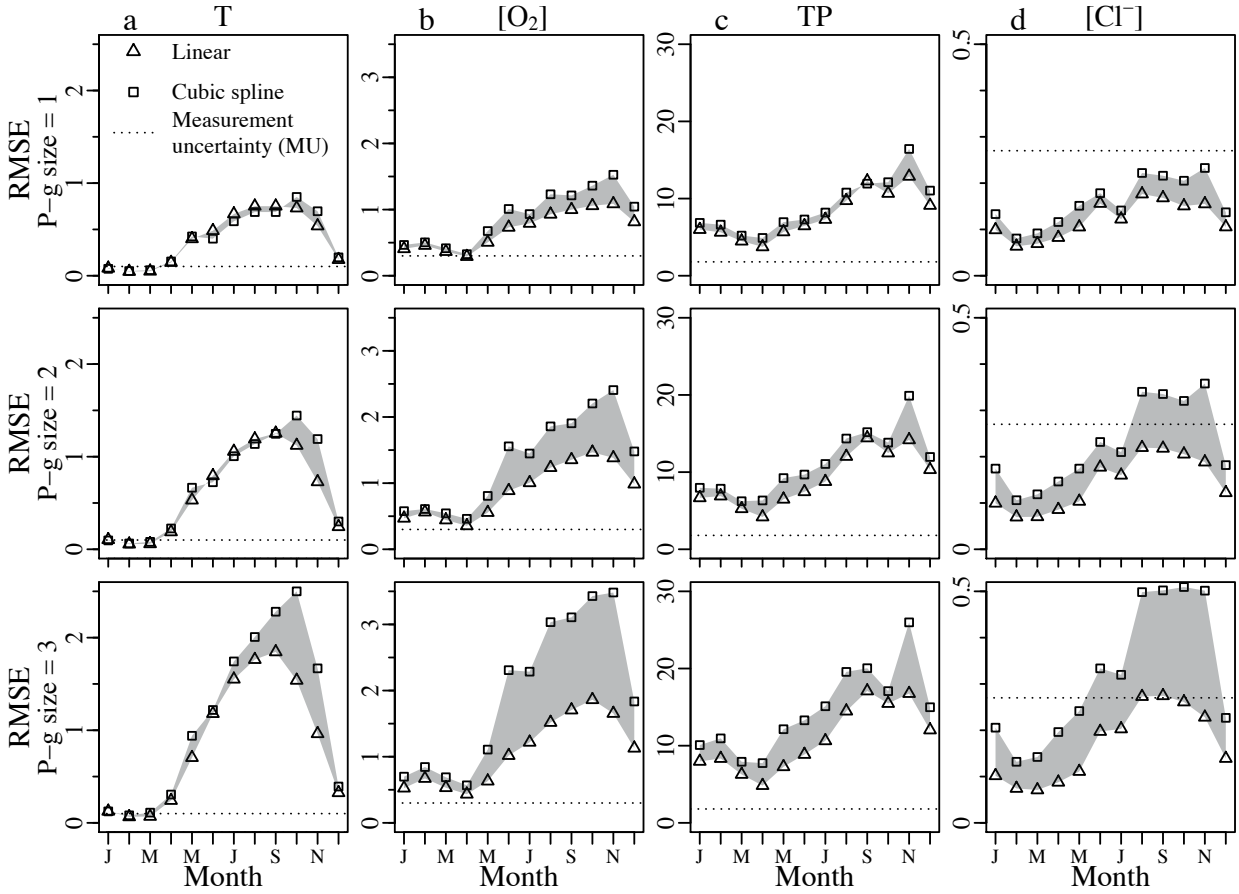

Figure 3.3: Seasonal variation in the root mean square error (RMSE) associated with linear interpolation and with cubic spline interpolation, for pseudo-gap sizes of 1, 2, and 3. The variables are a) temperature (T,°C), b) oxygen concentration ([O_2], mg L^{-1}), c) total phosphorus concentration (TP, μg L^{-1}), and d) chloride concentration ([Cl^-], mg L^{-1}). Dotted lines indicate measurement uncertainty (MU). The shaded areas indicate the difference of the RMSEs associated with each of the two methods.

dependence on pseudo-gap size (i.e., RMSE increasing with pseudo-gap size) was once again evident. Additionally, the results showed a concentration of high RMSEs in the metalimnion and upper hypolimnion, centered around a depth of 20 m (Figure 3.4). The RMSEs of TP were also high near the lake bottom, while for the other three variables the RMSEs were low below approximately 80 m, remaining near or below the respective MUs for all three pseudo-gap sizes. The RMSEs for $[Cl^-]$ exceeded the MU from August to November for depths above 20 m for linear interpolation and above 40 m for cubic spline interpolation. This depth limitation of $[Cl^-]$ was present for all three pseudo-gap sizes; however, the frequency of occurrence of cases in which the RMSE exceeded the MU tended to increase with pseudo-gap size.

For the majority of depths and months, the RMSEs associated with linear interpolation were lower than those associated with cubic spline interpolation (Figure 3.4). For all three pseudo-gap sizes, the RMSE differences were largest at depths above 80 m for temperature, $[O_2]$ and $[Cl^-]$, and below 100 m for TP (Figure 3.4, shaded areas). Between June and November, the RMSE associated with linear interpolation occasionally exceeded that associated with cubic spline interpolation for temperature in the lower epilimnion and the metalimnion, and for TP at the lake bottom. However, the number of such occurrences was comparatively low.

3.3.4 Mean bias error

The effectiveness of the two interpolation methods was also assessed for all three pseudo-gap sizes using the MBE and the same grouping method used for the RMSE (i.e., pseudo-gap size, month, and depth). For the most part, the MBEs remained below or near the respective MUs. Therefore, only the MBEs for a pseudo-gap size of 2, sorted by depth and month, are presented as an example (Figure 3.5). In the cases when the MBE did exceed the MU, the magnitudes of the MBE associated with cubic spline interpolation were smaller than those associated with linear interpolation. The MBEs for temperature, $[O_2]$, and $[Cl^-]$ showed similar seasonal and spatial patterns to those exhibited by the RMSEs; i.e., the MBEs were low in winter and spring and high in summer and fall, with the largest bias occurring in the metalimnion and upper hypolimnion (Figure 3.5). The MBE for TP followed the same seasonal pattern but the highest values occurred below 100 m. The MBE differences for temperature, $[O_2]$, and $[Cl^-]$ generally increased with increasing pseudo-gap size, as the magnitude of the MBEs of both methods increased proportionally. While the MBE difference for TP increased with pseudo-gap size, this was mainly accounted for by an increase in the MBE associated with linear interpolation, as the MBE associated with cubic spline interpolation changed very little with pseudo-gap size.

3.4 Discussion

Two-point linear interpolation and cubic spline interpolation are both simple to apply, but from the outset each can be seen to have both advantages and disadvantages. Because the values resulting from linear interpolation always lie between the adjacent measured values, linear interpolation will always overestimate the minima in profiles and underestimate the maxima, resulting in reduced variability within the profile and a bias towards the mean. The values produced by cubic spline interpolation do not suffer from this bias and may yield more realistic values for the extrema within a profile, but this comes at a cost: because spline-interpolated data can lie outside the range of measured data, unrealistically low minima and unrealistically high maxima may result. This tends to happen when adjacent measurements are spatially close but differ substantially in magnitude from one another, which is most likely to result when the sampling interval is small but measurement error is large. The likelihood of this kind of overshoot makes it necessary to check

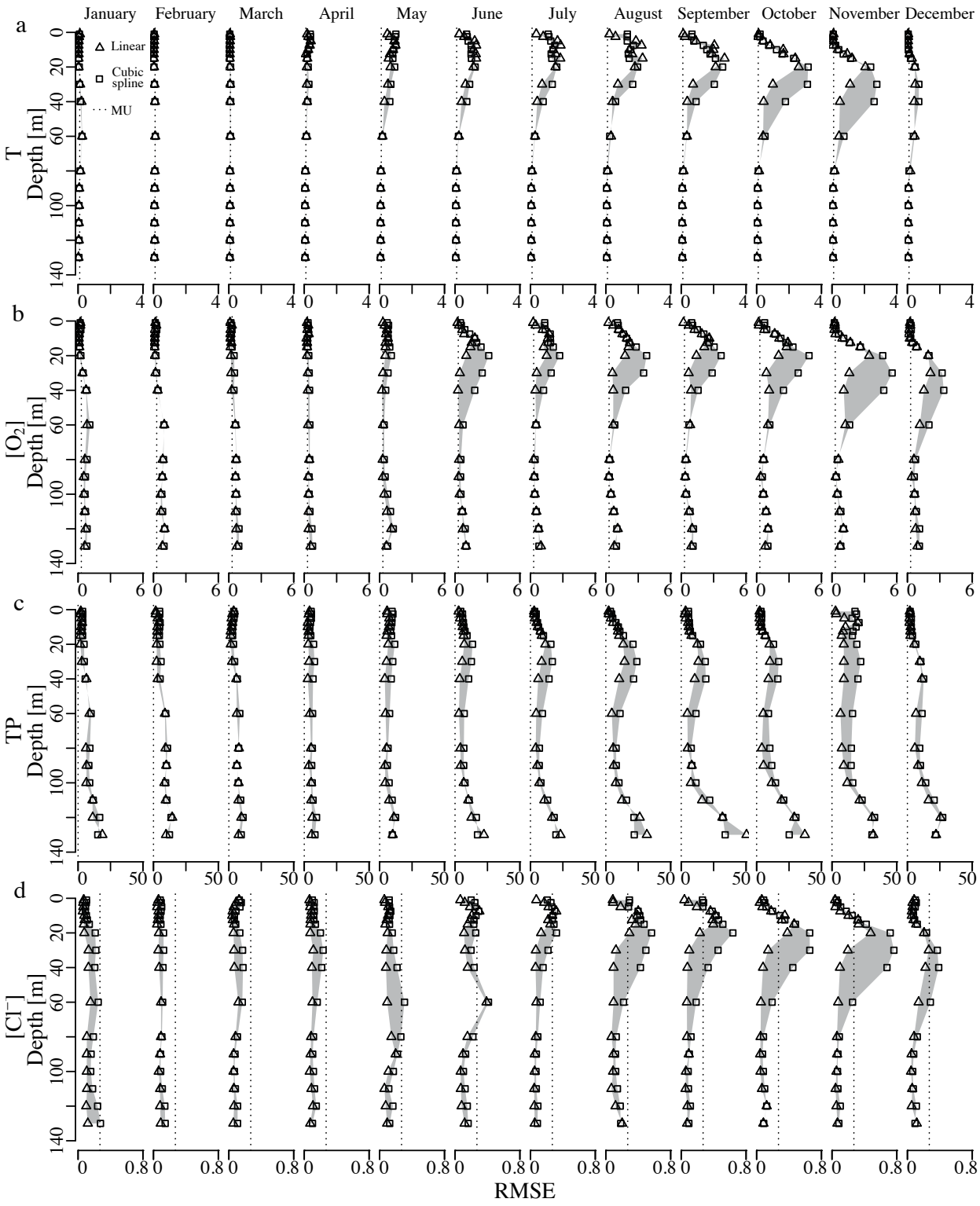

Figure 3.4: Monthly profiles of the root mean square errors (RMSEs) associated with linear interpolation and cubic spline interpolation. Calculated interpolation errors for a pseudo-gap size of 2 were grouped by measurement depth and month. The variables are a) temperature (T,°C), b) oxygen concentration ([O_2], mg L^{-1}), c) total phosphorus concentration (TP, μg L^{-1}), and d) chloride concentration ([Cl^-], mg L^{-1}). Dotted lines indicate measurement uncertainty. The shaded areas indicate the difference of the RMSEs associated with each of the two methods.

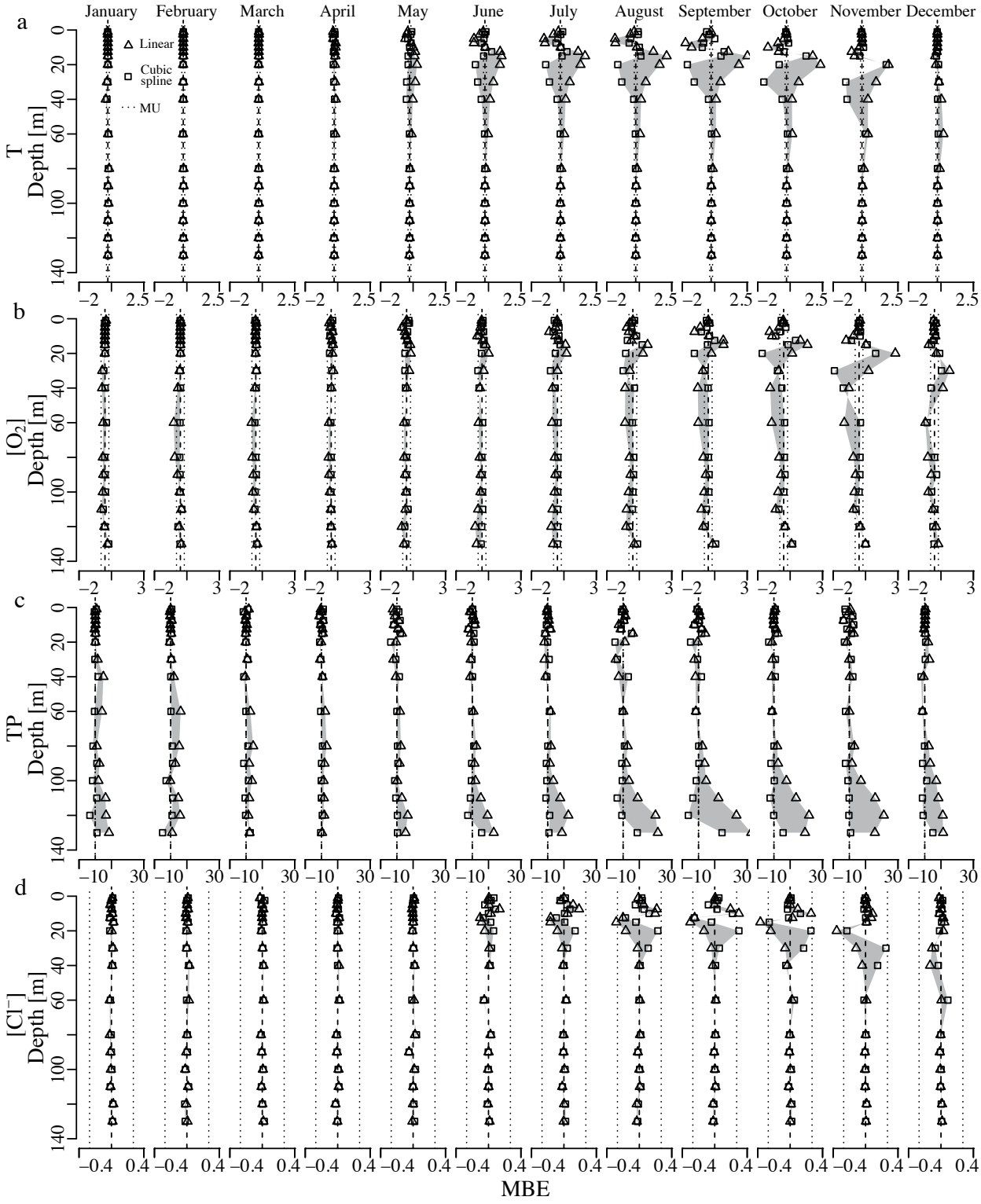

Figure 3.5: Monthly profiles of the mean bias error (MBE) for linear interpolation and cubic spline interpolation. Calculated interpolation errors for a pseudo-gap size of 2 were grouped by measurement depth and month. The variables are a) temperature (T,°C), b) oxygen concentration ([O_2], mg L^{-1}), c) total phosphorus concentration (TP, μg L^{-1}), and d) chloride concentration ([Cl^-], mg L^{-1}). Dotted lines indicate measurement uncertainty. The shaded areas indicate the difference of the MBEs associated with each of the two methods.

spline-interpolated data to ensure that they are physically reasonable. This can be done either by eye or by adding an additional automatic stage to the interpolation process to flag values that are physically impossible (e.g., negative concentrations) or unlikely (e.g., extremely high concentrations or extremely high concentration gradients within the interpolated profile, or interpolated concentrations that differ excessively from the measured values above and below them). If profile interpolation is to be completely automated, with no checking by eye, then linear interpolation is safer because unpleasant surprises are much less likely. However, the interpolated profile resulting from a spline interpolation is by definition continuous with respect to its first and second derivatives, which is not the case for a linearly interpolated profile. Thus the gradients of linearly interpolated profiles are discontinuous, making flux calculations unreliable.

This study has shown the errors associated with two-point linear interpolation to be consistently smaller than those associated with cubic spline interpolation. Additionally, the analysis provides useful insight into how interpolation is affected by season, depth, and spatial data gap size. For all four variables investigated, the two methods performed equally well throughout the entire profile in winter and spring, when the RMSEs and MBEs associated with each of the two methods did not generally exceed the MU (Figures 3.4, 3.5). In summer and fall the same was true below approximately 60 m for water temperature, $[O_2]$, and $[Cl^-]$ (but not for TP). Where there was a measurable difference in performance, linear interpolation produced consistently smaller errors than cubic spline interpolation. Although the RMSE increased with pseudo-gap size for both methods, the errors associated with cubic spline interpolation increased at a faster rate than those associated with linear interpolation, and as a result the RMSE difference also increased with increasing pseudo-gap size. In the rare situations in which the RMSE associated with cubic spline interpolation was smaller than that associated with linear interpolation, the difference between the RMSE was small and did not increase with pseudo-gap size (e.g., temperature in Figure 3.4).

Despite the fact that the RMSE values associated with linear interpolation were consistently lower than those associated with cubic spline interpolation (Figure 3.4), the bias associated with the latter was smaller (Figure 3.5). Cubic spline interpolation both overestimated and underestimated the true values over a wide range of error magnitude, while linear interpolation consistently produced overestimates or underestimates (depending on the profile shape), but within a smaller range of error magnitude. The difference between the methods can be illustrated using density distribution plots of the errors (Figure 3.6). The distributions of the errors associated with cubic spline interpolation have a broad, shallow peak near zero, with long tails, whereas those associated with linear interpolation are either slightly negative or slightly positive, with a high, narrow peak, and short tails.

The reason for the difference in the density distributions is made clear by the example shown in Figure 3.7. In Figure 3.7a, observed water temperatures at 5 m, 7.5 m, and 10 m have been removed to create a 3-point pseudo-gap, which is then filled using both two-point linear interpolation and cubic spline interpolation. The interpolation errors (listed in Figure 3.7a) associated with the cubic spline interpolation are slightly smaller than those associated with the linear interpolation (see also Figure 3.4). In Figure 3.7b, a 3-point pseudo-gap created by removing the measurements at 20 m, 30 m, and 40 m, and interpolated similarly, results in the opposite situation: the interpolation error associated with the two-point linear interpolation is much smaller than that associated with the cubic spline interpolation. There are two key differences between the two scenarios. The first is in the magnitude of the errors: while cubic spline interpolation errors can be small (Figure 3.7a) they can also be large (Figure 3.7b), whereas linear interpolation errors are consistently small. The second is in physical plausibility: under normal conditions, the spline-interpolated profile of Figure 3.7b is not physically realistic (assuming the temperature of maximum density to be 4°C, then between approximately 20 m and 30 m denser water would be overlying lighter water,

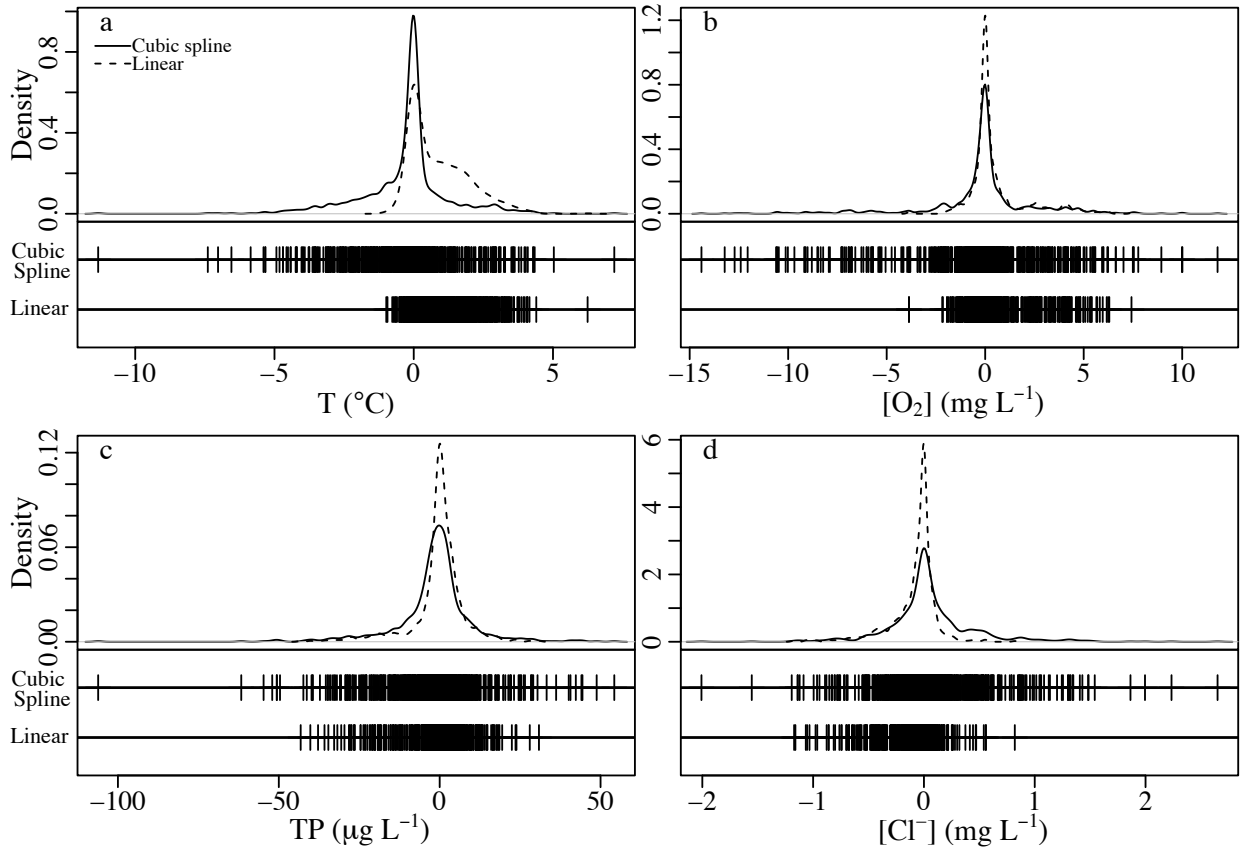

Figure 3.6: Density distribution plots of interpolation errors (interpolated minus observed) for a) temperature (T_e), b) oxygen concentration ($[O_2]_e$), c) total phosphorus concentration (TP_e), and d) chloride concentration ($[Cl^-]_e$) at 20 m depth for all three pseudo-gap sizes (1, 2, and 3) combined. Two types of distribution plot are shown for each variable to highlight the width and height of peaks, as well as tail sizes.

and between about 30 m and 40 m water temperatures would be < 0°C). The large interpolation errors depicted in Figure 3.7b occur only when data points are missing in regions where gradients are changing; i.e., where $d^2C/dz^2 \neq 0$, where C is concentration or temperature and z is depth. In regions where d^2C/dz^2 is zero or close to zero, less information is lost when data points are missing, making it easier for either interpolation method to accurately fill the data gap.

The density distribution of errors associated with the linear interpolation of temperature (T) at 20 m depth, where d^2T/dz^2 can be large during certain times of the year, differs clearly from that associated with the linear interpolation of the other three variables at the same depth (Figure 3.6). Instead of a high, narrow peak, the error distribution for temperature has a small peak near zero and a large shoulder up to approximately 2°C. At 20 m depth, the temperature profile is typically either uniform (e.g., during winter) or is transitioning from a low to a high gradient (e.g., during summer stratification, Figure 3.7). In the former case, linear interpolation can accurately interpolate any data gaps and the interpolation errors are small, giving rise to the peak in the distribution near zero. In the latter case, linear interpolation will consistently overestimate the observed values, and interpolation errors will be positive (Figure 3.7b). As the pseudo-gap size increases, the magnitudes of the interpolation errors also increase, leading to a concentration of interpolation errors T_e within the approximate range $0°C \leq T_e \leq 2°C$ (Figure 3.6a). This can be seen clearly in Figure 3.7b, where a 3-point pseudo gap produces a linear interpolation error of $T_e = 2.1°C$ at a depth of 20 m. The contrast in density distribution between cubic spline interpolation and linear interpolation at 20 m depth illustrates very well the trade-offs between the advantages and

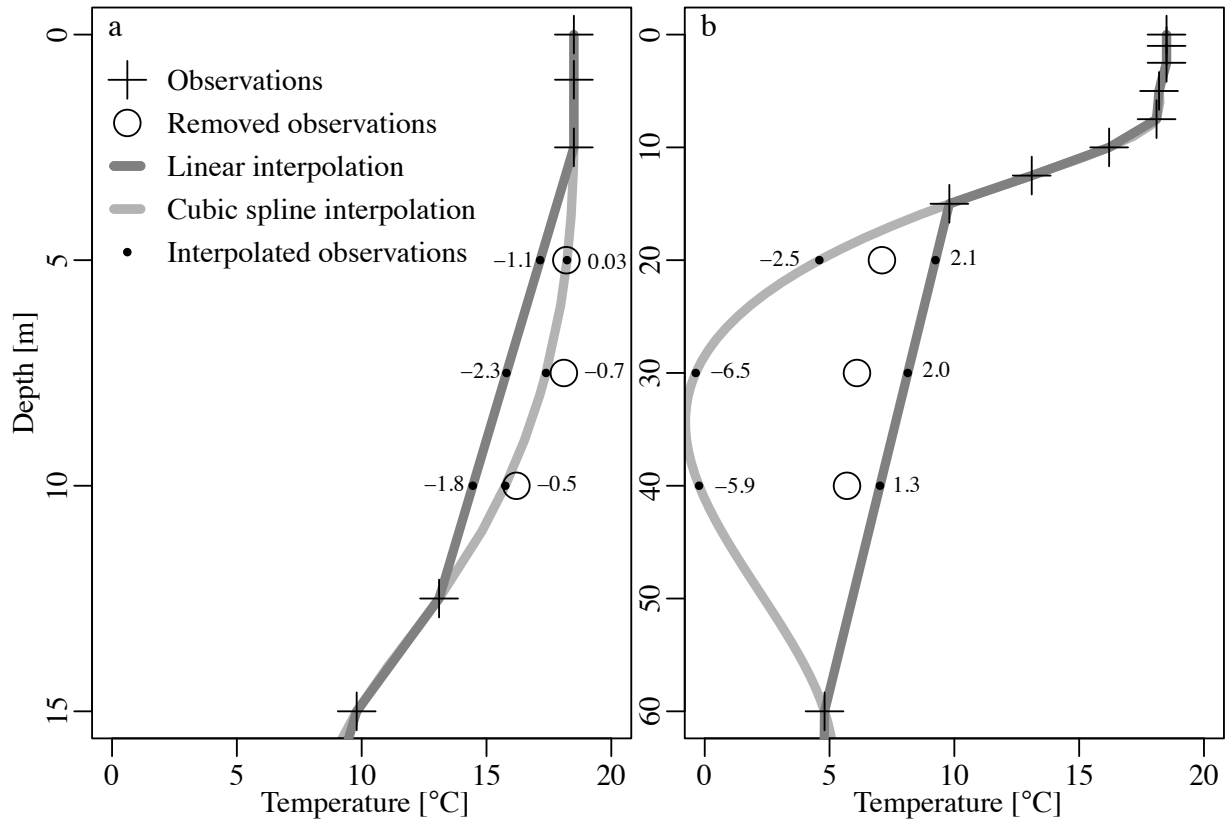

Figure 3.7: Two examples of the linear interpolation and cubic spline interpolation of part of a temperature profile (measured in the Lake of Zurich on 08 September 1993) for a pseudo-gap size of 3, showing a) a situation in which cubic spline interpolation is the more accurate (interpolation over the pseudo-gap from 2.5 to 12.5 m depth) and b) a situation in which two-point linear interpolation is the more accurate (interpolation over the pseudo-gap from 15 to 60 m depth). The magnitudes of the interpolation errors for both methods are marked on the figure. The profiles of observed temperature are plotted at the standard measurement depths, while the interpolated profiles are shown with a uniform sampling interval of 1 m to highlight differences between the results of the two interpolation methods.

disadvantages of the two interpolation methods discussed above. During the stratification period, d^2T/dz^2 is large and as a result linear interpolation consistently overestimates the temperature, but without creating unrealistically high or low values. Cubic spline interpolation is able to accurately interpolate the temperature at 20 m (peak at approximately zero), but does so at the risk of creating unrealistically high or low values, which are reflected in the large tails in the density distribution of T_e (Figure 3.6a).

Interpolation errors associated with both linear and cubic spline interpolation show a strong seasonal dependence. Errors are low in winter and spring, increase during summer and are high in fall. The same seasonal pattern also holds true for the RMSE difference and for the MBE difference. The homogeneity of the winter and spring profiles makes it easy for both methods to interpolate all three pseudo-gap sizes accurately. During summer and fall, the existence of gradients in the profiles (Figure 3.1) makes interpolation difficult, particularly over large gaps (e.g., Figure 3.7). Even TP profiles, which do not show much seasonal variation themselves (Figure 3.1), show a seasonal pattern in their RMSE values (Figure 3.3c).

Figures 3.4 and 3.5 show that most of the seasonal pattern in RMSE and MBE can be attributed to interpolation errors in and near the metalimnion (and in the case of TP, near the lake bottom). For water temperature, $[O_2]$, and $[Cl^-]$, interpolation errors were small and rarely exceeded MU below

approximately 60 m. This pattern of error distribution also held true for the RMSE difference between the two methods. As discussed above, changing gradients in a profile result in large errors during summer and fall. As these gradients are located around the metalimnion and upper hypolimnion (and near the lake bottom for TP), this is where the largest interpolation errors occur. Below approximately 60 m, profiles are generally homogeneous (except for TP), and are therefore easier to interpolate accurately. The depth dependence of the magnitude of the interpolation errors can be linked to the physics of an individual lake. A lake that does not mix regularly will develop varying thermal and chemical gradients, giving rise to large interpolation errors. In contrast, a lake subjected to consistently strong mixing events will have weaker thermal or chemical stratifications, minimizing changes in gradients and therefore interpolation errors. Existing information on typical lake profiles and mixing patterns can therefore give a preliminary indication of how successful empirical interpolation is likely to be in filling any data gaps.

This discussion has focused on a comparison of the size of the errors produced by the two interpolation methods. However, the size of the errors should also be considered in the context of the usefulness of the interpolated values. The MABE values in Table 3.1 show that for all pseudo-gap sizes and variables, both interpolation methods have the potential to produce large errors. Although the magnitude of the MABEs is disconcerting, density distribution plots of the errors (Figure 3.6) show that extremely large MABEs are in fact rare, and that most interpolation errors (concentrated in the vicinity of the peaks in Figure 3.6) are small. Nevertheless, because both interpolation methods have the potential to produce large errors in a number of situations, further steps (e.g., visual inspection of the interpolated profiles) may be necessary to identify unacceptably large errors.

3.5 Comments and recommendations

The two methods compared in this study, two-point linear interpolation and cubic spline interpolation, are two of the simplest gap-filling methods available. Yet the results of this study show that both linear and cubic spline interpolation can provide reasonably accurate results when interpolating gaps of various sizes in lake profiles. For both methods, interpolation errors were smallest when the pseudo-gap size was small, and increased as the pseudo-gap size grew. However, the rate of increase with pseudo-gap size was lower for linear interpolation than for cubic spline interpolation, and as a result, linear interpolation was substantially more accurate than cubic spline interpolation when interpolating over large pseudo-gaps. Two-point linear interpolation is therefore generally recommended for the interpolation of data gaps in lake profiles, as it is likely to yield more accurate and more consistent results than cubic spline interpolation.

However, the limitations discussed above must be taken into consideration. In addition, when either interpolation method is applied, it is important to be aware of the size and location of data gaps, and to verify the results of the interpolation. Interpolation is in a sense a necessary evil, and Figures 3.3-3.6 show that errors associated with any automatic interpolation can be unacceptably high. Automatic profile interpolation therefore needs to be supplemented with an automatic method of detecting physically implausible interpolation errors, and, ideally, with visual inspection of the interpolated profiles. Furthermore, the results suggest that neither method can satisfactorily interpolate a 3-point pseudo-gap, so that for gap sizes of 3 or more points, a process-based physical model may be the only feasible method of interpolation.

This study has also highlighted the importance of selecting proper sampling intervals. The data set used for the analysis seemed well-designed, with measurement densities high near the lake surface, decreasing through the metalimnion and upper hypolimnion, and increasing again slightly towards the lake bottom. However, the cross-validation analysis found the highest interpolation

errors for all variables in the metalimnion and upper hypolimnion, and near the lake bottom for TP. Clearly, smaller spatial sampling intervals at these depths would not only reduce interpolation errors, but also capture gradients and variations with greater accuracy.

4

The physical impact of the late 1980s climate regime shift on Swiss rivers and lakes

North, R. P.[1,2], Livingstone, D. M.[1], Hari, R. E.[3], Köster, O.[4], Niederhauser, P.[5], and Kipfer, R.[1,2]

1. Eawag, Swiss Federal Institute of Aquatic Science and Technology, Department of Water Resources and Drinking Water, Überlandstrasse 133, CH-8600 Dübendorf, Switzerland.

2. ETH Zurich, Department of Environmental Systems Science, Institute of Biogeochemistry and Pollution Dynamics, Universitätsstrasse 16, CH-8092 Zürich, Switzerland

3. Eawag, Swiss Federal Institute of Aquatic Science and Technology, Department of Systems Analysis, Integrated Assessment and Modelling, Überlandstrasse 133, CH-8600 Dübendorf, Switzerland.

4. Zurich Water Supply, Hardhof 9, P.O. Box 1179, CH-8021 Zürich, Switzerland

5. Amt für Abfall, Wasser, Energie und Luft des Kantons Zürich (AWEL), Hardturmstrasse 105, CH-8090 Zürich, Switzerland

Accepted for publication in *Inland Waters*

Abstract In the late 1980s, a sudden climate regime shift (CRS) occurred throughout the Northern Hemisphere that affected both marine and inland waters. In Switzerland, rivers and lakes underwent an abrupt warming. A month-by-month comparison of water temperatures before and after the late 1980s CRS shows seasonal differences in the magnitude of the warming, which was stronger in winter, spring, and summer than in autumn. In lakes, the magnitude of the increase and the abruptness of the change diminished with increasing depth. Surface temperatures showed

Acknowledgements Appreciation is extended to the numerous individuals who participated in many decades of measuring temperature profiles in the Lower Lake of Zurich, the Upper Lake of Zurich, Greifensee, and the Lake of Walenstadt. River and stream temperatures were kindly provided by the Swiss Federal Office of the Environment (FOEN) and air temperature data by the Swiss Federal Office of Meteorology and Climatology (MeteoSchweiz).

the most consistent abrupt warming. Hypolimnetic temperatures also increased, but the change was gradual in three of the four lakes studied. The abrupt warming in the late 1980s contributed substantially to the overall increase in temperature that has occurred in water bodies in Switzerland over the last few decades.

4.1 Introduction

At the end of the 1980s, a large-scale, abrupt climate regime shift (CRS) occurred over large parts of the Northern Hemisphere, associated with a shift in the Arctic Oscillation and in related climate modes such as the North Atlantic Oscillation and the Pacific Decadal Oscillation (Yasunaka and Hanawa, 2002; Alheit et al., 2005; Rodionov and Overland, 2005; Lo and Hsu, 2010). It affected not only Northern Hemisphere temperatures, but also other climatic variables such as the frequency and intensity of cyclones (McCabe et al., 2001). Its impact on the marine environment is especially well documented. Sea surface temperatures throughout the Northern Hemisphere were affected (Yasunaka and Hanawa, 2002), as were the physics and biology of marine areas as diverse as the North Pacific (Hare and Mantua, 2000; Benson and Trites, 2002), Bering Sea (Hare and Mantua, 2000; Benson and Trites, 2002; Rodionov and Overland, 2005), North Sea (Reid et al., 2001; Beaugrand, 2004; Alheit et al., 2005), Baltic Sea (Alheit et al., 2005), Mediterranean Sea (Conversi et al., 2009, 2010), and Sea of Japan (Tian et al., 2004; Zhang et al., 2007; Tian et al., 2008; Kidokoro et al., 2010). The influence of the late 1980s CRS was not confined to marine systems, however; it has also been detected in lake ecosystems in Germany (Gerten and Adrian, 2000; Jochimsen et al., 2012) and Sweden (Temnerud and Weyhenmeyer, 2008). In Switzerland, the influence of the late 1980s CRS has been detected in lakes (Anneville et al., 2004, 2005), rivers (Hari et al., 2006), and, even groundwater (Figura et al., 2011). Here we investigate in more detail the physical impact of the late 1980s CRS on Swiss river and lake temperatures.

4.2 Study sites and data

Time-series of water temperature from 18 river and stream measuring stations and four perialpine lakes in Switzerland were analysed. The main analysis was limited to data measured from 1972 onwards, as data quality before 1972 was considered inadequate at one or more locations.

For several decades, water temperatures have been measured at sub-daily intervals in many Swiss rivers and streams, allowing the computation of reliable daily means (Hari et al., 2006). Reliable daily mean water temperature data were available for each day of the period 1972 - 2001 from 15 measuring stations and for over 99.9% of the same period from an additional three stations. Based on these daily data, a monthly mean water temperature time-series was computed for each measuring station. As the river temperature time-series are broadly coherent within Switzerland (Hari et al., 2006), the 18 time-series were aggregated to yield one monthly mean time-series representative of the general behaviour of river water temperatures (RWTs) in Switzerland.

The four study lakes – the Lower Lake of Zurich, the Upper Lake of Zurich, Greifensee, and the Lake of Walenstadt – are all located in northeastern Switzerland (Table 4.1). The Upper Lake of Zurich and Greifensee are considerably shallower than the other two lakes. The Lake of Walenstadt mixes twice a year but has never been known to freeze over (Zimmermann et al., 1991); in the other three lakes, the presence or absence of ice cover and the frequency and intensity of mixing vary depending on the severity of the winter (Zimmermann et al., 1991; Livingstone, 1993; Hendricks Franssen and Scherrer, 2008; Rempfer et al., 2010). For further details on the limnological characteristics of the four lakes see Zimmermann et al. (1991) and Rempfer et al. (2010). For the

Lower Lake of Zurich, the Upper Lake of Zurich, and Greifensee, reliable water temperature data measured at approximately monthly intervals at the deepest point of each lake were available from 1972 - 2005; for the Lake of Walenstadt, the monthly time-series extended only from 1972 - 2000. Lake temperature profiles were interpolated spatially at intervals of 1 m using linear interpolation (Chapter 3). From the resulting interpolated profiles, volume-weighted mean temperatures were derived for the full water column, the epi/metalimnion, and the hypolimnion. The depth of the upper boundary of the hypolimnion (z_h) varies among the lakes (Table 4.1). For each lake, values of the Schmidt stability – a measure of overall thermal stability – were calculated from the interpolated temperature profiles (Schmidt, 1928; Idso, 1973). Time-series of surface water temperature, the three volume-weighted mean temperatures, and Schmidt stability were interpolated temporally at daily intervals using cubic spline interpolation. These daily values were then aggregated to yield monthly and annual means. From the Lower Lake of Zurich, reliable water temperature data covering a much longer period are available. This extended Lower Lake of Zurich dataset, covering the period 1944-2010, was also analysed.

Table 4.1: Characteristics of the four study lakes (z_h = depth of the upper boundary of the hypolimnion in summer). Morphometric data from Zimmermann et al. (1991)

	Lake of Walenstadt	Greifensee	Lower Lake of Zurich	Upper Lake of Zurich
Altitude a.s.l. (m)	419	435	406	406
Surface area (km^2)	24	8	65	20
Volume (km^3)	2.42	0.15	3.3	0.47
Mean depth (m)	103	18	51	23
Maximum depth (m)	145	33	136	48
z_h (m)	20	17	20	30
Mean retention time (yr)	1.4	1.5	1.2	1.4
Trophic status	Oligotrophic	Hypertrophic	Mesotrophic	Mesotrophic

Because air temperatures fluctuate with a very high degree of coherence over the entire Swiss Plateau, the behaviour of the regional air temperature on the Swiss Plateau is characterized well by an averaged time-series of the air temperatures measured at the four Swiss Meteorological Office stations of Zurich, Berne, Basle, and Neuchâtel (Livingstone and Lotter, 1998). Daily maximum and minimum temperatures were used to calculate daily means for each station, from which the regional mean was determined. The resulting time-series of daily means was aggregated to yield monthly and annual means.

4.3 Methods

Change-points between regimes were detected using the sequential t-test STARS (Rodionov and Overland, 2005). Mean annual temperatures were tested using a threshold significance level $p = 0.15$, a Huber weight parameter h = 1 (Rodionov, 2006), and a cut-off length L = 15 yr. The threshold significance level and the cut-off length determine the magnitude of the shifts detected by STARS (Rodionov and Overland, 2005). The cut-off length determines the detection scale of interest (Rodionov and Overland, 2005), which in this case was approximately 15 yr (1972-1987 and 1988-2005). The Huber weight parameter accounts for outliers when calculating the mean value of a regime (Rodionov, 2006). The cut-off length was reduced to 10 yr for the RWT time-series and the Lake of Walenstadt time-series because of their shorter lengths. When STARS detected a shift, an additional (and more stringent) t-test was applied to the two regimes. While the STARS threshold significance level was set to $p = 0.15$, any shift that did not satisfy a significance criterion

of $p < 0.05$ was rejected. As the focus of this study was the impact of the late 1980s CRS, the discussion focuses on shifts detected between 1984 and 1991. The non-parametric Mann-Kendall test was used to test for significant monotonic trends within individual regimes.

4.4 Results

4.4.1 Air temperature

Annual mean regional air temperatures on the Swiss Plateau underwent an abrupt increase of 0.9°C from 1987 to 1988 ($p < 0.001$), dividing the period 1972-2005 into two regimes: Regime I from 1972-1987 and Regime II from 1988-2005 (Figure 4.1a). Comparing the two regimes month by month, the regional air temperature increased from Regime I to Regime II by over 0.7°C from January to August and in October (Figure 4.1b; Table 4.2). No statistically significant monotonic trend was found in either Regime I or Regime II ($p < 0.05$), suggesting that the entire increase in air temperature during the period 1972-2005 resulted from the late 1980s CRS.

4.4.2 River and stream temperatures

River and stream temperatures in Switzerland closely follow regional air temperature (Livingstone and Hari, 2008). The abrupt increase in air temperature in Switzerland associated with the late 1980s CRS was therefore reflected in a corresponding abrupt increase in river and stream temperatures (Hari et al., 2006). Analysis of the annual mean 18-station RWT time-series confirmed the existence of an abrupt increase from Regime I to Regime II ($p < 0.001$) with a magnitude of $\Delta T = 0.7$°C (Figure 4.1c). As in the case of air temperature, this increase was more pronounced from January to August and in October than during the rest of the year (Figure 4.1d; Table 4.2). No statistically significant monotonic trend was found in either Regime I or Regime II ($p < 0.05$), suggesting, in agreement with Hari et al. (2006), that the entire temperature increase in Swiss rivers and streams from 1972-2001 can be explained by the late 1980s CRS.

4.4.3 Lake temperatures

Lake surface temperature: In all four of the study lakes, an abrupt increase in annual mean lake surface water temperature was detected during the late 1980s ($p < 0.01$) (Figure 4.2a-d, Table 4.3). The regime shift occurred from 1987 to 1988 in the Lake of Walenstadt and Greifensee, from 1988 to 1989 in the Lower Lake of Zurich, and from 1989 to 1990 in the Upper Lake of Zurich. The magnitude of the regime shift ranged from 0.6°C to 0.8°C (Table 4.3). In general, the regime shift tended to be more coherently pronounced in all four lakes from April to August (Table 4.2). In Regime I, no statistically significant trends were found for any of the lakes ($p < 0.05$). In Regime II, a significant (upward) trend was found only for the Lower Lake of Zurich ($p < 0.05$).

Mean lake temperature: For the annual, volume-weighted mean lake temperature, a regime shift of 0.3 - 0.4°C was detected in all four lakes in the late 1980s (Figure 4.2e-h, Table 4.3). The regime shift occurred from 1988 to 1989 in the Lake of Walenstadt, from 1987 to 1988 in Greifensee, and the Lower Lake of Zurich, and from 1984 to 1985 in the Upper Lake of Zurich. The largest temperature increases between Regimes I and II occurred from January to August (Table 4.2), except for Greifensee (April to August). A statistically significant upward trend was found in Regime II for the Lake of Walenstadt ($p < 0.05$); otherwise, no monotonic trends were found in either of the two regimes.

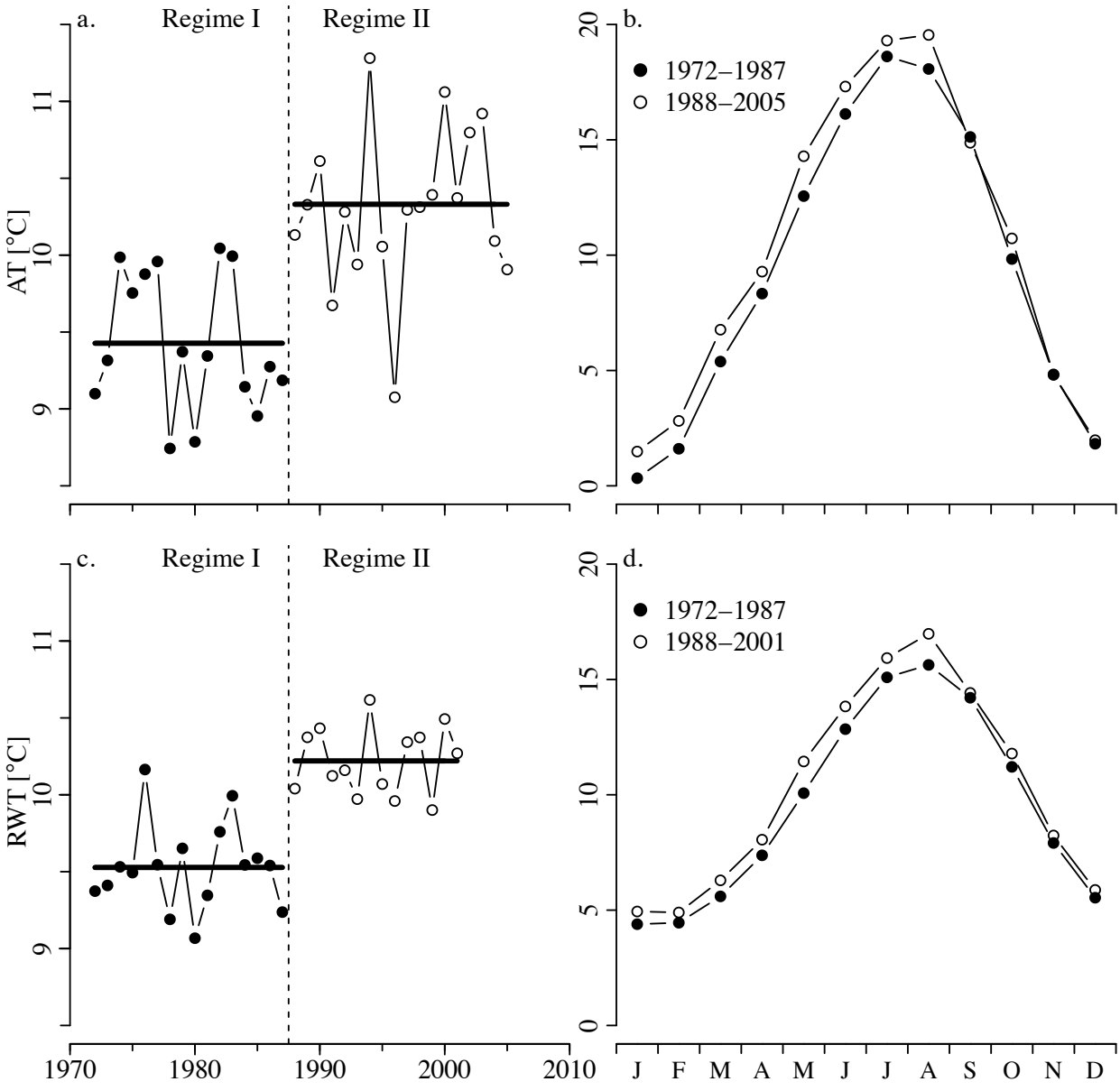

Figure 4.1: a) Annual mean regional air temperature (AT) in northern Switzerland in Regimes I (1972-1987) and II (1988-2005) based on data from the meteorological stations of Zurich, Berne, Basle, and Neuchâtel. b) Comparison of monthly mean AT in Regimes I and II. c) Combined mean annual river water temperatures (RWT) from 18 rivers and streams across Switzerland in Regimes I (1972-1987) and II (1988-2001). d) Comparison of monthly mean RWT in Regimes I and II. The thick horizontal lines illustrate the mean temperatures in Regimes I and II.

Table 4.2: Change in monthly mean temperature [°C] and thermal stability [J m^{-2}] from Regime I (up to and including 1987) to Regime II (1988 and after). Statistical significance: $p < 0.05$ (*).

	Jan	Feb	Mar	Apr	May	Jun	Jul	Aug	Sep	Oct	Nov	Dec
Air temperature	1.2	1.2	1.4*	1.0*	1.7*	1.2*	0.7	1.5*	-0.3	0.9	0.0	0.2
River water temperature	0.6*	0.4*	0.7*	0.7*	1.4*	1.0*	0.8*	1.4*	0.2	0.6*	0.3	0.3
Lake surface water temperature												
Lake of Walenstadt	0.4*	0.4*	0.1	0.4	2.0*	1.8*	1.6*	1.3*	0.2	0.3	0.5*	0.3
Greifensee	0.5	0.2	-0.1	1.2*	2.1*	0.8	1.0*	0.8	0.3	0.5	0. 5	0.2
Lower Lake Zurich	0.4*	0.6*	0.6	0.9	1.9*	0.6	1.1	1.2*	0.3	0.4	0.5	0.4
Upper Lake Zurich	0.2	0.4	0.3	1.5*	1.6*	-0.1	1.4	0.9	-0.1	-0.1	0.2	0.2
Volume-weighted mean lake temperature												
Lake of Walenstadt	0.4*	0.4*	0.5*	0.5*	0.5*	0.4*	0.3	0.3*	0.3*	0.2	0.3*	0.3*
Greifensee	0.3*	-0.1	0.2	0.6*	0.6*	0.5*	0.5*	0.5*	0.3	0.2	0.3	0.3
Lower Lake Zurich	0.4*	0.5*	0.5*	0.5*	0.5*	0.5*	0.4*	0.3*	0.2	0.2	0.3*	0.3*
Upper Lake Zurich	0.5*	0.5*	0.5*	0.7*	0.7*	0.5	0.5*	0.3	-0.1	0.0	0.2	0.3
Volume-weighted mean epi/metalimnetic temperature												
Lake of Walenstadt	0.4*	0.4*	0.5*	0.6*	1.3*	1.2*	0. 7	0.8*	0.5*	0.4	0.4*	0.3
Greifensee	0.4*	-0.1	0.2	0.7*	0.8*	0.7*	0.7*	0.8*	0.4	0.3	0.4	0.4
Lower Lake Zurich	0.4*	0.5*	0.6*	0.9*	1.1*	0.9*	0.6	0.6*	0.4	0.4	0.4	0.5
Upper Lake Zurich	0.5*	0.5*	0.5	0.7*	0.8*	0.5	0.6*	0.3	-0.1	0.0	0.2	0.3
Volume-weighted mean hypolimnetic temperature												
Lake of Walenstadt	0.4*	0.4*	0.6*	0.5*	0.4*	0.3*	0.2	0.3*	0.3*	0.1	0.2*	0.3*
Greifensee	0.3*	-0.1	0.2	0.2	0.1	0.0	-0.1	-0.2	-0.2	-0.2	-0.1	0.3
Lower Lake Zurich	0.3*	0.4*	0.4*	0.4*	0.3*	0.3*	0.3*	0.2	0.2	0.2	0.2	0.2*
Upper Lake Zurich	0.5*	0.6*	0.4*	0.2	0.1	0.0	0.1	-0.1	-0.1	-0.1	0.0	0.4*
Schmidt stability												
Lake of Walenstadt	17	-1	24	187*	1071*	1385*	775	1131*	512	282	295	104
Greifensee	-3	0	-3	40*	102*	112*	120*	148*	61	40	20	2
Lower Lake Zurich	48*	16	11	228*	741*	725*	805*	984*	409	252	268	124
Upper Lake Zurich	-2	2	1	55*	83*	87	191*	169*	49	19	2	-14

Table 4.3: Temporal location, statistical significance, and magnitude (ΔT) of abrupt shifts in annual mean Swiss lake temperatures and thermal stability as detected by the STARS test (Rodionov and Overland, 2005). The lake temperatures listed are: surface temperature (T_0); mean lake temperature (T_l); epi/metalimnetic temperature (T_{em}); hypolimnetic temperature (T_h). Thermal stability calculated as Schmidt stability (S). Statistical significance: $p < 0.05$ (*); $p < 0.01$ (**); $p < 0.001$ (***). ΔT is given only for regime shifts detected in the 1980s.

		Lake of Walenstadt	Greifensee	Lower Lake of Zurich	Upper Lake of Zurich
T_0	STARS	1987/88 (***)	1987/88 (***)	1988/89 (***)	1989/90 (**)
	ΔT_0 (°C)	0.8	0.6	0.8	0.6
T_l	STARS	1988/89 (***)	1987/88 (*)	1987/88 (***)	1984/85 (**)
	ΔT_l (°C)	0.4	0.3	0.4	0.4
T_{em}	STARS	1987/88 (***)	1981/82 (***)	1987/88 (***)	1984/85 (**)
	ΔT_{em} (°C)	0.6	-	0.6	0.4
T_h	STARS	-	-	1987/88 (**)	-
	ΔT_h (°C)	-	-	0.3	-
S	STARS	1982/83 (**)	1980/81 (***)	1989/90 (***)	1988/89 (***)
	ΔS (J m^{-2})	-	-	422	55

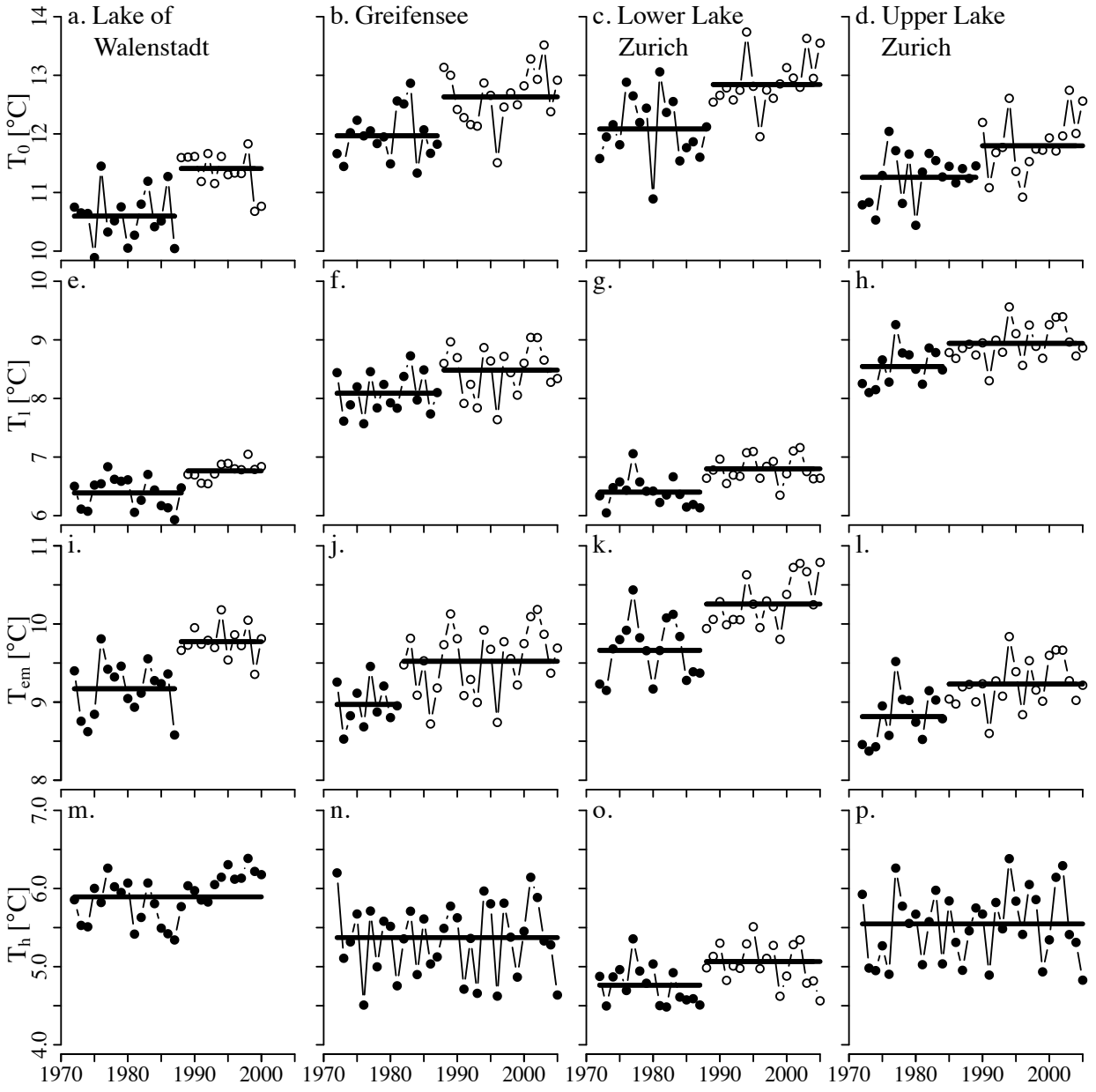

Figure 4.2: Annual mean lake surface water temperatures (T_0) for the Lake of Walenstadt, Greifensee, the Lower Lake of Zurich, and the Upper Lake of Zurich (a, b, c, d), and the corresponding mean lake temperatures (T_l) (e,f,g,h), mean epi/metalimnetic temperatures (T_{em}) (i,j,k,l), and mean hypolimnetic temperatures (T_h) (m,n,o,p). All means are volume-weighted. The thick horizontal lines illustrate the mean temperatures in Regimes I and II.

An exceptionally long temperature time-series, encompassing over 60 yr of data, is available from the Lower Lake of Zurich (Figure 4.3). When the time window was increased to span the period 1944 - 2010, the STARS test identified two regime shifts in mean lake temperature: a main regime shift of 0.4°C from 1987 to 1988 ($p < 0.001$) and a smaller regime shift of 0.2°C from 1964 to 1965 ($p < 0.05$). The main regime shift involved a year-round increase in mean lake temperature and a significant shift ($p < 0.05$) in each individual month from December to May, as well as August. Despite the smaller regime shift from 1964 to 1965, the extended Lower Lake of Zurich temperature data show no significant trend ($p < 0.05$) before or after the regime shift in 1987/88. The abrupt temperature increase of 0.4°C in the late 1980s therefore contributed substantially to the overall increase in mean lake temperature that has occurred over the last few decades.

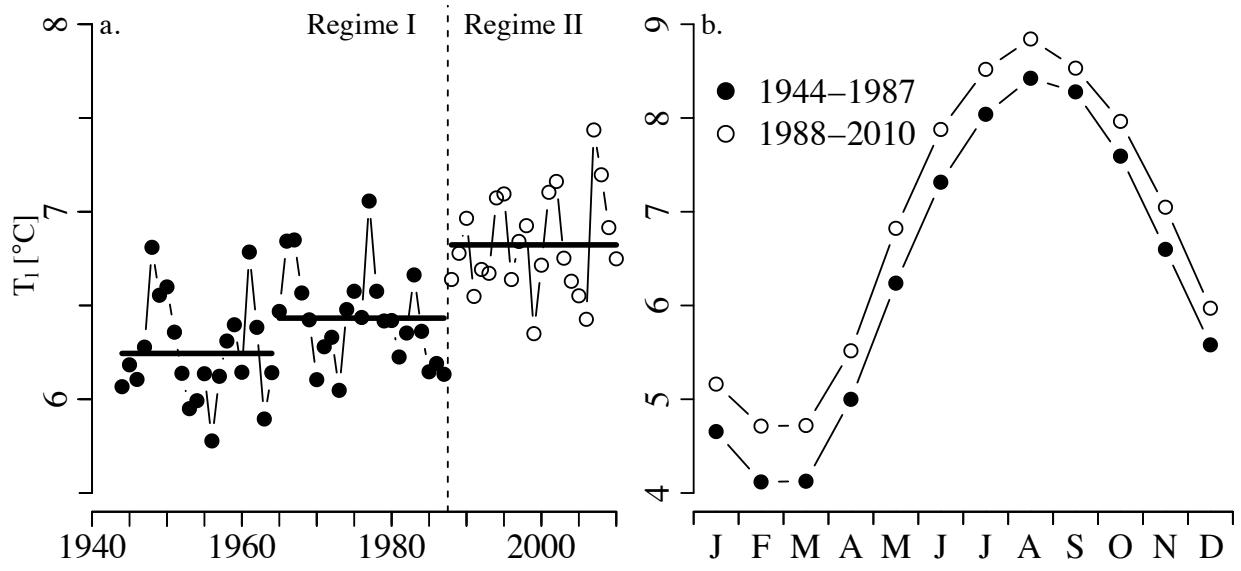

Figure 4.3: a) Annual volume-weighted mean lake temperature (T_l) of the Lower Lake of Zurich (extended data series, 1944 - 2010). The thick horizontal lines illustrate the mean temperatures in Regimes I and II. b) Comparison of monthly mean air temperatures in Regimes I and II.

Epi/metalimnetic temperature: Coarse estimates of the dependence of the temperature regime shift on depth were obtained by analysing the mean volume-weighted epi/metalimnetic and hypolimnetic temperatures separately. Significant shifts in annual mean epi/metalimnetic temperature occurred in the Lake of Walenstadt and the Lower Lake of Zurich from 1987 to 1988 ($p < 0.001$), and in the Upper Lake of Zurich from 1984 to 1985 ($p < 0.01$), although in Greifensee, a shift was detected in the early 1980s (Table 4.3, Figure 4.2i-l). Comparing Regimes I and II month by month, epi/metalimnetic temperatures in all four lakes increased in nearly every month of the year, with the largest increases occurring from April to August (Table 4.2). As in the case of lake surface water temperature, a significant (upward) trend in epi/metalimnetic was found for the Lower Lake of Zurich in Regime II ($p < 0.05$).

Hypolimnetic temperature: The Lower Lake of Zurich was the only lake with a statistically significant regime shift in annual mean hypolimnetic temperature ($p < 0.01$; ΔT=0.3°C) (Figure 4.2m-p, Table 4.3), although an increase in hypolimnetic temperature from Regime I to Regime II occurred in every month of the year not only in the Lower Lake of Zurich, but also in the Lake of Walenstadt (Table 4.2). The largest increases in temperature in the hypolimnion of the Lake of Walenstadt, the Lower Lake of Zurich, and the Upper Lake of Zurich occurred from January to

April, while in Greifensee changes were small (≤ 0.3°C) throughout the year (Table 4.2). A test for monotonic trends in hypolimnetic temperature ($p < 0.05$) revealed no trend for any of the four lakes in Regime I, and no trend for three of the lakes in Regime II (the exception was the Lake of Walenstadt, for which the Regime II time-series extends only up to 2000).

4.4.4 Lake thermal stability

A late 1980s regime shift in the annual mean Schmidt stability (S) was detected in the Lower Lake of Zurich and the Upper Lake of Zurich ($p < 0.001$), but not in the other two lakes (Figure 4.4a-d, Table 4.3). In all four lakes, the Schmidt stability increased from Regime I to Regime II during the stratified period (from late spring to early autumn), when thermal stability is high (Table 4.2). During winter and early spring, when thermal stability is low and the lakes undergo mixing, the Schmidt stability changed very little from Regime I to Regime II (Table 4.2). The largest increases tended to occur between April and August, and in all four lakes a significant regime shift ($p < 0.05$) was detected for this five-month period (Figure 4.4e-h). A significant upward trend in Regime II was found in Greifensee ($p < 0.05$) and the Lower Lake of Zurich ($p < 0.01$). Otherwise, the Schmidt stability was statistically stationary in both Regimes I and II.

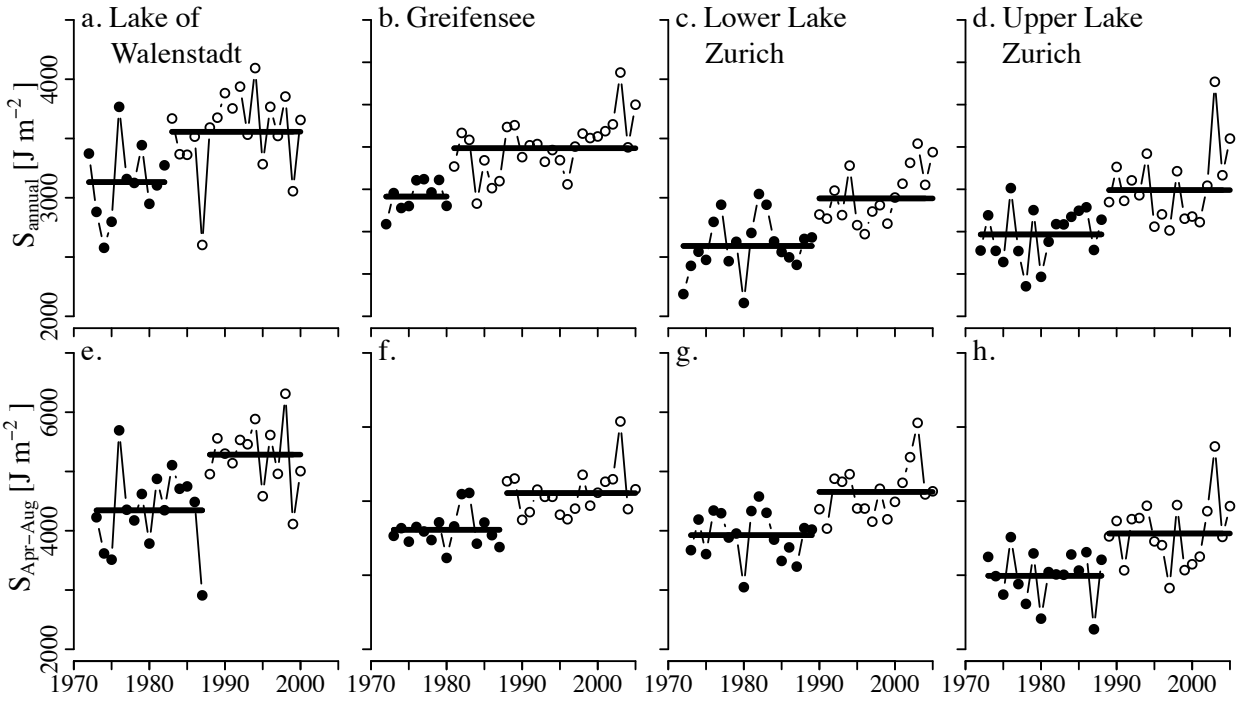

Figure 4.4: Schmidt stability of the Lake of Walenstadt, Greifensee, the Lower Lake of Zurich, and the Upper Lake of Zurich, averaged over the full year (S_{annual}) (a,b,c,d) and over April to August ($S_{Apr-Aug}$) (e,f,g,h). The thick horizontal lines illustrate the mean Schmidt stabilities in Regimes I and II.

4.5 Discussion

In the late 1980s, water temperatures in rivers and lakes in Switzerland (along with some groundwaters: see Figura et al. 2011) clearly underwent a regime shift corresponding to, and presumably caused by, the late 1980s CRS. The late 1980s CRS was associated with, and may ultimately have been triggered by, a shift in the Arctic Oscillation and other large-scale climate modes (Rodionov

and Overland, 2005; Lo and Hsu, 2010). The shift in water temperature occurred in conjunction with an abrupt increase of 0.9°C in annual mean air temperatures on the Swiss Plateau, centred around 1987/88. The shift was reflected most strongly in river water temperatures (ΔT = 0.7°C) and lake surface water temperatures (ΔT = 0.6 - 0.8°C), which are tightly related both to each other and to regional air temperature (Livingstone and Hari 2008).

In all four study lakes the magnitude of the shift decreased with depth, from the lake surface through the epi/metalimnion to the hypolimnion. No temperature regime shift in the late 1980s was detected in the epi/metalimnion of Greifensee, and only the Lower Lake of Zurich showed an abrupt temperature shift in the hypolimnion. Nonetheless, all four lakes showed an abrupt regime shift in mean lake temperature (ΔT = 0.3 - 0.4°C; $p < 0.05$). This indicates that, although the late 1980s CRS had a detectable effect on the heat budgets of all four lakes, its effect on the internal distribution of heat varied from lake to lake, presumably depending on individual lake characteristics, which differ substantially (Table 4.1).

Applying the STARS test to the extended Lower Lake of Zurich time-series of mean lake temperature (1944 - 2010), the regime shift from 1987 to 1988 was still easily detectable, statistically highly significant, and strong. Despite a small additional regime shift detected from 1964 to 1965 (Figure 4.3a), the extended time-series showed no significant monotonic trend ($p < 0.05$) during Regime I, even when this regime was extended back to 1944. The lack of trend across the small regime shift, and its relatively low significance ($p < 0.05$), suggest that it might not be a true regime shift, but rather the realisation of an autoregressive stationary red-noise process (Rudnick and Davis, 2003). To distinguish between the two possibilities, prewhitening can be applied to the time-series to remove its red noise component prior to testing for a regime shift (Rodionov, 2006). When this was done, the shift from 1964 to 1965 became non-significant ($p > 0.05$), and the magnitude of the shift from 1987 to 1988 increased to 0.5°C ($p < 0.001$). Thus, most of the increase in the mean lake temperature of the Lower Lake of Zurich over the past 65 years appears to be associated with the late 1980s CRS.

No significant trends ($p < 0.05$) in the air temperature or river water temperature time-series were detected during either Regime I or Regime II, suggesting, in agreement with Hari et al. (2006), that the entire recent increase in river water temperatures in Switzerland can be interpreted as a result of the of the late 1980s CRS. This is not necessarily true, however, for all the lake surface water temperature records. Although no significant trends ($p < 0.05$) in lake surface water temperature were found in Regime I for any of the lakes, one of the four lakes showed a significant warming trend during Regime II. This one exception was the Lower Lake of Zurich, in which the surface water temperature showed a significant upward trend ($p < 0.05$) of approximately 0.04°C yr^{-1} during Regime II, which is similar to the global lake surface water warming rate of 0.045 ± 0.011°C yr^{-1} determined for 1985-2009 from satellite data (Schneider and Hook, 2010). Thus, although the late 1980s CRS can statistically explain the entire observed increase in the surface water temperature of some Swiss lakes over the past few decades, this is not true of all. The surface water temperature of the Lower Lake of Zurich, in common with the temperatures of some Swiss groundwaters (Figura et al., 2011), has continued to increase even after the late 1980s CRS.

Comparing the two regimes month by month, the regional air temperature, mean river water temperature, and lake water temperatures (excluding the hypolimnion) increased from Regime I to Regime II throughout most of the year, with the exception of part of autumn and early winter. The largest increases tended to occur from January to August for air temperature, from March to August for river water temperature, and from approximately April to August for lake surface water temperatures. The lack of any strong increase in the temperatures of rivers or the uppermost layers of lakes from Regime I to Regime II in the first two months of the year, despite comparatively large

increases in air temperature, is not surprising. In January and February, snow in river catchment areas (and often ice in the rivers themselves) buffers the effect of changes in air temperature on river water temperatures, so the increase in the mean air temperature from Regime I to Regime II is unlikely to have been fully reflected in river temperatures in these winter months. In lakes, partial ice cover (e.g., in Greifensee and the Upper Lake of Zurich; see Hendricks Franssen and Scherrer 2008) also has a buffering effect. Even in lakes not subject to ice cover, however, vertical mixing during winter and spring, when thermal stability is low and wind-induced mixing is common, also buffers the effect of changing air temperatures, diminishing the impact of a rise in mean air temperature from Regime I to Regime II. After the establishment of a stratified water column in April, the relatively thin epilimnion responds much more sensitively to changes in air temperature (Livingstone and Lotter, 1998), explaining the greater differences in lake temperatures between the two regimes that are apparent from April to August.

The asymmetric warming between the surface and bottom waters of the lakes, with the epi/metalimnion warming more than the hypolimnion, resulted in a general increase in thermal stability. The increase was strongest from April to August in all four lakes, and thermal stabilities averaged over these months showed an abrupt increase in the late 1980s. Despite the general increase in thermal stability from Regime I to Regime II, the frequency of occurrence of complete mixing (defined here as occurring when the Schmidt stability < 15 J m^{-2}) did not change noticeably in three of the four lakes. The exception was the Lower Lake of Zurich, which underwent complete mixing in 13 out of the 16 years of Regime I, but in only 9 out of the 18 years of Regime II, suggesting a shift from monomixis in Regime I to oligomixis in Regime II. Because the Lower Lake of Zurich did not undergo complete mixing every year during Regime II, on several occasions hypolimnetic temperatures were able to increase over a period of several consecutive years as a result of the gradual downward transport of heat from the lower metalimnion by turbulent diffusion (Livingstone, 1993, 1997). Although mixing episodes always eventually returned the hypolimnetic temperature approximately to its long-term mean value, the existence of this multi-annual "sawtooth" mixing pattern in Regime II automatically resulted in hypolimnetic temperatures that were on average higher in Regime II than in Regime I.

The existence of a regionally coherent response of lake water temperatures to climatic forcing in general has been well documented in previous studies (e.g., Magnuson et al., 1990; Blenckner et al., 2007; Livingstone et al., 2010). In the specific case of the abrupt CRS in the late 1980s, the present study has confirmed that rivers and lakes in Switzerland responded coherently to the step-change in external forcing, but has also demonstrated a certain degree of heterogeneity in the response, especially in lake hypolimnia. Regional coherence among lakes is known to be strongest for physical variables that have a direct causal link to climatic forcing (Magnuson et al., 1990). Thus, inter-lake coherence in lake temperature is strongest at the surface, but weakens with depth as the influence of climatic forcing becomes more indirect and individual lake processes become more dominant. Differences in the mixing characteristics of the individual lakes, related, for instance, to differences in lake morphometry (Table 4.1), are likely to be primarily responsible for this. Rempfer et al. (2010) have already shown, for example, that morphometric differences among the same four Swiss lakes (Table 4.1) result in different hypolimnetic responses to wind forcing in winter.

Research on the physical impact of climate change on aquatic systems has tended to focus on gradual long-term trends (e.g., Schneider and Hook, 2010), but the present study shows clearly that abrupt changes in large-scale climatic forcing can result in similarly abrupt regime shifts in the physical environments of rivers and lakes. In addition to the late 1980s CRS, at least two other abrupt, large-scale CRSs appear to have occurred in the past few decades; i.e., in the mid 1970s and the late 1990s (Hare and Mantua, 2000; Rodionov and Overland, 2005; Overland et al., 2008). It is

likely that the impact of such unannounced and, perhaps, ultimately unpredictable abrupt shifts in physical boundary conditions on aquatic ecosystems will differ from the impacts of more gradual change. Thus, if drastic changes in their functionality are to be avoided, aquatic ecosystems may have to adapt not only to gradual changes in water temperature as climate change progresses, but also to abrupt changes. This emphasizes the importance of maintaining the resilience of aquatic ecosystems (Scheffer et al., 2001; Folke et al., 2004) in the face of climate change.

5

Long-term changes in hypoxia in a large temperate lake: consequences of a climate regime shift

North, R. P.[1,2], North, R. L.[3], Livingstone, D. M.[1], and Kipfer, R.[1,2]

1. Eawag, Swiss Federal Institute of Aquatic Science and Technology, Department of Water Resources and Drinking Water, Überlandstrasse 133, CH-8600 Dübendorf, Switzerland.
2. ETH Zurich, Department of Environmental Systems Science, Institute of Biogeochemistry and Pollution Dynamics, Universitätsstrasse 16, CH-8092 Zürich, Switzerland
3. University of Saskatchewan, Department of Biology & Global Institute for Water Security, 112 Science Place, Saskatoon SK, S7N 5E2

In preparation for submission

Abstract The Lower Lake of Zurich provides an ideal system for studying the impact of climate change due to its sensitivity to climate variability, history of eutrophication and subsequent nutrient controls, and the quality and length of its data set. A long time-series of measured temperature, oxygen and phosphorus profiles made it possible to separate out the potentially confounding effects of climatic forcing and oligotrophication on the occurrence and extent of hypoxia. A change in thermal stability associated with an abrupt increase in regional air temperature (that was ultimately related to a change in the behavior of the Arctic Oscillation) resulted in a general expansion of the hypoxic zone in the fall, the period of minimum deep-water oxygen concentration. Dissolved phosphorus concentrations in the bottom water were strongly correlated with the extent of the hypoxic zone, suggestive of internal phosphorus loading. Despite 25 years of declining external phosphorus loading, this unaccounted for source of phosphorus may provide an alternative explanation

Acknowledgements We would like to thank all who contributed to the collection of the lake data used in this study, which were kindly provided by the City of Zurich Water Supply, Switzerland, by Amt für Abfall, Wasser, Energie und Luft, Canton of Zürich, Switzerland and by Anne Dietzel. We also thank the entire environmental isotopes group at Eawag and the participants in the annual HYPOX meetings for discussions that improved the manuscript greatly. This research forms part of project "HYPOX", funded under the European Commission's Seventh Framework Programme (contract no. 226213).

for recent increases in the toxic cyanobacterium *Planktothrix rubescens*. These climate-induced ecosystem scale changes may result in declines in water quality and coldwater fish habitats, and provide further evidence of the vulnerability of lakes to predicted increases in global air temperatures.

5.1 Introduction

Hypoxia occurs when dissolved oxygen (O_2) concentrations drop below the threshold at which life can no longer be sustained (Diaz and Rosenberg, 2008). This threshold is conventionally assumed to be 2 mg O_2 L^{-1}, although its value differs greatly among organisms (Vaquer-Sunyer and Duarte, 2008). Hypoxia is an important indicator of ecosystem health: as the extent, duration, and frequency of occurrence of hypoxia increases, ecosystem health declines. The occurrence of a drastic increase in hypoxia in aquatic ecosystems over the past few decades has been attributed to the combined effects of eutrophication and climate change (Diaz, 2001; Diaz and Rosenberg, 2008; Vaquer-Sunyer and Duarte, 2008). Lakes are particularly susceptible to variations in climatic forcing (Adrian et al., 2009; Schindler, 2009; Shimoda et al., 2011). For numerous lakes across the globe, evidence is accumulating that their thermal regimes are undergoing fundamental changes as a result of climate warming, involving an increase in thermal stability and the partial suppression of mixing (e.g., Livingstone, 2003, 2008; Verburg and Hecky, 2009; Schneider and Hook, 2010; Stainsby et al., 2011). As a result of these changes, lakes are likely to experience an increase in the frequency of occurrence, duration, and extent of bottom-water hypoxia (Stefan and Fang, 1994a; Rempfer et al., 2010; Foley et al., 2012).

The (Lower) Lake of Zurich, located on the Swiss Plateau, has been the focus of several previous studies of the impact of increasing air temperature on lake mixing patterns and O_2 depletion (Livingstone, 1997; Jankowski et al., 2006; Rempfer et al., 2009, 2010). This study continues this work, focusing on the long-term relationship between climatic forcing, mixing, and bottom-water hypoxia, and considers implications for nutrient dynamics. Particular emphasis is placed on the effect of the late 1980s climate regime shift (CRS) that resulted from a change in the behaviour of the Arctic Oscillation (AO) and the North Atlantic Oscillation (NAO) (Yasunaka and Hanawa, 2002; Alheit et al., 2005; Rodionov and Overland, 2005), which has been linked to sudden regime shifts in the ecology of both oceans and lakes (e.g., Anneville et al., 2004; Alheit et al., 2005; Anneville et al., 2005).

5.2 Methods

5.2.1 Study lake

The Lake of Zurich is a perialpine lake with a surface area of 65 km^2, a volume of 3.3 km^3 and a maximum depth of 136 m (Livingstone, 2003). The lake usually undergoes complete mixing once per year (i.e., it is holomictic and monomictic), but it can mix twice per year (i.e., it is facultatively dimictic) (Peeters et al., 2002; Livingstone, 2003). During exceptionally cold winters when the lake freezes, it exhibits dimictic behaviour as it undergoes mixing and homothermy before and after the onset of inverse stratification in winter. However, the Lake of Zurich has been completely ice-covered only once (1962-63) in the period 1944-2010 (Peeters et al., 2002; Rempfer et al., 2010). During milder winters with no ice cover, the lake is monomictic, with homothermy and complete mixing occurring only in late winter and early spring. Finally, in exceptionally mild

winters the lake can remain positively stratified throughout the entire winter, severely suppressing mixing (Livingstone, 1993, 1997; Rempfer et al., 2010).

Several unique characteristics of the lake and its history make it an ideal study site for investigating the impact of changing air temperatures on lake processes (Peeters et al., 2002). It has an extensive data set (>70 yr) of lake profiles measured at approximately monthly intervals (year-round) at consistent depths. Approximately 84% of the inflow into the lake is over a sill 3 m deep that connects it to the Upper Lake of Zurich (Omlin et al., 2001), thus limiting the impact of hydrology on lake processes (Livingstone, 2003). The lake is convectively mixed (Peeters et al., 2002), and even severe winter storms have only a limited effect on lake mixing during mild winters (Rempfer et al., 2010).

5.2.2 Field measurements

The Lake of Zurich data set dates back to 1936, but for this study was restricted to the period 1972 - 2010 (unless otherwise noted). During this period, water column profiles of temperature (T) and of the concentrations of dissolved O_2, total phosphorus (TP), and soluble reactive phosphorus (SRP) were measured at consistent depths (0.3, 1, 2.5, 5, 7.5, 10, 12.5, 15, 20, 30, 40, 60, 80, 90, 100, 110, 120, 130, and 135 m) at the deepest point of the lake (136 m) by the same agency, the City of Zurich Water Supply (WVZ) (Zimmermann et al., 1991), thus ensuring a high quality data set. Temperatures were measured by thermistor and regularly calibrated with a mercury thermometer (Livingstone, 2003). O_2 concentrations were measured using the Winkler method until 2001, after which O_2 electrodes were used that were calibrated with the Winkler method (Jankowski et al., 2006). TP and SRP concentrations were consistently measured with VIS Photometry, German standard methods D11, SLMB 27A/4.7 (Gammeter and Forster, 1997). The WVZ laboratory has been ISO accredited (Standard ISO 17025) since late 1999, after which measurement accuracy was 0.03-0.1°C for temperature, 0.1-0.3 mg L^{-1} for O_2, 0.79-1.8 μg L^{-1} for TP and SRP. Prior to 2000, measurement accuracies were estimated at ±10% for chemical variables and ±5% for physical variables. Phytoplankton data (described in detail by Anneville et al. 2005, Pomati et al. 2012, and Posch et al. 2012) were available for the period 1976-2008. Further details on the Lake of Zurich data set are available from Zimmermann et al. (1991), Livingstone (2003), and Jankowski et al. (2006).

5.2.3 Data analysis

The measured water column profiles were interpolated spatially at intervals of 1 m using linear interpolation, as described in Chapter 3. The resulting profiles were then interpolated temporally at daily (24-hr) intervals. A comparison of cubic spline and linear interpolation for filling gaps in the time domain revealed that cubic spline interpolation was the more accurate for temperature and O_2 concentration, but linear interpolation was the more accurate for phytoplankton biomass, TP concentration and SRP concentration. In each case the more accurate interpolation method was employed to yield consistent daily sampling intervals. The daily profiles were then aggregated to yield monthly mean profiles. Based on the spatially and temporally uniform data sets resulting from the two-stage interpolation process, the following were calculated: Nürnberg's hypoxic factor (HF) for an oxycline at 2 mg O_2 L^{-1} (Nürnberg, 2002, 2004); the concentrations of O_2, TP and SRP for various layers of the lake; and the Schmidt stability S (Schmidt, 1928; Idso, 1973), which is a measure of the overall thermal stability of the lake. HF, which was chosen to characterize the spatial and temporal extent of hypoxia during a given calendar year, was defined for our purposes

as follows:

$$\mathrm{HF} = \frac{1}{A_o} \sum_{i=1}^{n} t_i A_i \tag{5.1}$$

where n is the number of days in the year; i is the day of the year from 1 to n; A_0 is the lake surface area; A_i is the areal extent of the hypoxic zone on day i; and t_i is the time interval between consecutive vales of A_i. In this specific case, t_i was set to 1 day. The lake was considered to be stratified if the temperature gradient attained or exceeded 1°C m^{-1}. Similarly, the boundaries between the epilimnion, metalimnion and hypolimnion are typically defined by a temperature gradient of 1 °C m^{-1}. Following the protocols of previous work on the Lake of Zurich (e.g., Livingstone, 2003), these regions were instead defined by fixed depths. Mean deep-water O_2 and SRP concentrations were defined as volume-weighted means from 100 m to 135 m. Mean epi/metalimnetic SRP concentrations were defined as volume-weighted means from 0 m to 20 m. The lake was assumed to be stratified when S > 200 J m^{-2}, and homothermic when S < 200 J m^{-2} (Livingstone, 2003). In the Lake of Zurich, the summer stratification period typically extends from April to September. The annual minimum hypolimnetic O_2 concentration occurs at the end of the stratification period, generally sometime between September and November. Because the annual minimum varied from year to year, in some years mixing between the surface and the deep water occurred in October or November. Therefore, when estimating the annual maximum extent of the hypoxic zone, concentrations of O_2 from September were always used.

Monthly mean time-series of the measured and derived variables were either grouped by month to compare changes in seasonality, or were aggregated to yield time-series of annual means. Monthly mean loading rates of TP (t yr^{-1}) entering the Lake of Zurich over the sill connecting it with the Upper Lake of Zurich cover the years 1976 to 2005. The loading was determined from measured TP concentrations at the sill and the measured flow of the Linth Canal, which is the major inflow to the Upper Lake of Zurich. This loading was multiplied by a factor of 1.6 to account for other smaller inflows into the Upper Lake of Zurich (Gammeter and Forster, 2002). Daily mean air temperature data from a nearby meteorological station (Zurich-Fluntern) run by the Swiss Federal Office of Meteorology and Climatology were aggregated to yield monthly and annual means.

The sequential t-test STARS (Rodionov and Overland, 2005) was used to detect abrupt regime shifts in the annual mean time-series of measured and derived variables. The magnitude of the shifts detected by STARS was determined by the threshold significance level ($p = 0.15$) and the cut-off length (L = 10 yr) (Rodionov and Overland, 2005). The latter determines the detection scale of interest (decadal). When STARS detected a shift, the mean of each regime was calculated and tested with a second t-test. For this second test, any shift that satisfied a significance criterion of $p < 0.05$ was accepted.

The time-series were tested for monotonic trends using the Mann-Kendall test as implemented in the 'Kendall' R-package (McLeod, 2011). If a time-series contained a significant shift (as detected by STARS), the Mann-Kendall test was applied to each regime separately. The Pearson product-moment correlation coefficient test built into R was used to assess correlations computed between time-series (R Development Core Team, 2011).

Wavelet analysis was used to capture changes in seasonal and interannual variability in deep-water temperatures and O_2 concentrations. Wavelet analysis can be used to analyse non-stationary time-series and captures both the frequency distribution of the signal and how this distribution varies with time (Torrence and Compo, 1998; Benincà et al., 2009). Before conducting the wavelet analysis, the time-series were filtered using singular spectrum analysis, SSA (Ghil et al., 2002). Filtering removed any trend, and also frequencies that were too low to be captured by the wavelet analysis. The filtered time-series were standardized by their standard deviation and then decomposed

using the Morlet wavelet. The wavelet analysis was accomplished using the Matlab wavelet software provided by C. Torrence and G. Compo (http://atoc.colorado.edu/research/wavelets/). The SSA analysis was conducted using the RSSA package for R (Korobeynikov, 2010).

5.3 Results

5.3.1 Oxygen dynamics

Based on annual HF values for the Lake of Zurich (Figure 5.1a), the 39-year study period can be roughly divided into three segments. In Segment I (1972 - 1987), with the exception of the first two years, HF was never larger than 30 days yr^{-1}. Segment II (1988 - 2000) represents a transitional phase during which HF is extremely variable, ranging between approximately 8 days yr^{-1} and 64 days yr^{-1}. Finally, in Segment III (2001 - 2010), with the exception of only one year (2003), HF consistently exceeded 30 days yr^{-1}. The transition from Segment II to Segment III corresponded to a statistically significant abrupt (upward) shift of 21 days yr^{-1} ($p < 0.001$) as detected by the STARS test (Table 5.1). No statistically significant monotonic trend was found before the shift (Segment I plus Segment II, $p > 0.05$) or after (Segment III, $p > 0.05$), suggesting that the majority of the increase in HF occurred as a result of an abrupt shift at the end of the 1990s (Table 5.1).

The annual duration and maximum areal extent of hypoxia both showed the same 3-segment pattern and shift as the HF values, confirming that HF could be used to represent changes in the duration and spatial extent of hypoxia (data not shown).

Table 5.1: Statistical significance of abrupt shifts and trends in annual hypoxic factor (HF) for a threshold of $[O_2] \leq 2$ mg L^{-1}, annual mean thermal stability (S), total phosphorus concentration (TP), external TP loading (ETP), and deep-water soluble reactive phosphorus concentration (SRP). Shifts were detected by the STARS test (Rodionov and Overland, 2005), and trends were detected by the Mann-Kendall test (MK). Indicated in the table are the temporal location of an abrupt shift detected by STARS and for the MK test the direction of the trend - positive (+) or negative (−). The tests were applied to one or more of the following: the full time-series (I, II, III), Segment I (1972-1987), Segment I & II (1972-2000), Segment II & III (1988-2010), and Segment III (2001-2010). Statistical significance: $p > 0.05$ (ns); $p < 0.05$ (*); $p < 0.01$ (**); $p < 0.001$ (***); test not applied (NA). ETP time-series limited to 1976-2005.

	STARS			MK		
	I, II, III	I, II, III	I	I, II	II, III	III
HF	2000/2001 (***)	ns	NA	ns	NA	ns
S	1987/88 (**)	NA	ns	NA	ns	NA
TP	NA	− (***)	− (***)	NA	− (***)	− (*)
ETP	NA	− (***)	ns	NA	ns	ns
SRP	NA	− (***)	− (***)	NA	ns	ns

The time-series of September deep-water O_2 concentration (Figure 5.1b) can also be divided into three distinct segments: mean O_2 concentrations below 100 m are generally above 4.4 mg L^{-1} in Segment I, variable in the transitional Segment II, and at or below 4.5 mg L^{-1} in Segment III (Figure 5.1b). The mean deep-water O_2 concentration in September mirrors that in the preceding April, when the deep-water O_2 concentration is generally at its annual maximum (Figure 5.1b; R^2=0.62, $p < 0.001$). This suggests that deep-water O_2 concentrations in September are dependent to a large extent on the mixing conditions prevailing during the previous winter and spring, which in the deep Swiss perialpine lakes largely determine the annual maximum hypolimnetic O_2 concentration (Livingstone and Imboden, 1996).

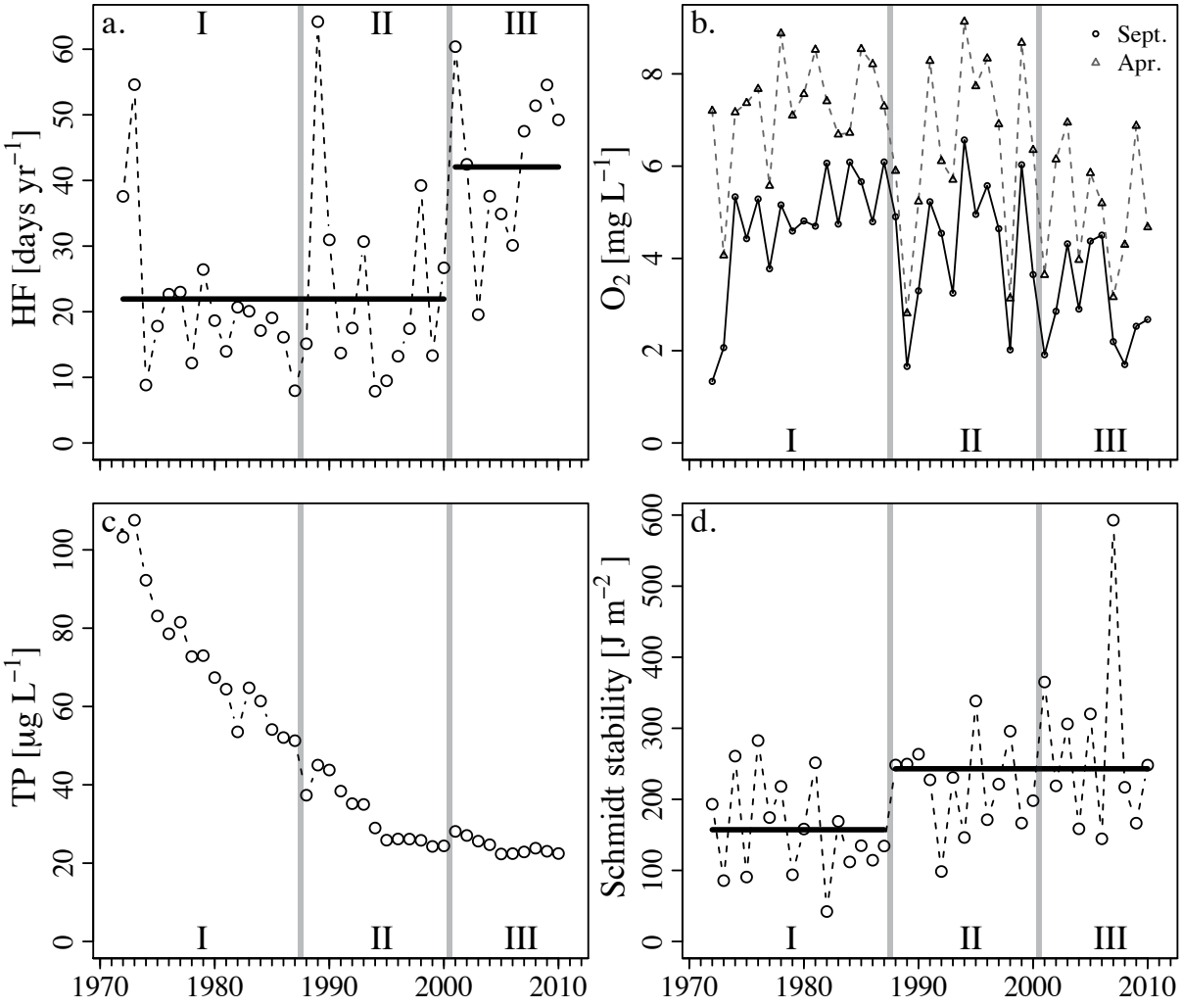

Figure 5.1: Time-series of a) annual hypoxic factor (HF) for a threshold of $[O_2] \leq 2$ mg L^{-1}, b) volume-weighted mean deep-water (≥ 100 m) O_2 concentrations in September (Sept) and April (Apr), c) volume-weighted mean annual TP concentration in the entire lake, and d) mean annual Schmidt stability. The solid lines in a) and d) show the mean values on either side of the abrupt shift detected by the STARS test (Rodionov and Overland, 2005). The grey vertical lines separate Segments I, II and III.

5.3.2 Eutrophication

An increase in the duration and extent of hypoxia can often be attributed to an increase in lake eutrophication (Diaz, 2001). However, the study period (1972-2010) corresponds to a period of decreasing TP concentration ($p < 0.001$; Figure 5.1c) and stable phytoplankton biomass (Posch et al., 2012) in the Lake of Zurich. This combination suggests that the observed increase in hypoxia from Segment II to Segment III is not the result of eutrophication. The decrease in lake water column TP concentrations resulted from improved wastewater treatment and the banning of phosphates in detergents, and is reflected in decreasing external TP loading from the Upper Lake of Zurich ($p < 0.001$; Figure 5.2a). In the mid-1990s the rate of decline in lake TP concentration slowed (Figure 5.1c), likely due to a corresponding steadying of external TP loading (Figure 5.2a). Nonetheless, the long-term downward trend in both external loading and lake TP concentration continued until the end of their respective time-series. Lake TP concentrations showed a noticeable jump from 2000 to 2001 (approximately 12×10^3 t), corresponding to the transition from Segment II to Segment III (Figure 5.1c). This increase resulted entirely from an increase in the hypolimnetic SRP concentration, 40 % of which was due to an increase in the deep-water SRP concentration (Figure 5.2b). The increase was not due to an increase in external loading, as this declined slightly (1.7×10^{-3} t) from 2000 to 2001 (Figure 5.2a). The increase in deep-water SRP concentration in Segment III is discussed in further detail in Section 5.3.4.

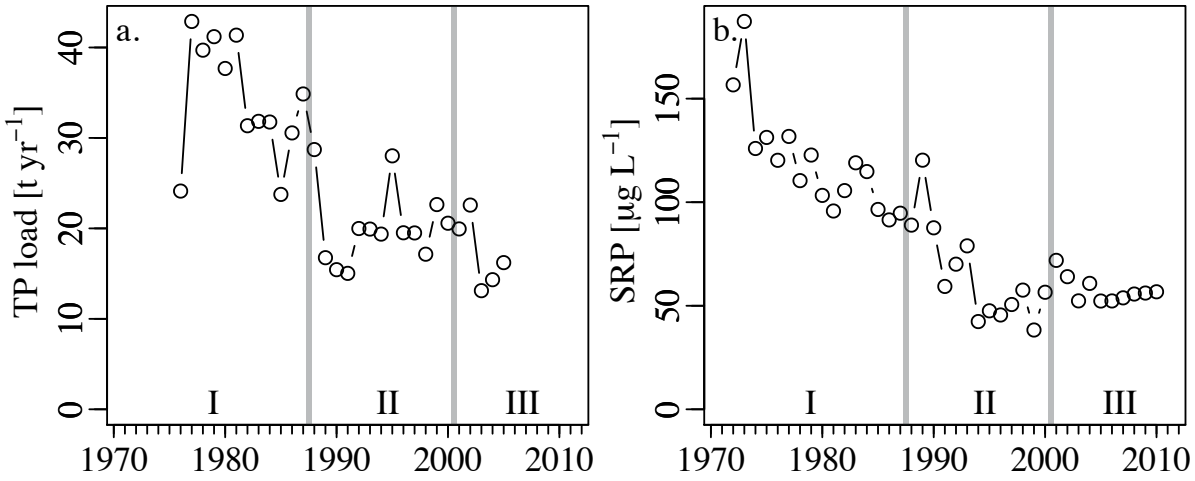

Figure 5.2: Time-series of a) estimated annual TP load entering the Lake of Zurich from the Upper Lake of Zurich (1976-2005) and b) volume-weighted mean annual SRP concentrations in the deep water (≥ 100 m) (1972-2010).

5.3.3 External forcing and mixing dynamics

The transition from a low to a variable HF (Segment I to Segment II) coincided with an abrupt shift in the mean air temperature on the Swiss plateau (see Chapter 4). This abrupt shift was linked to the now well-documented large-scale late 1980s CRS. In the Lake of Zurich, the increase in air temperature was reflected in an abrupt increase in the mean water temperature of the epi/metalimnion and, to a smaller degree, in the hypolimnion (see Chapter 4). As a result of the difference in warming between the epi/metalimnion and the hypolimnion, the Schmidt stability of the lake (S) in winter/spring (December to April) increased abruptly from Segment I to Segment II (Figure 5.1d; $\Delta S = 86$ J m^{-2}, $p < 0.01$).

Wavelet analysis was used to assess temporal changes in dominant mixing cycles. In Segment I, the power spectrum of deep-water temperature shows a peak centered on a period (T_W) of approximately 2 to 3 yr (Figure 5.3a). In Segments II and III, additional peaks appear, with periods ranging up to approximately 8 yr (Figure 5.3a). Throughout the time-series there is little power at a period of 1 yr, indicating that the annual cycle does not appear very strongly in the deep-water temperature.

The power spectrum of deep-water O_2 concentration shows significant peaks at a period of 1 yr throughout most of the time-series (Figure 5.3b). However, in Segments II and III the annual component is less consistent, and the power of the multiannual cycles (approximately $2 < T_W < 6$ yr) is greater than in Segment I (Figure 5.3b). The decrease in power at lower periods in the time-series of O_2 concentration and the increase in power at higher periods in both the temperature and O_2 time-series suggest that annual renewal of the deep water occurred less consistently in Segments II and III than in Segment I. Instead, multiannual cycles began to dominate lake mixing patterns after the late 1980s CRS.

To confirm the results of the frequency analysis, it was assumed that if the deep-water temperature (O_2 concentration) increased (decreased) over two or more consecutive years, then the lake did not completely mix in the intervening winter. In Segment I, incomplete mixing occurred once based on deep-water temperature (1973-1975), and once based on deep-water O_2 concentration (1984-1986). In contrast, in Segments II and III incomplete mixing occurred five times based on deep-water temperature (1987-1990, 1991-1993, 1996-1998, 1999-2002, 2006-2008) and five times based on deep-water O_2 concentration (1987-1989, 1991-1993, 1996-1998, 1999-2001, 2006-2008). These results confirm that the frequency of occurrence and/or intensity of annual renewal of the deep-water decreased after the late 1980s CRS.

The transition from a variable HF to a consistently high HF (Segment II to Segment III) does not correspond with an abrupt change in any of the climatic or physical lake variables considered in this study. However, Livingstone (2003) found that in the Lake of Zurich the duration of the stratified period has been steadily increasing over the past few decades; i.e., the date of the onset of stratification (in spring) occurred earlier and the date of the onset of homothermy (in fall) occurred later. This trend continued into Segment III ($p < 0.05$), and on four separate occasions between 2000 and 2010, the date of the onset of homothermy was after December 31st. Between 1944 and 1999 this occurred only once, in 1987. Therefore, it appears that near the end of Segment II a threshold was crossed, and the combined effect of reduced winter mixing and a longer stratification period resulted in the abrupt increase in HF from Segment II to Segment III (Figure 5.1a).

5.3.4 Phosphorus dynamics

Annual mean deep-water SRP concentrations increased sharply at the end of Segment II, and, after a short decrease, continued to increase with a significant trend from 2005 onwards ($p < 0.01$; Figure 5.2b). The increase corresponded with the period of increased HF (Figure 5.1a), and occurred despite almost 20 years of declining lake TP concentrations (Figure 5.1c). Three possible causes of the abrupt increase in deep-water SRP were investigated: i) increased external TP loading, ii) reduced deep-water renewal, leading to an accumulation of phosphorus (P) in the deep water, and iii) increased internal P loading (re-dissolution from the sediments). Of these three potential causes, the latter two are tightly related and difficult to distinguish.

i) External loading – While TP concentrations in the Lake of Zurich have declined since the 1970s, it is possible that a change in weather patterns (e.g., increased rainfall) in Segment III could have led to an increase in external TP loading. However, as discussed earlier, external TP loading from the Upper Lake of Zurich remained relatively stable throughout Segments II and III

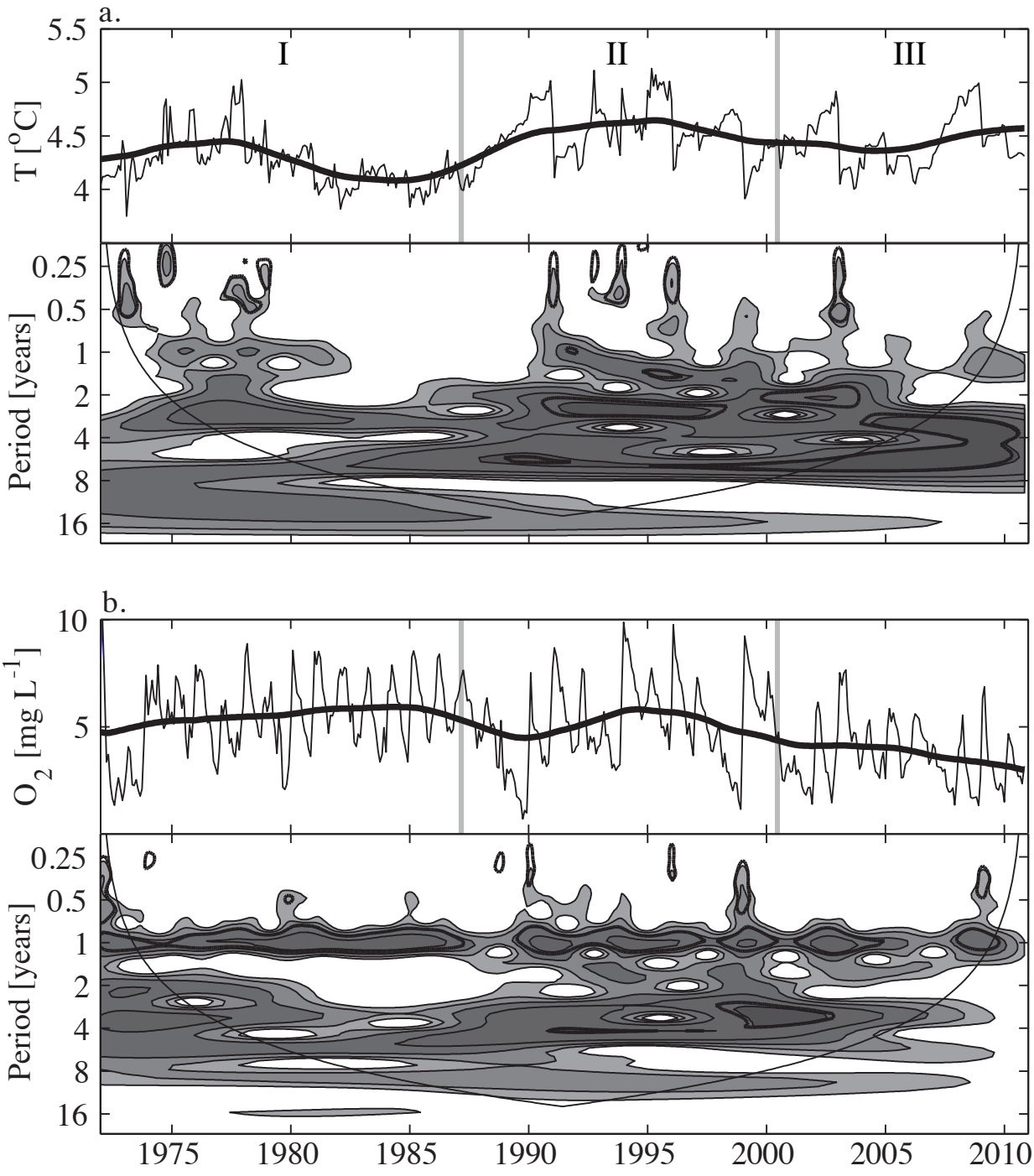

Figure 5.3: Time-series (upper panels) and local wavelet power spectrum (lower panels). a) Volume-weighted deep-water temperature (≥ 100 m). b) Volume-weighted deep-water O_2 concentration (≥ 100 m). The time-series show the original monthly mean time-series (thin line) and the component of the time-series that was filtered out prior to wavelet analysis using SSA (thick line). The contour plot shows the wavelet power spectrum ($|\text{Power}|^2$) of the standardized filtered time-series. The units of the spectrum are the same as the variance – a. $(°C)^2$; b. $(\text{mg L}^{-1})^2$ – and the filled contours represent variances of 1, 2, 4, 8, and 16. The x-axis is the wavelet location in time and the y-axis (note that the scale is logarithmic) is the wavelet period. The thick black contour is the 5% confidence level against red noise. In both lower panels the area below the thin black line is the "cone of influence" where edge effects limit the ability to interpret the results.

(Figure 5.2a), and there was no significant correlation between annual values of external TP loading and annual concentrations of deep-water SRP ($p > 0.1$). Additionally, there was no observed increase from Segment II to Segment III in P input through wastewater discharge (AWEL, 2010).

ii) Reduced deep-water renewal – A reduction in either the frequency of occurrence or the intensity of deep, penetrative mixing events (deep-water renewal), could hinder the transport of SRP from the hypolimnion to the epilimnion. SRP released from decaying particulate matter would then be trapped in the hypolimnion and would begin to accumulate over consecutive years. However, throughout Segment III, monthly mean SRP concentrations showed a strong annual cycle, and did not increase over consecutive years (Figure 5.4). For all three segments, a month-by-month comparison showed an increase in the mean deep-water SRP concentration from April to November and a decrease from November to April (Figure 5.5b). From November to April stratification was weak and epi/metalimnetic SRP concentrations were high (Figure 5.5a), suggesting that in all three segments, SRP was consistently mixed from the deep-water into the epi/metalimnion once per year. Therefore, although mixing patterns changed after the late 1980s CRS (Figure 5.3), during Segment III mixing was still strong enough to prevent the accumulation of SRP in the deep water.

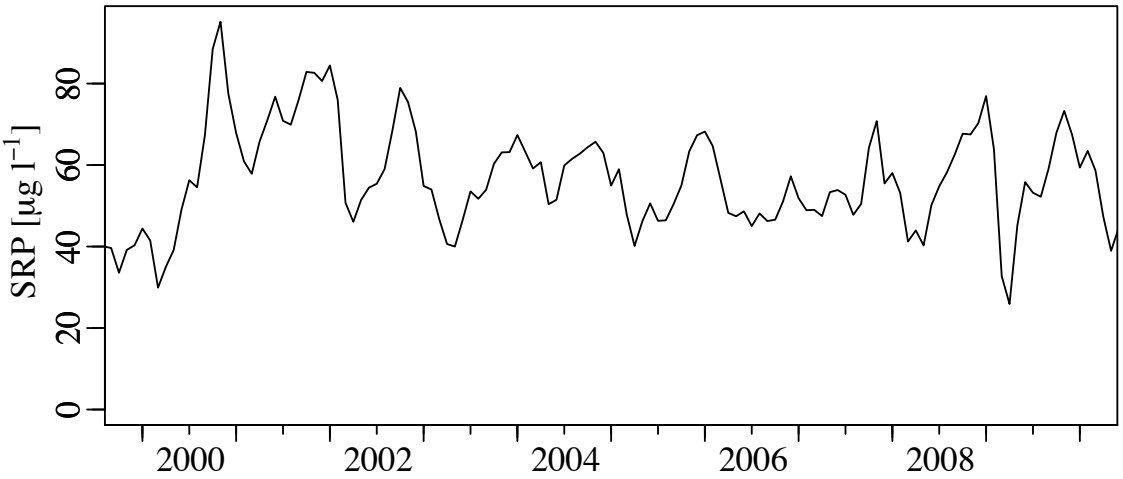

Figure 5.4: Time-series of volume-weighted monthly mean SRP concentration in the deep-water. The long and short ticks on the x-axis indicate January and July values, respectively.

iii) Internal P loading – Annual HF values and September deep-water SRP concentrations were separated into Segments I, II, and III, and each segment was linearly detrended. The three detrended segments of the time-series were re-combined prior to comparing the two variables. The resulting time-series of linearly detrended annual HF values and linearly detrended September deep-water SRP concentrations share the 3-segment pattern described earlier – consistently low values (Segment I), high variability (Segment II), and consistently high values (Segment III) – and are highly correlated (Figure 5.6a; R^2=0.54, $p < 0.001$). Significant correlations were also found between (detrended) September deep-water SRP concentrations and other indicators of hypoxia, such as the (detrended) areal extent of hypoxia in September (Figure 5.6b; R^2=0.64, $p < 0.001$) and the (detrended) annual duration of hypoxia at a depth of 130 m (Figure 5.6c; R^2=0.51, $p < 0.001$). The strong correlations suggest that the increase in the deep-water SRP apparent in Segment III has at least in part resulted from an increased dissolution of P from the sediment; i.e., an increase in internal P loading related to the increasing extent and duration of hypoxia.

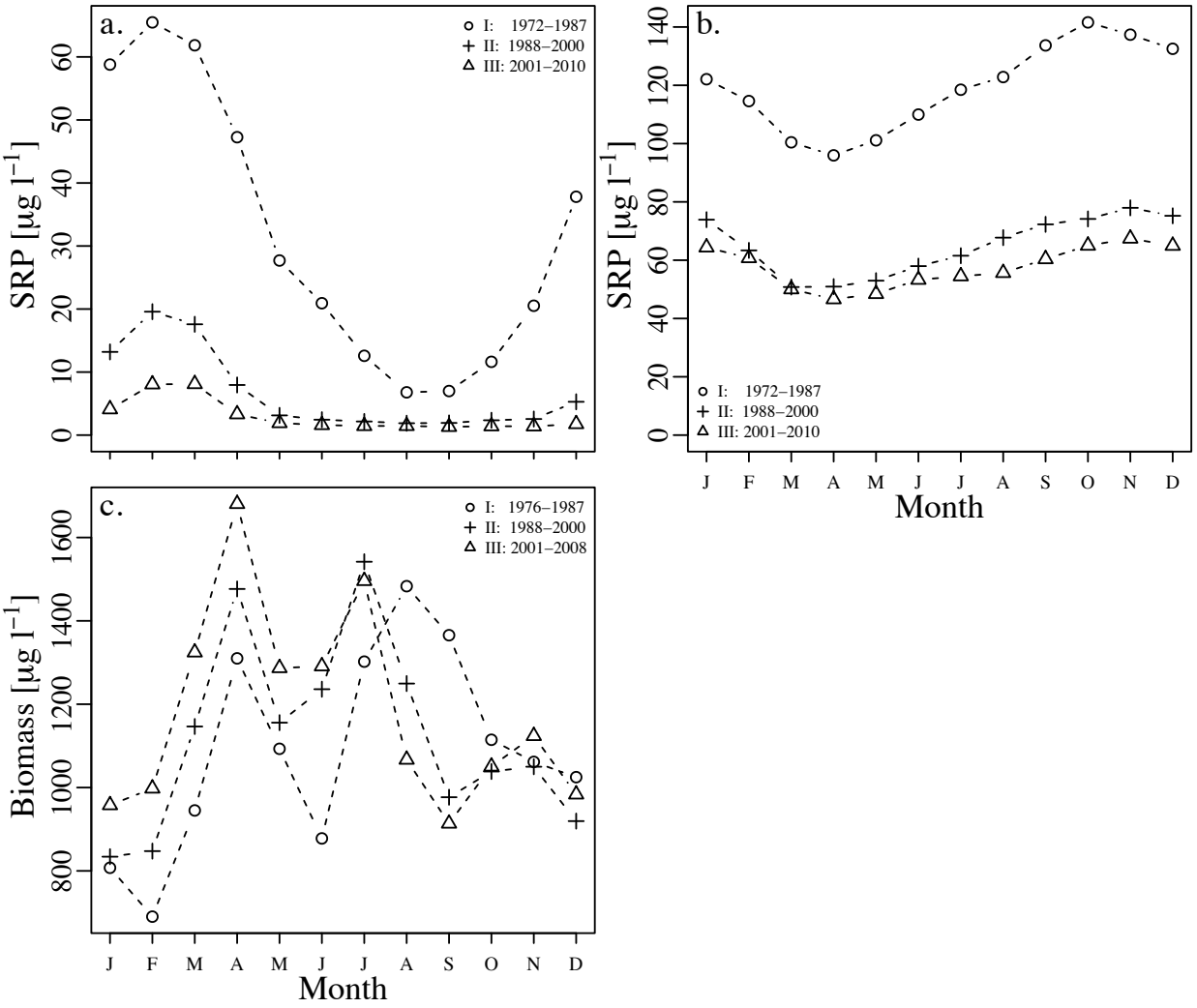

Figure 5.5: Seasonality comparison between Segment I, II, and III. a) Volume-weighted SRP concentration in the epi/metalimnion. b) Volume-weighted SRP concentration in the deep-water. c) Phytoplankton biomass of the epi/ metalimnion.

5.3.5 Phytoplankton biomass

The seasonal pattern of total phytoplankton biomass in the epi/metalimnion (Figure 5.5c) changed from bimodal in Segment I (typical for temperate freshwater lakes) – with a peak in April and the largest peak in August – to trimodal in Segments II and III – with the largest peak in April, a second peak in July, and a new peak in November. Despite the change in seasonality, the mean annual total phytoplankton biomass in the entire lake remained relatively constant between 1976 and 2010 (Posch et al., 2012).

In all three segments, phytoplankton biomass in the epi/metalimnion increased from February to April (Figure 5.5c), which corresponded to a period of drawdown in epi/metalimnetic SRP concentrations, indicating uptake by phytoplankton (Figure 5.5a). The November peak in phytoplankton biomass in Segments II and III (Figure 5.5c) can be attributed to an increase in the total biomass of *P. rubescens*. The *P. rubescens* biomass was much higher in Segments II and III than in Segment I, and reached an annual maximum in November (Posch et al., 2012). In late fall and early winter, deep-water SRP concentrations declined (Figure 5.5b) as decreasing water column stabilities resulted in the mixing of SRP into the epi/metalimnion (Figure 5.5a). During this period,

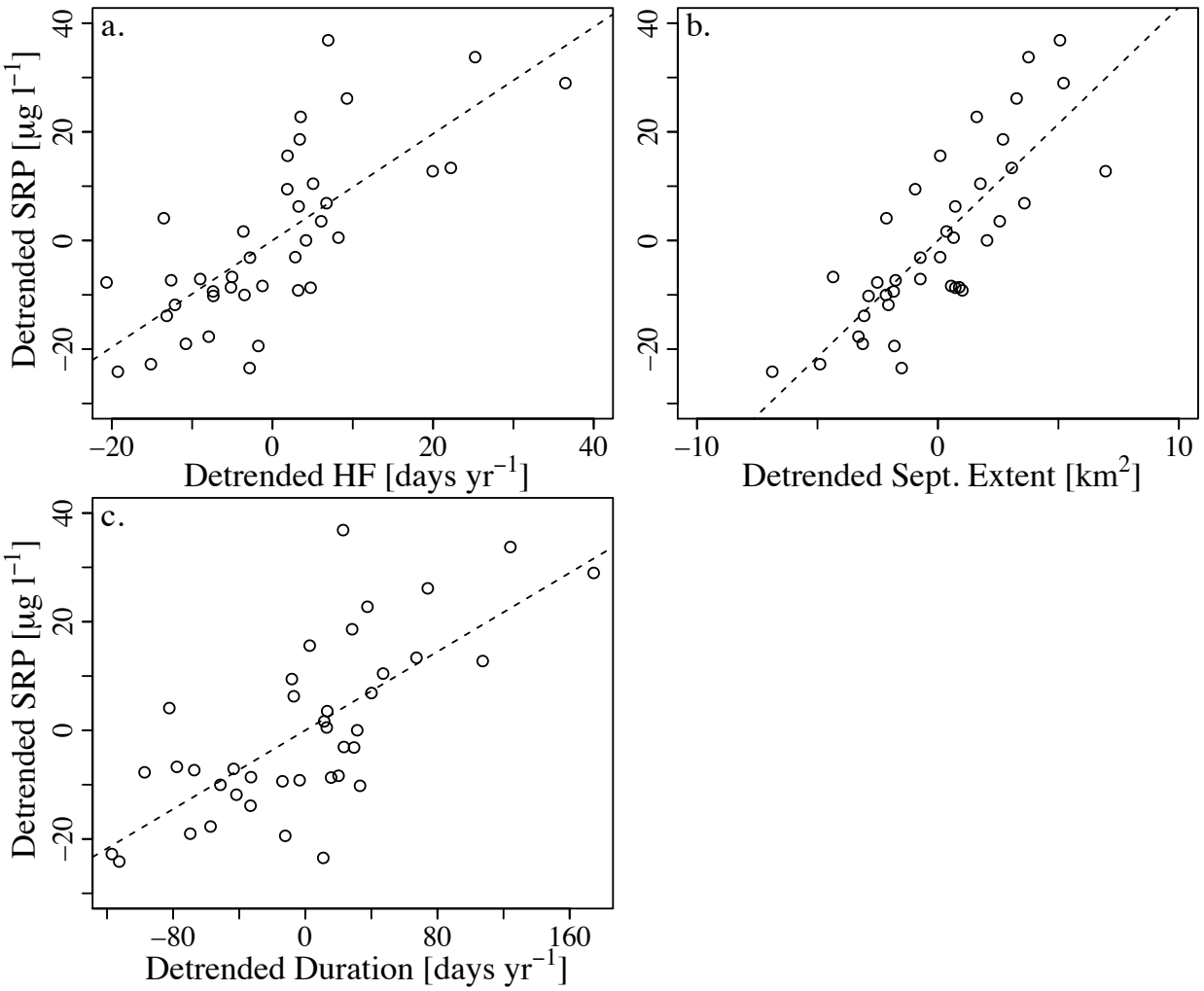

Figure 5.6: Plot of linearly detrended September deep-water (≥ 100 m) SRP concentrations against linearly detrended values of a) HF, b) the areal extent of hypoxia in September, and c) the annual duration of hypoxia at a depth of 130 m. The dashed line is the fit of the linear regression.

P. rubescens biomass in the epi/metalimnion was at its highest (Posch et al., 2012), suggesting that the SRP mixing into the epi/metalimnion was contributing to the increase in *P. rubescens*. Note that summer and fall epi/metalimnetic SRP concentrations during Segments II and III cannot be accurately interpreted as they are near the detection limit (1.0 μg L^{-1}).

5.4 Discussion

An abrupt rise in air temperature over the Swiss Plateau at the end of the 1980s likely led to a similarly abrupt increase in winter/spring water temperature and thermal stability in the Lake of Zurich (see Chapter 4). The increased stability has suppressed annual mixing, limiting replenishment of O_2 in the hypolimnion, and resulting in an increase in the extent and duration of seasonal hypoxia. The period of consistent seasonal hypoxia (Segment III) corresponded to an increase in deep-water SRP concentrations. The increase in SRP is most likely the result of internal P loading, and may have influenced phytoplankton seasonal patterns and contributed to recent increases in the potentially toxic cyanobacterium *P. rubescens*.

The observed changes in winter thermal stability, mixing patterns, and deep-water O_2 concentrations had been predicted in previous studies of the Lake of Zurich, through the use of models (Peeters et al., 2002) or extrapolations from the analysis of isolated extreme events, such as particularly mild winters or hot summers (Livingstone, 1997; Jankowski et al., 2006; Rempfer et al., 2009, 2010; Gallina et al., 2011). The consistency between the predictions of these studies and the observations presented here provide a good indicator of the validity of models and case studies when predicting the impacts of climate change on lakes. This is particularly important for infrequently monitored lakes, for which the type of time-series analysis used in this study is not possible.

What is driving the increase in hypoxia?

The observed increase in the duration and extent of hypoxia corresponded to a reduction in the frequency and/or intensity of annual winter/spring deep-water renewal. In a monomictic lake, deep-water renewal typically occurs once a year, sometime in winter or early spring. Deep-water O_2 is depleted during summer stratification and is replenished by deep mixing events. If the annual renewal of the deep water does not occur, or is incomplete (weak), deep-water O_2 concentrations will decrease over consecutive years (Livingstone, 1997). Wavelet analysis showed that after the late 1980s CRS, the power spectrum of deep-water O_2 concentration and temperature shifted to include more power at low frequencies, which represent multiannual cycles of deep-water renewal. This change in the power spectrum provides strong evidence that the increase in winter thermal stability is resulting in a reduction in the frequency and/or intensity of occurrence of deep, penetrative winter mixing events, leading to an increase in the duration and extent of hypoxia in the Lake of Zurich.

Throughout all three segments, the duration of the stratified period gradually increased in the Lake of Zurich. It appears that a threshold was crossed near the end of Segment II, and the combined effect of a reduction in deep-water renewal and an increase in the duration of stratification severely limited O_2 replenishment of the deep water. In Segments I and II, strong mixing events – identified by sharp drops in deep-water temperature, e.g. 1995/1996 (Figure 5.3a, upper panel) – generally increased the deep-water O_2 concentration to at least 7.5 mg O_2 L^{-1} (Figure 5.3b, upper panel). Similar events in Segment III (e.g., 2008/2009), rarely resulted in a deep-water O_2 concentration greater than 6 mg O_2 L^{-1} (Figure 5.3b, upper panel). With less O_2 in the deep water at the start of the stratification period, combined with a longer stratification period, hypoxic conditions occurred more consistently, lasted longer, and extended across a larger area during Segment III than during Segments I and II.

What are the impacts of increasing thermal stability and hypoxia on nutrient dynamics?

Three potential causes of an observed increase in deep-water SRP concentration from Segment II to Segment III were investigated; namely, an increase in external TP loading, a reduction in the frequency and/or intensity of deep-water renewal, and an increase in internal P loading. We rejected the hypothesis that the increased SRP in the deep water during Segment III was due to external TP loading, as external TP loading from the Upper Lake of Zurich decreased from Segment I to Segment II, and from Segment II to Segment III. Additionally, there was no correlation of external TP loading with deep-water SRP concentration. Changes in the frequency or intensity of deep-water renewal could also be rejected, as the time-series of monthly mean deep-water SRP concentration did not show evidence of a gradual accumulation over multiple consecutive years. If SRP was accumulating in the deep-water, the time-series of deep-water SRP concentration would be expected to show a "sawtooth" pattern, similar to that described by Livingstone (1997) for deep-water temperature (i.e., a gradual increase during consecutive years of weak mixing, followed by a sharp drop after a strong mixing event). Furthermore, throughout all three segments, the seasonality plot of deep-water SRP concentration consistently showed a gradual increase dur-

ing the stratification period, and a decrease in fall and winter. The consistent seasonality and lack of accumulation of SRP in the deep-water suggests that in all three segments mixing was strong enough to prevent SRP from being trapped in the deep water.

Deep-water SRP concentration was strongly correlated with the extent and duration of hypoxia; i.e., an increase in the extent and duration of hypoxia coincides with an increase in the concentration of SRP in the deep-water. This suggests that the increase in deep-water SRP concentration is a result of an increase in the re-dissolution of P from the sediment, associated with the observed increase in extent and duration of hypoxia, combined with the seasonal pattern of P-release. Several of the indicators of internal P loading in stratified lakes, as outlined by Nürnberg (2009), were present in the Lake of Zurich. The profiles of concentrations of TP and SRP increased with depth, indicating a sediment source. Deep-water SRP concentration increased from April to October/November, corresponding to the stratification period, when hypoxic conditions develop and internal P loading is expected to occur. Although the Lake of Zurich does not experience severe anoxia, both the duration and spatial extent of seasonal hypoxia have increased. In Segments II and III, phytoplankton biomass showed a new peak in November, corresponding to the period of decreasing thermal stability and upwelling of SRP from the hypolimnion. The combination of indicators suggests that internal P loading is likely the dominant process controlling the observed increase in deep-water SRP concentration in Segment III. The internal P loading hypothesis could not, however, be confirmed with 100% certitude because low deep-water O_2 concentrations do not always result in an increase in the re-dissolution of P from the sediment (Hupfer and Lewandowski, 2008). Instead, it is likely that a variety of factors control the nutrient flux across the sediment-water interface, and a much more detailed assessment would be required to fully understand the effect of the observed change in deep-water O_2 concentrations on redox processes.

How have the changes in mixing, hypoxia, and internal P loading influenced the pelagic phytoplankton community?

The observed increase in temperature and thermal stability in the Lake of Zurich (see Chapter 4) has been previously linked to changes in phytoplankton community composition (Anneville et al., 2005), phytoplankton richness (Pomati et al., 2012), and the abundance of *P. rubescens* (Gallina et al., 2011; Posch et al., 2012). In this study, the late 1980s CRS was linked to a change in the seasonal pattern of phytoplankton biomass in the epi/metalimnion. After the CRS, the April phytoplankton peak increased, the summer phytoplankton peak occurred one month earlier (from August to July), and a new peak appeared in November. The new November phytoplankton peak in Segments II and III was temporally consistent with the annual peak in *P. rubescens* biomass and the period of upwelling of SRP from the deep water. This combination suggests that the November peak in phytoplankton biomass is due to an increase in *P. rubescens* relative to the other phytoplankton groups in the lake, which in turn resulted from an increase in bioavailable P (i.e., SRP mixing up from the hypolimnion). This is contrary to the results of Posch et al. (2012), who concluded that the increase in *P. rubescens* resulted from a long-term increase in NO_3^- concentration. However, the mean NO_3^- concentration in the lake declined from Segment II to Segment III, while the abundance of *P. rubescens* increased (Figure 1a,b of Posch et al. 2012). In addition, the molar dissolved inorganic nitrogen (DIN):dissolved P (DP) ratio remained well above the 16:1 Redfield ratio threshold (Redfield et al., 1963) throughout all three segments (Figure 1c of Posch et al. 2012). The consistently high DIN:DP ratio, combined with the seasonal drawdown in SRP concentrations, indicates that the pelagic phytoplankton community was deficient in P. Therefore, it appears that the increase in *P. rubescens* was not entirely due to the increase in NO_3^- concentrations, but was more strongly associated with the increase in deep-water SRP, the limiting nutrient. It does not lie within the scope of this work to determine whether one of the two nutrients is the leading cause of the increase in *P. rubescens*, particularly considering the current debate

over whether or not there is one "ultimate" limiting nutrient (e.g., Schindler et al., 2008; Scott and McCarthy, 2010). We can, however, advise caution and further research before implementing expensive measures to reduce nitrogen loading, as in the long term this may not result in any improvement to the water quality of the Lake of Zurich.

The lake is home to a commercial coldwater fishery, with lake trout (*Salvelinus namaycush*) the most abundant fish species (Massol et al., 2007). The observed increase in water temperature and decrease in deep-water O_2 concentration combine to reduce the size of the coldwater fish habitat (Coutant, 1985; Arend et al., 2010). The constraint of fish between a region of detrimentally high temperatures and a region of detrimentally low O_2 concentrations is referred to as a "thermal-dissolved O_2 squeeze" (Coutant, 1985). Throughout Segments II and III in the Lake of Zurich, at least once per year, O_2 concentrations throughout the entire hypolimnion were below the hypoxic threshold for juvenile lake trout ($[O_2] < 7$ mg L^{-1}; Evans 2007). In contrast, this only occurred in 50% of years in Segment I. Combined with observed increases in epi/metalimnetic surface water temperatures, it is likely that in the fall, the habitable region for lake trout has decreased since the late 1980s CRS. While oligotrophication and increasing water temperature have in some ways been beneficial for fish stocks in perialpine lakes (Gerdeaux et al., 2006), the combined effect of the thermal-dissolved O_2 squeeze and the increasing abundance of *P. rubescens*, a type of phytoplankton that serves as a poor nutritional food source to higher organisms (Martin-Creuzburg et al., 2008), could begin to have a negative effect on the coldwater fish population of the Lake of Zurich in the near future.

Outlook

Like any environmental system, lakes are driven by a multitude of competing factors, making it difficult to associate an observed change with any one specific driver. In this study, external P loading was clearly excluded as the main driver of increasing deep-water hypoxia. However, it cannot be eliminated as an indirect driver. During a period of high external P loading (e.g., pre-1980 in the Lake of Zurich), large amounts of P can be buried in the lake sediment. Eventually, the buried P may be reintroduced into the lake through internal loading. Similarly, the response of a lake variable to change is rarely straightforward, as demonstrated by the deep-water O_2 concentration in the Lake of Zurich. Instead of reacting in an abrupt manner to the late 1980s CRS (e.g., by an abrupt increase in the extent of hypoxia), the deep-water O_2 concentration underwent a transition phase of high variability during Segment II, before steadying in Segment III.

Previous studies have shown that lakes respond coherently to changing climatic forcing, particularly in the case of physical lake variables (Magnuson et al., 1990; Kratz et al., 1998; Magnuson and Kratz, 2000; Anneville et al., 2005; Livingstone et al., 2010). While chemical and biological variables behave less coherently than physical variables (Magnuson et al., 1990; Kratz et al., 1998; Magnuson and Kratz, 2000), there is growing evidence that an increase in hypoxia, as observed in the Lake of Zurich, is becoming more common across the northern hemisphere (e.g., Foley et al., 2012; Rösner et al., 2012) in response to a large-scale increase in lake surface water temperature (Schneider and Hook, 2010). The Lake of Zurich is therefore an important example of how a continued global rise in air temperature could have a negative impact on lakes around the world, through an increase in the frequency of occurrence and extent of hypoxia, and in the re-dissolution of P from the sediment.

6

Annual prediction of hypolimnetic oxygen depletion in lakes

North, R. P.[1,2], and Livingstone, D. M.[1]

1. Eawag, Swiss Federal Institute of Aquatic Science and Technology, Department of Water Resources and Drinking Water, Überlandstrasse 133, CH-8600 Dübendorf, Switzerland.

2. ETH Zurich, Department of Environmental Systems Science, Institute of Biogeochemistry and Pollution Dynamics, Universitätsstrasse 16, CH-8092 Zürich, Switzerland

In preparation for submission

Abstract A hypolimnetic oxygen depletion model was reconfigured to predict annual oxygen concentrations at the end of the stratification period. The model was calibrated and tested using measured profiles of oxygen concentration from four Swiss lakes (the Upper Lake of Zurich, the Lower Lake of Zurich, the Lake of Walenstadt, and Aegerisee), of varying trophic states and depths. The model was able to accurately predict individual oxygen concentrations in the hypolimnion, and the volume-weighted mean oxygen concentration for the hypolimnion. In combination with a lake monitoring program, the model provides a simple tool for lake managers to estimate oxygen concentrations immediately prior to fall mixing, based on a profile of oxygen concentrations measured just before the onset of summer stratification.

6.1 Introduction

A recent rise in air temperatures across Europe has been linked to an increase in the duration and extent of hypoxia in lakes, undermining recent efforts to improve lake water quality by eliminating anthropogenic eutrophication through the reduction of nutrient loadings (Livingstone, 1997;

Acknowledgements Appreciation is extended to the numerous individuals who participated in many decades of measuring temperature profiles in the Lower Lake of Zurich, the Upper Lake of Zurich, Aegerisee and the Lake of Walenstadt. This research forms part of project "HYPOX", funded under the European Commission's Seventh Framework Programme (contract no. 226213).

Straile et al., 2003; Jankowski et al., 2006; Foley et al., 2012). Increasing occurrences of hypoxia can affect aquatic ecosystems negatively, leading to a loss of habitat and biodiversity (Diaz and Rosenberg, 2008; Foley et al., 2012). Hypoxia in the bottom waters of lakes may occur intermittently, seasonally or permanently. The frequency of occurrence, duration and spatial extent of hypoxia depend on many factors, including the extent of winter mixing, the duration of summer stratification, and oxygen consumption rates in the water column and at the sediment-water interface. The complexity of the relationship between bottom-water oxygen concentrations and these many drivers can result in interannual variability in the duration and extent of hypoxia. It is therefore difficult to predict whether a lake will become hypoxic in any given year. This can be problematic for lake resource managers if the presence of hypoxia affects management decisions. To address this problem, an existing hypolimnetic oxygen depletion model was modified to create a tool to predict hypolimnetic oxygen concentrations at the end of the summer. Ideally, the ability to predict minimum lake oxygen concentrations would allow lake resource managers and operators (e.g., fisheries, hatcheries, drinking water suppliers, and wastewater treatment plants) to make more informed resource management decisions. For example, knowing end-of-summer oxygen concentrations could help determine whether artificial lake mixing is needed to prevent the development of hypoxic conditions in the upcoming summer. In this study, we aimed to develop a tool that is widely applicable (e.g., to numerous lake types) and easy to use. The modelling tool must be robust and simple enough that all users can understand, modify, and apply the model to their particular needs.

Hypolimnetic oxygen depletion models are usually either empirically based (e.g., Molot et al., 1992) or mechanistically based (e.g., the biogeochemical model of Omlin et al. 2001). The validity of empirical models is generally restricted to the lake or set of lakes from which they were derived, and their predictions decrease in accuracy when the model is extended beyond their original data set (e.g., Clark et al., 2002). Complex mechanistic models often require extensive calibration (Clark et al., 2002) and are typically used as "black boxes" because the user does not have a complete understanding of model functionality, uncertainties and limitations. Therefore, the model that was selected for this study is simple and deductively based, so that it can be applied to a wide range of lake types, and to ensure ease of use for a variety of users. The selected model of Livingstone and Imboden (1996) was originally tested on Aegerisee in Switzerland, and has since been successfully applied to several lakes in Ireland and Canada (Rippey and McSorley, 2009; Lin, 2010).

The model was calibrated and tested using measured oxygen concentration profiles from four Swiss lakes: the Lower Lake of Zurich, the Upper Lake of Zurich, the Lake of Walenstadt, and Aegerisee. The model configuration allows lake managers to estimate an oxygen concentration profile just prior to fall mixing (referred to here as the fall profile) from an oxygen concentration profile measured before the onset of stratification (referred to here as the spring profile) and an estimated oxygen consumption rate. The model can be continuously evaluated and updated by comparing the modelled fall oxygen profile with a measured profile. Through this iterative process, the model continuously checks its accuracy and updates the oxygen consumption rate, accounting for any changes in consumption patterns.

6.2 Methods

6.2.1 Study Area

Four lakes were chosen for this study in order to test the model over a range of different bathymetries, trophic statuses, mixing patterns and hypolimnetic oxygen concentrations. Three of the four

lakes are directly connected; the Linth Canal flows out of the Lake of Walenstadt and becomes the major inflow to the Upper Lake of Zurich, which in turn flows across a sill into the Lower Lake of Zurich (Figure 6.1). Aegerisee lies approximately 10 km southwest of the Lower Lake of Zurich (Figure 6.1). Relevant properties of the four lakes and their locations are shown in Figure 6.1.

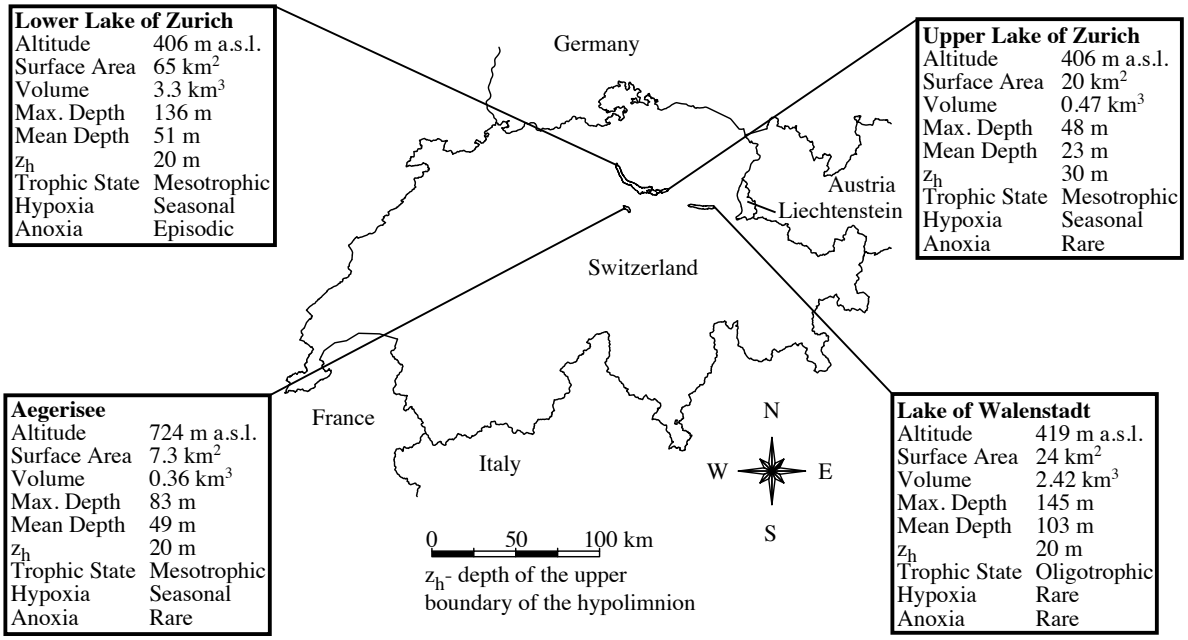

Figure 6.1: Map of Switzerland showing the location and characteristics of the four study lakes. Data from Zimmermann et al. (1991), Livingstone and Imboden (1996), and Rempfer et al. (2010)

In all four lakes, oxygen concentration profiles were measured approximately once a month over the full calendar year. However, beginning in 2005, profiles for the Upper Lake of Zurich were only taken in February, March, May, August, September, and November. Similarly, beginning in 2001, the Lake of Walenstadt's profiling was limited to February, May, August, and November. As these sampling programs still capture typical spring and end-of-summer or early fall profiles, these years were included in the analysis. Hypolimnetic oxygen concentrations were modelled in the Lower Lake of Zurich at 8 depths from 1944 to 2010; in the Upper Lake of Zurich at 3 depths from 1972 to 2009; in the Lake of Walenstadt at 6 depths from 1976 to 2010; and in Aegerisee at 5 depths from 1976 to 1982, and at 6 depths from 1983 to 1994 (Table 6.1). In order to include more profiles from Aegerisee, during data preparation (see below) the profiles measured between 1976 and 1981 were interpolated to match the depths used between 1982 and 1994 (i.e., oxygen concentrations at 40 m and 60 m were linearly interpolated from concentrations measured at 30 m, 50 m, and 70 m). The upper boundary of the hypolimnion in each of the four lakes was originally determined from values established in previous studies (Zimmermann et al., 1991; Livingstone and Imboden, 1996; Rempfer et al., 2010). However, during model optimization, the upper boundary of the hypolimnion in the Lower Lake of Zurich and the Lake of Walenstadt was lowered from 20 m to 40 m, and was raised from 30 m to 20 m for the Upper Lake of Zurich (Table 6.1). Lowering the hypolimnetic boundary eliminated the effects of abnormal morphometry that could not be accounted for by the model. For the Upper Lake of Zurich the boundary was raised to include more observation depths (from 2 to 3 points) in the model. Additionally, measurements taken very close to the lake bottom were removed to avoid measurement uncertainties related to bottom boundary effects. As these modifications were at the extreme upper and lower hypolimnetic

boundaries, they had little affect on modelled oxygen concentrations, particularly with regard to average concentrations in the hypolimnion.

6.2.2 Data preparation

The data sets from each lake were inspected to exclude profiles with two or more consecutive missing measurements in the hypolimnion (see Chapter 3). Based on this criterion, all Aegerisee profiles taken before 1976 were eliminated. Three profiles were removed from the Lake of Walenstadt data set, including the June profile from 2008, a year with only four measured profiles of oxygen concentration. Without the June profile there was no spring profile for the model input, and therefore 2008 was not modelled for the Lake of Walenstadt. Because measurements were not always taken at consistent depths in the hypolimnion of the Lower Lake of Zurich, it was assumed that a measurement interval greater than 40 m represented two or more consecutive missing measurements. This threshold was used because measurement intervals tended to be between 10 m and 20 m in the hypolimnion. Based on this criterion, two profiles were removed from the Lower Lake of Zurich dataset. No profiles were removed from the Upper Lake of Zurich dataset.

The resulting profiles were interpolated spatially with depth using linear interpolation (see Chapter 3) and temporally using cubic spline interpolation. The interpolation filled small data gaps and ensured that measurement depths were consistent throughout each lake's dataset. Because measurement intervals were small and consistent throughout most of the datasets, the interpolation did not drastically modify the measurement intervals (i.e., the distance between measurement depths and the time between profiles), which minimized interpolation error. Measured and modelled oxygen concentrations could therefore be directly compared, but as a result measurement intervals within a profile were not always uniform (Table 6.1).

Table 6.1: Lake properties used for calibration and testing. The depth of the upper boundary of the hypolimnion was obtained from Zimmermann et al. (1991), Livingstone and Imboden (1996), and Rempfer et al. (2010).

	Lower Lake of Zurich	Aegerisee	Upper Lake of Zurich	Lake of Walenstadt
Depth of the upper boundary of the hypolimnion [m]	20	20	30	20
Depth of the upper boundary of the modelled hypolimnion [m]	40	20	20	40
Modelled measurement depths [m]	40, 60, 80, 90, 100, 110, 120, 130	20, 30, 40, 60, 70, 80	20, 30, 36	40, 60, 80, 100, 120, 140
Data range [years]	1944 to 2010	1976 to 1994	1972 to 2010	1976 to 2007, 2009 to 2010

6.2.3 A hypolimnetic oxygen depletion model

The model of Livingstone and Imboden (1996) was designed to determine hypolimnetic oxygen depletion during the summer deoxygenation period. The authors successfully applied the model to hypolimnetic oxygen profiles in Aegerisee (for years 1950-51 and 1968-83) and the model has since been tested on both deep and shallow lakes in the UK and Canada (Rippey and McSorley, 2009; Lin, 2010).

Oxygen concentrations in a lake are a function of air-water exchange, primary production, advective-dispersive transport, and oxygen consumption in the water column and at the sediment-water boundary (Peña et al., 2010). During summer the hypolimnion is typically separated from the epilimnion by thermal stratification. The hypolimnion is therefore isolated from the primary sources of oxygen: air-water exchange and primary production. Vertical advective-dispersive transport of oxygen is also limited because the thermal stratification prevents wind-induced mixing from penetrating into the hypolimnion. Furthermore, horizontal advection and horizontal turbulent diffusion can be ignored in lakes, as horizontal transport processes proceed several orders of magnitude faster than vertical transport processes (Imboden and Emerson, 1978; Imboden and Wüest, 1995). Assuming oxygen consumption rates are constant throughout the summer (Livingstone and Imboden, 1996), the oxygen concentration at depth z (limited to the hypolimnion) at the end of the summer stratification period, $C(z)$, can be estimated from:

$$\frac{C_{max}(z) - C(z)}{\Delta t} = J(z) \tag{6.1}$$

where $C_{max}(z)$ is the oxygen concentration at depth z before the onset of stratification, Δt is the length of the stratification period, and $J(z)$ is the rate of oxygen consumption in the hypolimnion. The model divides the oxygen consumption rate, $J(z)$, into an areal component (at the sediment surface, including sediment oxygen demand), J_A, and a volumetric component (in the water column), J_V. Assuming J_A and J_V are constant over the summer stratification period, Equation 6.1 becomes:

$$C(z) = C_{max}(z) - (J_V(z) + \alpha(z)J_A(z))\Delta t \tag{6.2}$$

where the areal consumption rate changes with depth as a function of the ratio of sediment surface area to water volume, $\alpha(z)$, as follows (Livingstone and Imboden, 1996):

$$\alpha(z) = -\frac{dA(z)}{dV(z)} = -\frac{1}{A(z)}\frac{dA(z)}{dz} \tag{6.3}$$

The major update to the model from its original formulation (Livingstone and Imboden, 1996) was to allow C_{max} to vary with depth in the hypolimnion. This modification improved model accuracy as it allowed the model to account for non-uniformities in the spring oxygen profile. These non-uniformities often result from incomplete deep-water renewal in spring, which prevents the complete replenishment of deep-water oxygen (Livingstone, 1997). Henceforth, the hypolimnetic fall oxygen concentration profile ($C(z)$) will be referred to as the fall profile, and the hypolimnetic spring oxygen concentration profile ($C_{max}(z)$) as the spring profile.

6.2.4 Model calibration

During model calibration, an areal and a volumetric oxygen consumption rate for each year's stratification period were estimated from measured spring and fall hypolimnetic oxygen concentrations using Equation 6.2. The calibration process proceeded as follows. Starting with the known lake bathymetry (i.e., $\alpha(z)$), a measured spring profile ($C_{max}(z)$), the calculated duration of stratification (Δt) and initial estimates for the areal and volumetric consumption rates, Equation 6.2 was used to calculate a "modelled" fall oxygen concentration at every depth in the hypolimnion ($C(z)$). The model error was calculated as the sum of the square of the differences between the modelled and measured fall oxygen concentration at every depth in the hypolimnion. The consumption rates were gradually changed and the process repeated to find the set of consumption rates that minimized the model error. The iterative process was performed using the optimization function Optim,

which is built into the R software package (R Development Core Team, 2011). The consumption rates were assumed to be positive and constant for an individual profile (i.e., rates did not vary with depth). For each of the four lakes, the calibration was repeated for every measurement year, producing time-series of estimated annual volumetric and areal oxygen consumption rates.

The spring oxygen profile represents conditions just before the onset of stratification. This profile was taken to be the profile (between January and June) with the highest volume-weighted mean hypolimnetic oxygen concentration. This estimation assumed that the lake becomes stratified just after maximum oxygen concentrations are reached in the hypolimnion. This calculation always included the full hypolimnion, even when the model was only applied to a portion of the hypolimnion (which was the case for the Lower Lake of Zurich, the Upper Lake of Zurich and the Lake of Walenstadt). The fall oxygen profile represents conditions just before the onset of fall mixing; i.e., at the end of the summer stratification period. However, it is difficult to accurately determine when fall mixing has begun. Three methods were compared for fall profile selection. The first method assumed that fall mixing began in October or later every year, and therefore used an oxygen profile measured in September. The second method assumed that fall mixing began immediately after hypolimnetic oxygen concentrations reached their annual minimum. Therefore, the profile of oxygen concentration (between August and December) with the lowest volume-weighted mean hypolimnetic oxygen concentration was selected as the fall profile. In the third method the difference in volume-weighted mean hypolimnetic oxygen concentration was calculated between consecutive months (from August to December). A positive value represented an increase in hypolimnetic oxygen concentration and a negative value a decrease. Assuming that hypolimnetic oxygen concentrations decreased throughout the stratification period, a positive value would indicate the start of fall mixing. Therefore, the profile preceding the earliest positive value was chosen as the fall oxygen profile. During model calibration, all three methods were compared to determine the most accurate method for each lake. Only the results of the most accurate methods are provided, and only the most accurate methods were used for model testing (see next section).

6.2.5 Model testing

During model testing the model was used to predict fall oxygen concentrations. Figure 6.2 describes the simulation process for the current year. The first step, the calculation of J_A and J_V values, was accomplished during model calibration. The consumption rates were averaged over n years using four different averaging lengths, n=1, 2, 5 and 10 yr. The resulting average J_A and J_V values will be henceforth referred to as $J_{A,n}$ and $J_{V,n}$. Outliers in the time-series of calculated annual consumption rates were excluded from the calculation of $J_{A,n}$ and $J_{V,n}$. However, only one outlier was found: for the Lake of Walenstadt, in 2001 the J_V value lay more than 8 standard deviations from the mean. The particular reason for the occurrence of the outlier is discussed below.

A modelled fall profile, $C(z,t)$, was calculated from $J_{A,n}$, $J_{V,n}$, the measured spring profile, $C_{max}(z)$, and the estimated length of summer stratification, Δt – i.e., the mean Δt of the past n years. The model error was once again calculated as the difference between modelled and measured fall oxygen concentrations in the hypolimnion. Using the procedure outlined in the model calibration section, the measured fall profile was used to calculate J_A and J_V values for the current year's summer stratification period. These new consumption rates were then included in the calculation of the following year's $J_{A,n}$ and $J_{V,n}$ values, thus integrating changing oxygen consumption rates into the model results.

The initial values of $J_{A,n}$ and $J_{V,n}$ were calculated from the model calibration results, and the model was therefore not applied to the first 10 years of data. For each lake, the remaining years of data were used to test the ability of the model to accurately predict fall oxygen concentrations.

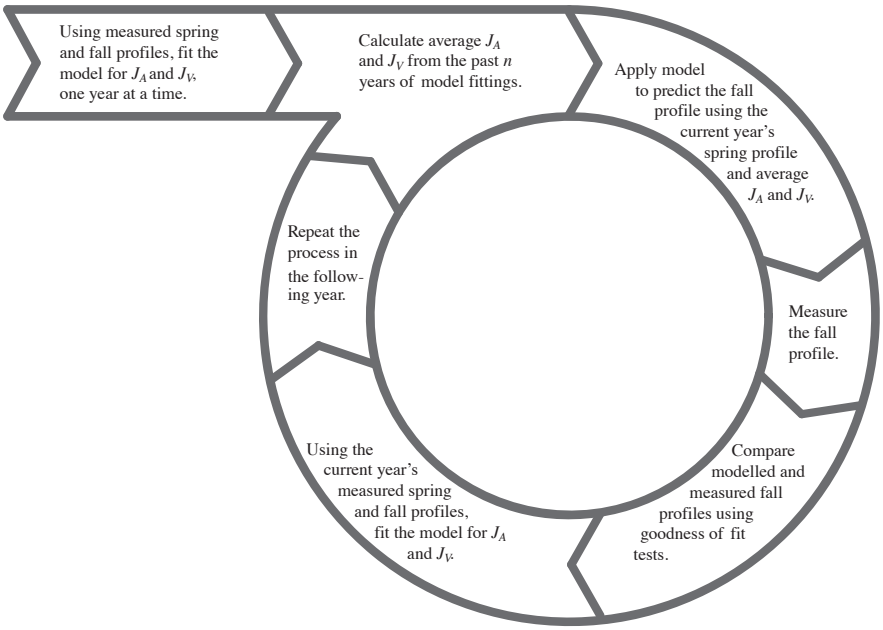

Figure 6.2: Outline of the modelling process used to predict annual fall profiles of hypolimnetic oxygen concentration.

6.3 Results

Regression analysis was used to measure the agreement or disagreement between measured oxygen concentration and modelled oxygen concentration. Following the method of Stefan and Fang (1994a), the model performance was assessed using the root mean square error (RMSE), the coefficient of determination (R^2) and its significance (p), and the slope of the regression line (S). It was assumed that the model accuracy increased as the RMSE approached zero, R^2 approached 1 for p <0.05, and S approached 1. Unless otherwise noted, all p values were <0.001. The analysis considered the hypolimnetic oxygen concentration profile and the volume-weighted mean hypolimnetic oxygen concentration (VWHO). For a given measurement depth in the hypolimnion, the error was defined as the difference between the measured and modelled oxygen concentration or VWHO.

6.3.1 Model calibration

In order to assess the accuracy of the estimated oxygen consumption rates, each set of J_A and J_V values was fed back into the model to determine a "modelled" fall profile of oxygen concentration. The resulting modelled fall oxygen concentrations could then be compared with the measured fall oxygen concentrations (Figure 6.3). For all four lakes the model results compared well with measurement results. RMSEs were relatively small at ≤ 0.83 mg O_2 L^{-1} for oxygen concentrations, and ≤ 0.33 mg O_2 L^{-1} for VWHO (Table 6.2). In addition, the fit of the regression was high for individual concentrations ($R^2 \geq 0.89$, $0.94 \leq S \leq 1.01$; Figure 6.3; Table 6.2) and for VWHO ($R^2 \geq 0.96$, $0.94 \leq S \leq 1.11$; Figure 6.4; Table 6.2).

As discussed in the Methods section, three different methods were used to select the fall profile. The model was run using all three methods, but only results for the most accurate method are presented here. Model accuracy was highest using a September oxygen profile for the Lower Lake of Zurich, Aegerisee and the Lake of Walenstadt. For the Upper Lake of Zurich the most accurate

Table 6.2: Model calibration for oxygen concentrations ($[O_2]$) and the mean volume-weighted hypolimnetic oxygen concentration (VWHO). The results are for the root mean square error (RMSE), the coefficient of determination (R^2), the slope of the regression line (S), and the coefficient of variation (CV). In all cases the significance of R^2 was $p < 0.001$.

	Lower Lake of Zurich	Aegerisee	Upper Lake of Zurich	Lake of Walenstadt
$[O_2]$				
RMSE [mg O_2 L^{-1}]	0.78	0.83	0.65	0.24
R^2	0.92	0.90	0.89	0.92
S	0.96	1.00	1.01	0.94
VWHO				
RMSE [m]	0.27	0.26	0.33	0.03
R^2	0.96	0.98	0.96	0.99
S	1.04	0.94	1.11	0.99
CV				
J_V	0.54	0.20	0.52	0.82 (0.37*)
J_A	1.1	0.45	0.49	0.79

* CV after removing the exceptionally high value of J_V from 2001 (Figure 6.5d).

method was to use a profile from the month before VWHO concentrations began to increase.

The mean estimated volumetric oxygen consumption rates (Figure 6.5) for the Lower Lake of Zurich (4.32 g O_2 m^{-3} yr^{-1}), Aegerisee (6.67 g O_2 m^{-3} yr^{-1}), the Upper Lake of Zurich (7.97 g O_2 m^{-3} yr^{-1}), and the Lake of Walenstadt (2.54 g O_2 m^{-3} yr^{-1}) were below previously published ranges (Figure 6.5); e.g., based on multiple studies, Snodgrass (1987) reported J_V values between 14.6 and 147 g O_2 m^{-3} yr^{-1}. Similarly, mean estimated areal oxygen consumption rates (Figure 6.6) were below the range published by Snodgrass (1987): 22 g O_2 m^{-2} yr^{-1} to 324 g O_2 m^{-2} yr^{-1}. There were two exceptionally high J_V values, one in 2003 for the Lower Lake of Zurich, and one in 2001 for the Lake of Walenstadt (Figure 6.5). Both years had abnormally high spring oxygen concentrations and a late onset of stratification, but typically low fall oxygen concentrations. A high volumetric oxygen consumption rate was therefore required to deplete an above average hypolimnetic oxygen content over a relatively short stratification period.

As the modelled consumption rates covered a wide range of values, the variability of consumption rates with time was assessed using the coefficient of variation (CV). The CV is defined as the standard deviation of the time-series divided by the absolute value of its mean. A low CV value corresponds to a low variability, indicating that the consumption rate of the current summer is likely to be similar to past rates. Thus, a low CV is an indication that upcoming end-of-summer concentrations can be accurately predicted using the oxygen consumption rates from preceding years. In contrast, a high CV indicates high interannual variability, and therefore less reliable predictions using consumption rates from preceding years. A CV threshold of 0.5 was chosen to indicate relatively low variability. Under this assumption, only Aegerisee had consistent volumetric consumption rates, and only the Upper Lake of Zurich had consistent areal oxygen consumption rates (Table 6.2). The CV for the volumetric consumption rate of the Lake of Walenstadt was particularly high (0.82). However, removing the J_V value from 2001 yielded a much lower CV value of 0.37. Nonetheless, the oxygen consumption rates of the four lakes generally have a large amount of interannual variation.

6.3.2 Model testing

The calibrated model was applied to the four lake data sets to predict fall oxygen concentrations in the hypolimnion. Four different averaging lengths (n=1, 3, 5, 10 years) were used to estimate

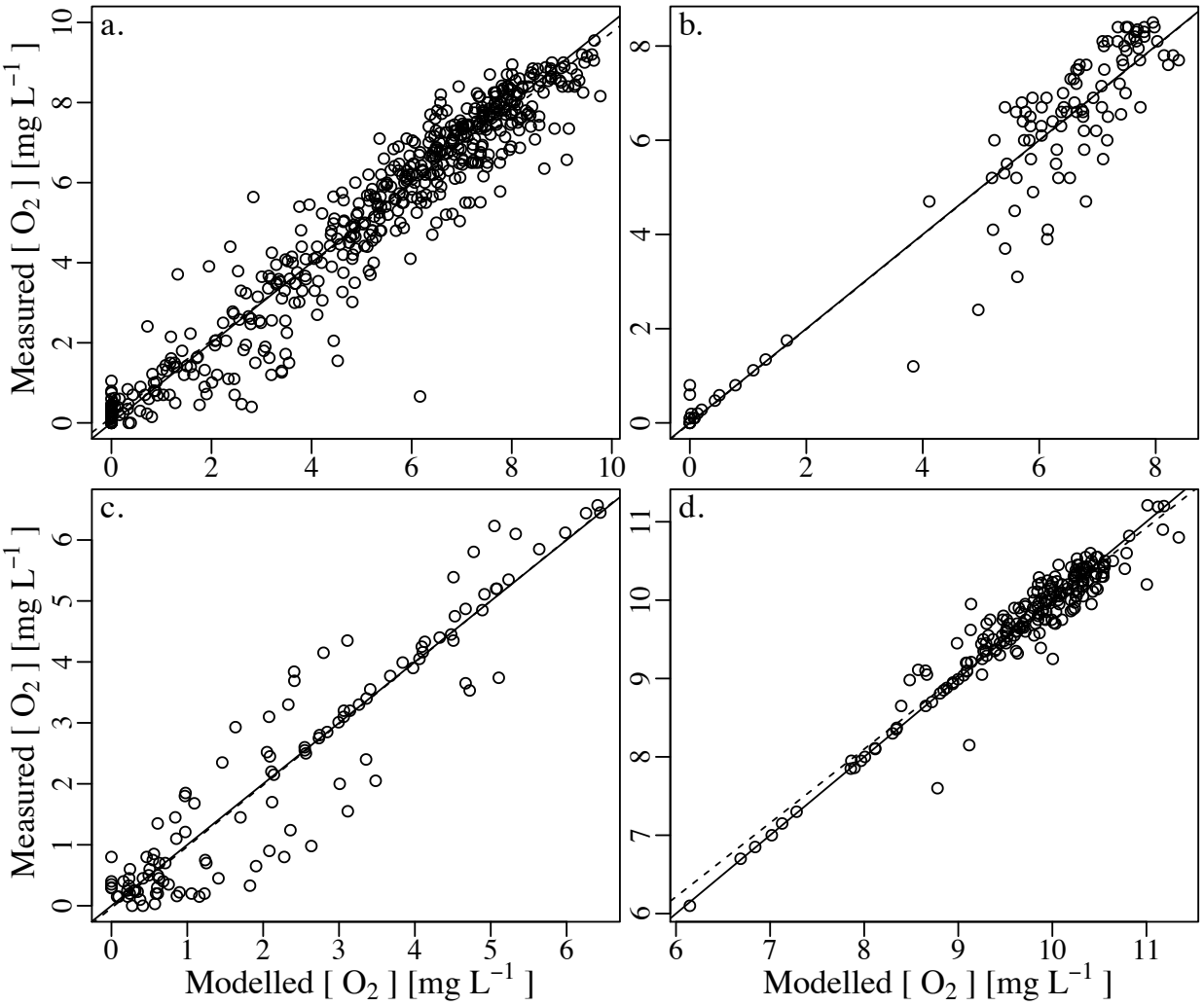

Figure 6.3: Comparing the modelled and measured fall hypolimnetic oxygen concentrations ([O_2]) at various depths in the hypolimnion. a) The Lower Lake of Zurich (1944 to 2010). b) Aegerisee (1976 to 1994). c) The Upper Lake of Zurich (1972 to 2009). d) The Lake of Walenstadt (1976 to 2010, except 2008). Linear regression lines are dashed and the 1:1 ratio lines are solid.

the oxygen consumption rates. However, the model accuracy did not change substantially with averaging length. An averaging length of 10 years generally provided the most accurate results. In order to limit redundancy, only results using this averaging length are presented.

The RMSE was lower for the Lake of Walenstadt at 0.7 mg O_2 L^{-1} than for the other three lakes (RMSE>1.1 mg O_2 L^{-1}; Table 6.3). The fit of the regression for oxygen concentrations was good for the Lower Lake of Zurich (R^2=0.77, S=0.87), Aegerisee (R^2=0.83, S=1.06), and the Upper Lake of Zurich (R^2=0.57, S=0.85), but was relatively weak for the Lake of Walenstadt (R^2=0.29, S=0.48; Figure 6.7; Table 6.3). Similarly, the goodness of fit between modelled and measured VWHO concentration was strong for the Lower Lake of Zurich (R^2=0.67, S=0.79), Aegerisee (R^2=0.77, $p < 0.005$, S=0.68), and the Upper Lake of Zurich (R^2=0.45, S=0.70), but was not significant for the Lake of Walenstadt ($p < 0.1$) ; Figure 6.8; Table 6.3).

The poor fit for the Lake of Walenstadt is largely due to the model results in 2001. During model calibration, the model found that the volumetric oxygen consumption rate in 2001 needed to be exceptionally high to account for high spring oxygen concentrations and a short stratification period. During model testing however, the consumption rate was determined from rates over the

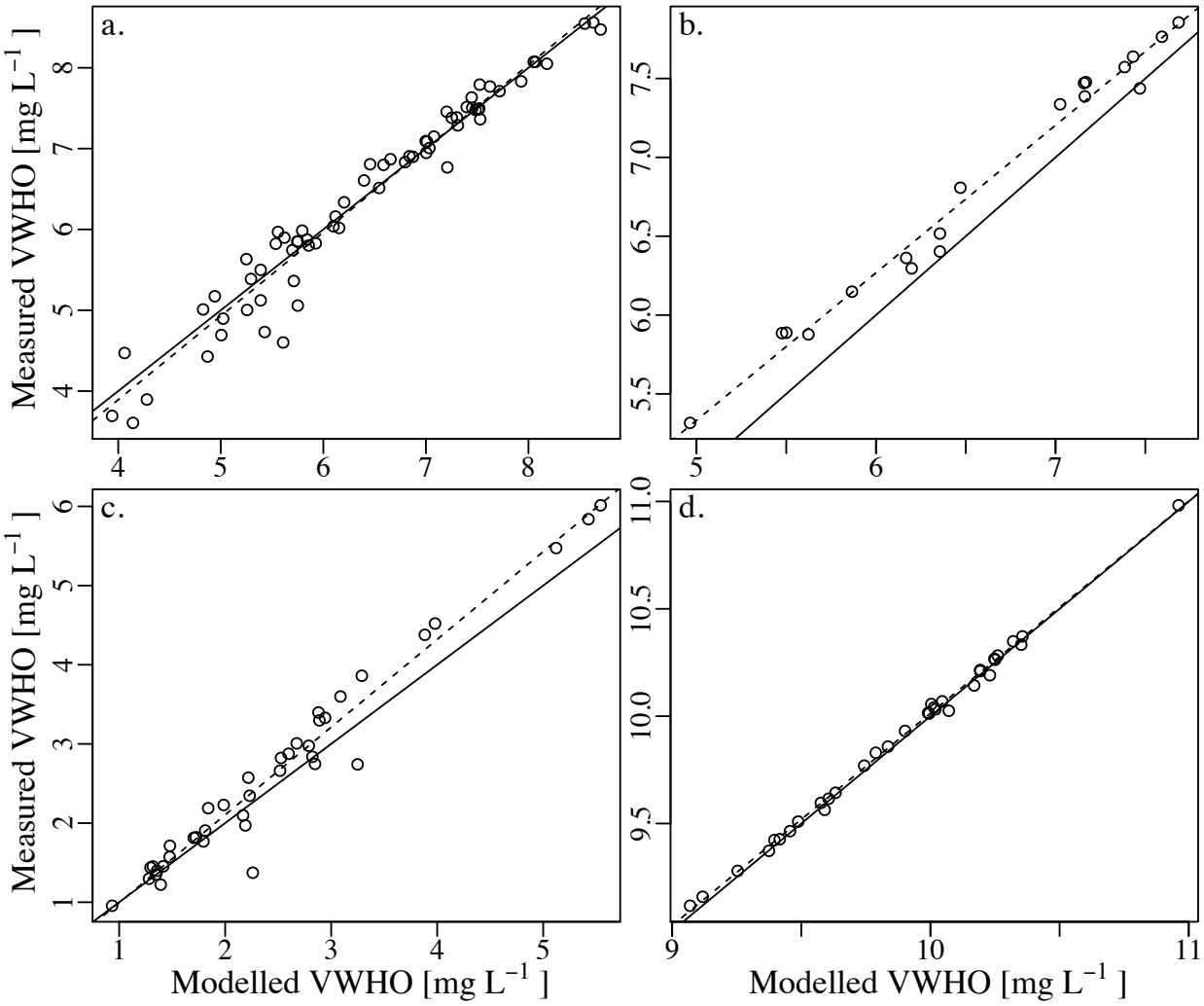

Figure 6.4: Comparing the modelled and measured volume-weighted mean hypolimnetic oxygen concentration (VWHO). a) The Lower Lake of Zurich (1944 to 2010). b) Aegerisee (1976 to 1994). c) The Upper Lake of Zurich (1972 to 2009). d) The Lake of Walenstadt (1976 to 2010, except 2008). Linear regression lines are dashed and the 1:1 ratio lines are solid.

preceding 10 years, which substantially underestimated the actual oxygen consumption. As a result, predicted fall oxygen concentrations in 2001 were well above measured concentrations (filled circles in Figure 6.7d and 6.8d). Ignoring the results from 2001, the model fit for the Lake of Walenstadt improved substantially for oxygen concentration (R^2=0.60, S=0.78) and VWHO (R^2=0.40, $p < 0.005$, S=0.83; Table 6.3).

As an additional test, the number of years that the model correctly predicted that hypoxia would occur anywhere in the hypolimnion (i.e., $[O_2] \leq 2$ mg O_2 L^{-1}) was calculated. This assessment did not consider at what depth hypoxia occurred, but only whether O_2 concentrations ≤ 2 mg L^{-1} were observed anywhere in the hypolimnion. Dividing by the number of years in which hypoxia was measured in the hypolimnion provided a quantitative assessment of the model's ability to predict upcoming hypoxic conditions in the hypolimnion. For all three lakes the model successfully predicted hypoxia in the majority of years - 76% of years for Lower Lake of Zurich, 67% of years for Aegerisee and 64% of years for Upper Lake of Zurich (Table 6.3). Hypoxic oxygen concentrations were not reached in the Lake of Walenstadt, and this lake was therefore excluded

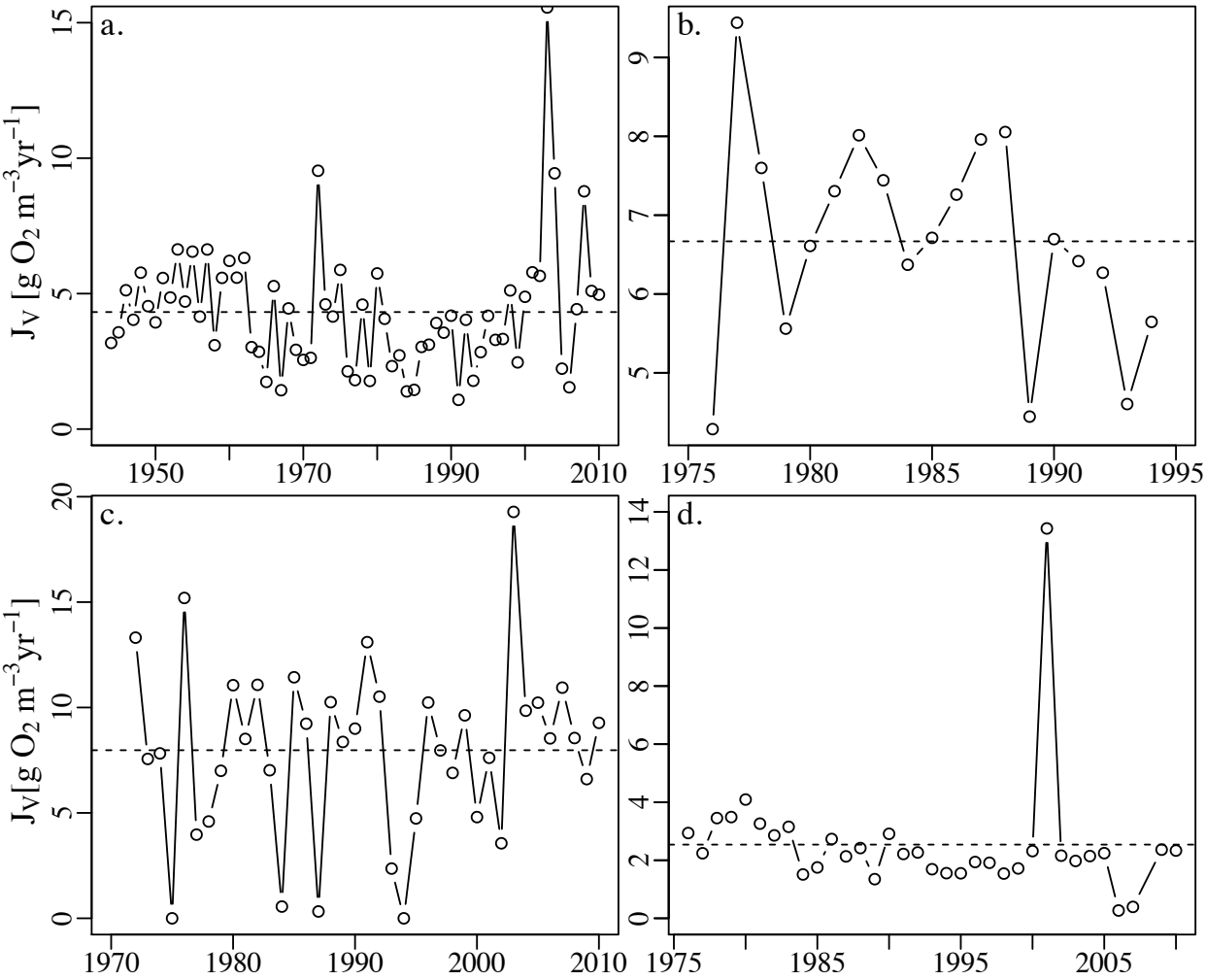

Figure 6.5: Time-series of volumetric oxygen consumption, J_V, determined from model fitting using observed spring and fall profiles. a) The Lower Lake of Zurich (1944 to 2010). b) Aegerisee (1976 to 1994). c) The Upper Lake of Zurich (1972 to 2009). d) The Lake of Walenstadt (1976 to 2010, except 2008). Dashed lines indicate mean J_V.

from this part of the analysis.

6.4 Discussion

The hypolimnetic oxygen depletion model of Livingstone and Imboden (1996) was calibrated and tested using long-term data sets from four Swiss lakes. During model calibration the model performed exceptionally well, as model error was low for both individual oxygen concentrations and VWHO. The model was also able to accurately predict upcoming hypolimnetic oxygen concentrations and VWHO. Furthermore, in the majority of years the model correctly predicted whether hypoxic conditions would be reached in the hypolimnion before the end of the stratification period.

Within the literature opinions differ on what type of information a model should provide to water resource managers and operators. Often, the debate considers oxygen concentrations at various depths or VWHO concentrations as the most applicable variables (Cornett and Rigler, 1979; Clark et al., 2002; Paterson et al., 2009). It is most likely that as the needs of operators differ, any modelling tool will need to accurately predict multiple measures of hypolimnetic oxygen content.

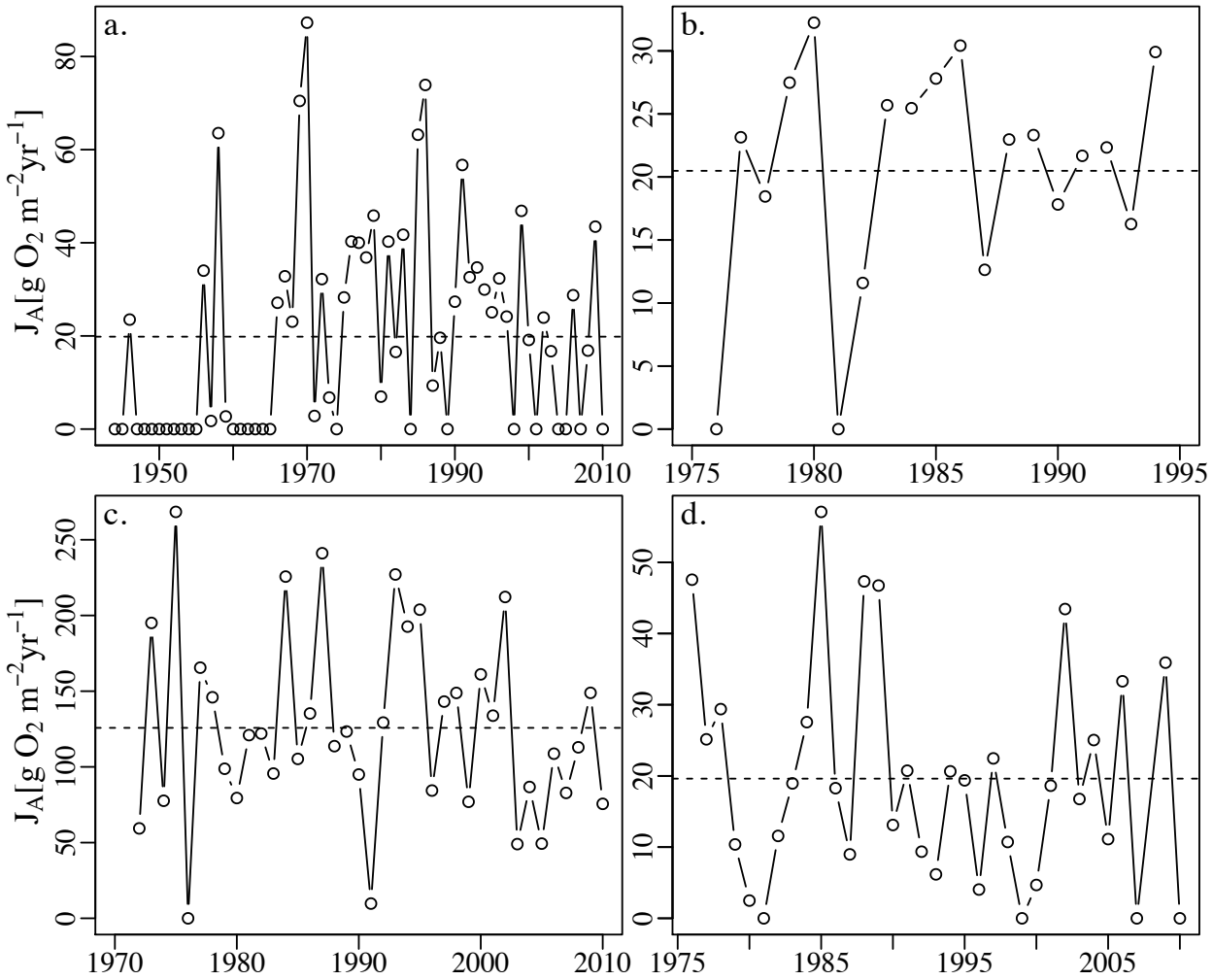

Figure 6.6: Time-series of areal oxygen consumption, J_A, determined from model fitting using observed spring and fall profiles. a) The Lower Lake of Zurich (1944 to 2010). b) Aegerisee (1976 to 1994). c) The Upper Lake of Zurich (1972 to 2009). d) The Lake of Walenstadt (1976 to 2010, except 2008). Dashed lines indicate mean J_A.

The model presented in this paper can accurately predict hypolimnetic oxygen concentrations as a function of depth, the occurrence of hypoxia or anoxia, VWHO concentrations and, to a lesser extent, the depth of the upper boundary of the hypoxic and anoxic zones (data not shown). This flexibility, combined with the model's simplicity and robustness, should allow operators to apply the model in a way that suits their individual needs.

The analysis found that the model accuracy was not affected by the surface area, maximum depth, or trophic state of the lake (Figure 6.1). The trophic states covered by the four data sets include mesotrophic, oligotrophic and eutrophic, as both the Lower Lake of Zurich and the Lake of Walenstadt were initially eutrophic. Therefore, the model not only works for different lake characteristics, but is also capable of accommodating changing trophic states. This robustness will be particularly useful if a lake is affected by climate change or exposed to variable external nutrient loadings.

The deterministic, one-dimensional, unsteady dissolved oxygen model of Stefan and Fang (1994a) provides a good comparison with the model tested in this study, as the former performed well for a variety of lake sizes and trophic states. For weakly stratified lakes, the results of the regression between modelled and measured oxygen concentrations in the Upper Lake of Zurich

Table 6.3: Model prediction for oxygen concentrations ($[O_2]$), the mean volume-weighted hypolimnetic oxygen concentration (VWHO), and the occurrence of hypoxia. The results are for the root mean square error (RMSE), the coefficient of determination (R^2), the slope of the regression line (S), and the coefficient of variation (CV). Hypoxia is defined as an oxygen concentration ≤ 2 mg O_2 L^{-1}. The significance of R^2, p, was < 0.001, except for VWHO in both Aegerisee ($p < 0.005$) and the Lake of Walenstadt ($p > 0.1$). ns = non-significant result ($p > 0.1$)

	Lower Lake of Zurich	Aegerisee	Upper Lake of Zurich	Lake of Walenstadt
$[O_2]$				
RMSE [mg O_2 L^{-1}]	1.34	1.13	1.34	0.73
R^2	0.77	0.83	0.57	0.29 (0.60*)
S	0.87	1.06	0.85	0.48 (0.78*)
VWHO				
RMSE [m]	0.79	0.72	1.11	0.62
R^2	0.66	0.77	0.45	ns (0.40*)
S	0.79	0.68	0.70	– (0.83*)
Occurrence of hypoxia				
% of years correctly detected	76	67	64	-

* Values for the Lake of Walenstadt after removing the results of 2001 ($p < 0.005$ for R^2 of VWHO).

(R^2=0.57) compared well with the R^2 values of 0.46–0.64 found by Stefan and Fang (1994a). For strongly stratified lakes, Stefan and Fang (1994a) found R^2 values between 0.70–0.92, which were similar to the results from this study's deepest lakes, the Lower Lake of Zurich and Aegerisee (R^2=0.77–0.83). The results suggest that both models are better suited to strongly stratified, deep lakes than to weakly stratified, shallow lakes. The advantage of the Stefan and Fang model is that it is able to simulate profiles of the entire water column throughout the year, and estimate impacts of future climate change scenarios on lake oxygen concentrations (Stefan and Fang, 1994b). The disadvantage is that the model requires a large amount of input data and lake process information (e.g., meteorological data, oxygen production by photosynthesis, light limitation, and surface reaeration rates) and is coupled with a heat transport model. In contrast, the Livingstone and Imboden (1996) model only requires spring and fall hypolimnetic oxygen profiles and lake morphometric data. The disadvantage of this simpler model stems from several major assumptions. Volumetric oxygen consumption was assumed to be constant with depth, and oxygen concentrations were not affected by changing summer water temperatures. The model also assumed that oxygen depletion rates (volumetric and areal) are constant over the summer stratification period. This is of particular importance when oxygen concentrations drop below 2 mg O_2 L^{-1} and rates of depletion may begin to slow (Wetzel, 2001); this likely led to inaccuracies at low oxygen concentrations, which is of particular importance when determining the depth of hypoxia. Based on the advantages and disadvantages of the two models, and given that neither model outperforms the other in terms of accuracy, it could be concluded that a more complex model than that of Livingstone and Imboden (1996) is not necessary to predict upcoming end-of-summer hypolimnetic oxygen concentrations.

Traditional lake monitoring programs typically obtain monthly profiles of multiple variables over the entire year, or at least during the ice-free period. Recently, monitoring programs in some lakes (e.g., the Upper Lake of Zurich and the Lake of Walenstadt) have been forced to reduce the frequency of their profile measurements due to funding cutbacks, improved lake conditions as a result of reduced nutrient loading, and other factors. In this study, we found that even with a reduced monitoring campaign, the model can be used to accurately predict oxygen concentrations in the hypolimnion. Combining the model with just two profile measurements per year – targeted to capture the period just prior to the onset and end of stratification – one can still obtain an accurate idea of hypolimnetic oxygen depletion in the summer. Additionally, these results can be

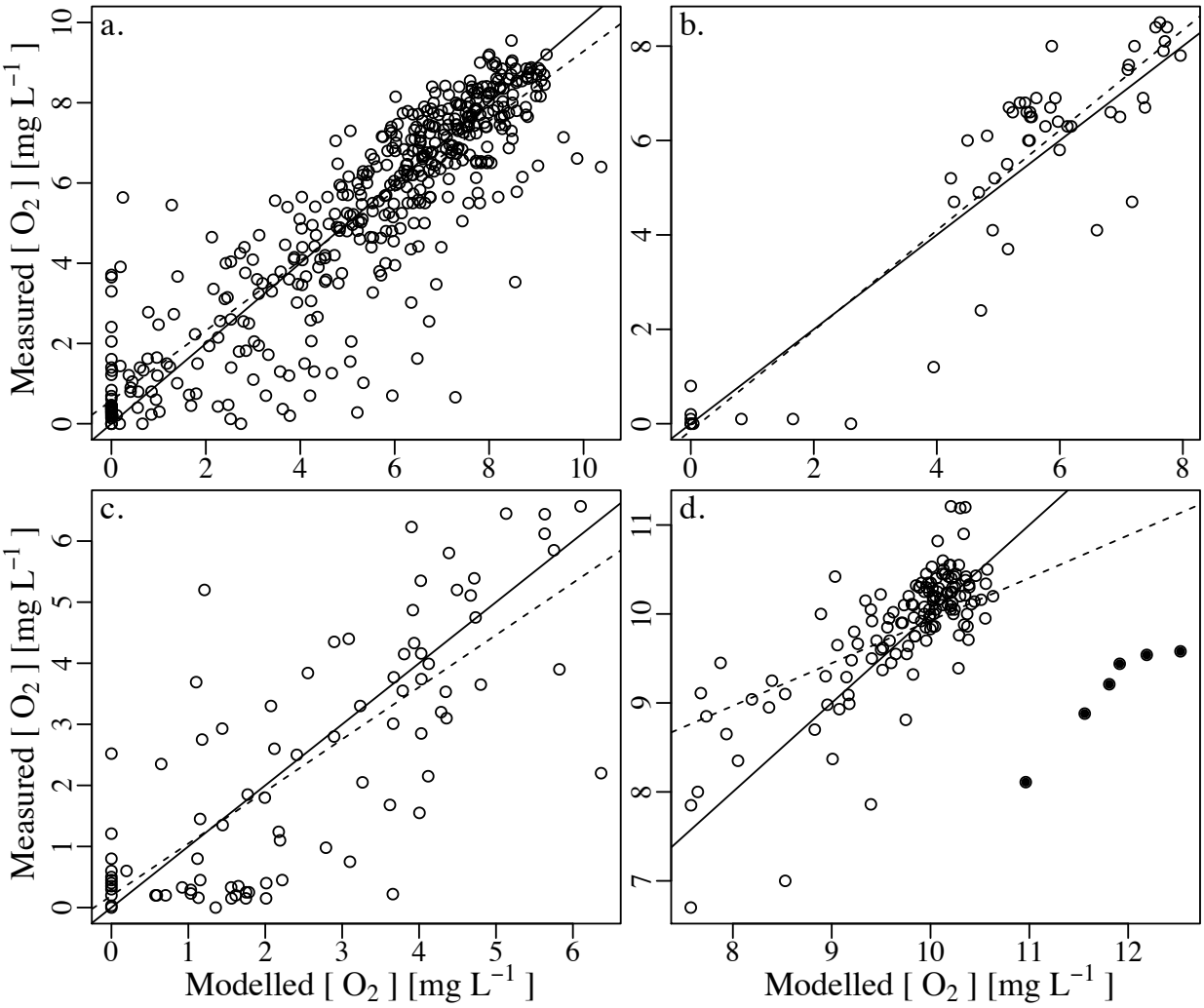

Figure 6.7: Comparing modelled (predicted) and measured fall oxygen concentrations ($[O_2]$) at various depths in the hypolimnion. a) The Lower Lake of Zurich (1944 to 2010). b) Aegerisee (1976 to 1994). c) The Upper Lake of Zurich (1972 to 2009). d) The Lake of Walenstadt (1976 to 2010, except 2008). Linear regression lines are dashed and the 1:1 ratio lines are solid. The filled circles in d) are the results of 2001, a year of particularly poor model results for the Lake of Walenstadt.

continuously validated and updated by comparing modelled and observed fall profiles. The model can also be used to fill in gaps between spring and fall profiles by progressively increasing Δt, thus predicting a hypolimnetic oxygen profile for each summer month.

In summary, the modelling tool tested in this study provides accurate insight into hypolimnetic oxygen content at the end of the summer stratification period. Although it must be accompanied by a lake monitoring campaign, it provides an effective, robust tool for water resource management under changing climatic conditions.

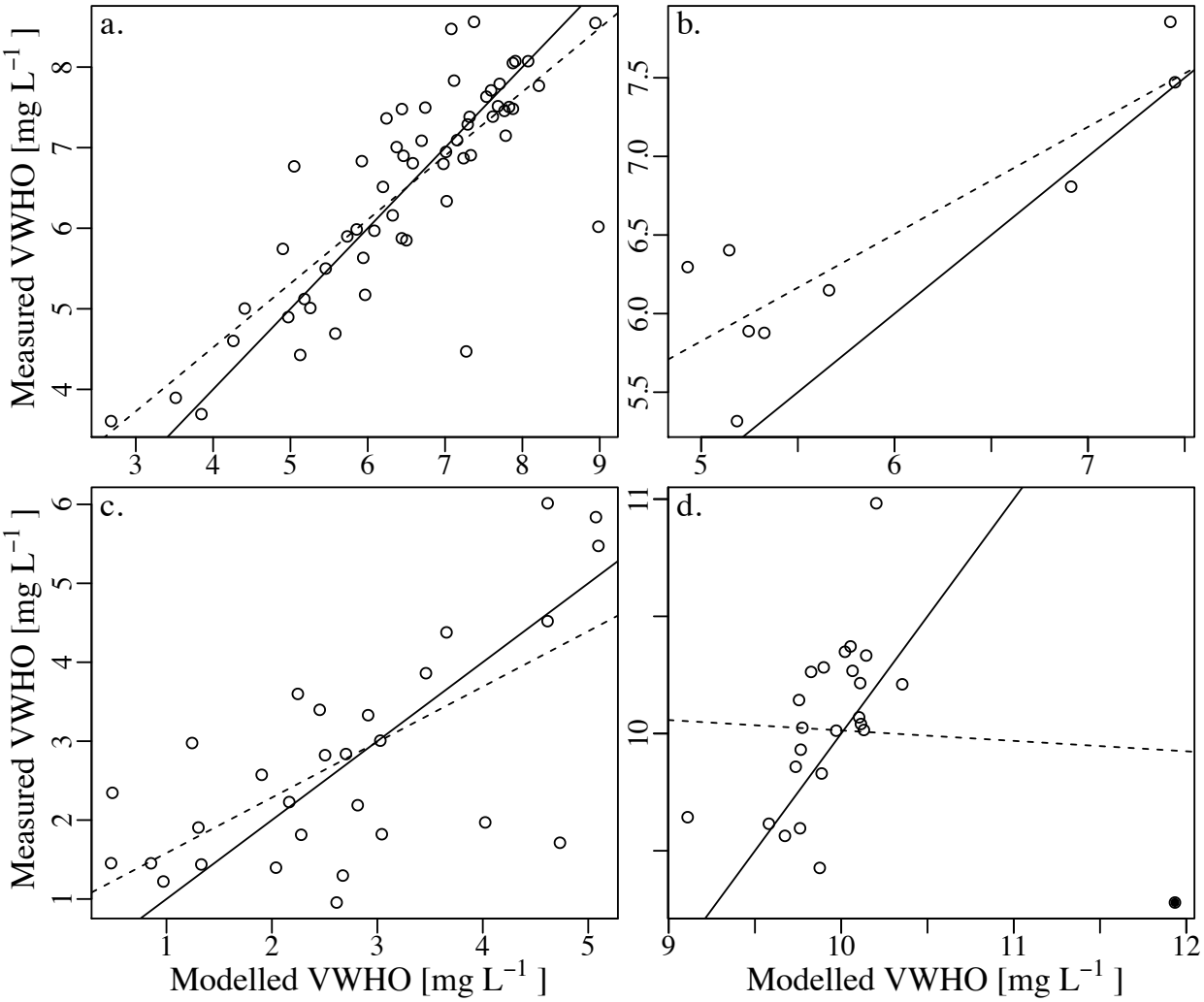

Figure 6.8: Comparing modelled (predicted) and measured fall volume-weighted hypolimnetic oxygen concentration (VWHO). a) The Lower Lake of Zurich (1944 to 2010). b) Aegerisee (1976 to 1994). c) The Upper Lake of Zurich (1972 to 2009). d) The Lake of Walenstadt (1976 to 2010, except 2008). Linear regression lines are dashed and the 1:1 ratio lines are solid. The filled circles in d) are the results of 2001, a year of particularly poor model results for the Lake of Walenstadt.

7

Conclusions and outlook

An increase in the frequency of occurrence, duration, and extent of lake hypoxia as a result of climate change has been predicted for some time (e.g., Blumberg and Di Toro, 1990; Stefan et al., 1996; Livingstone, 1997). However, past studies have often used modelling or extreme events to predict impacts, without actually observing long-term changes (e.g., Stefan et al., 1996; Jankowski et al., 2006; Rempfer et al., 2010). The work in this study was able to expand previous work by taking advantage of several exceptionally long lake monitoring programs in Switzerland. Through these unique lake data sets, it was possible to conclude confidently that an increase in the extent and duration of hypoxia in the Lower Lake of Zurich ultimately resulted from an abrupt increase in air temperature.

In order to analyse the long time-series used in the thesis, proper data set preparation was required. In historical data it is common to encounter missing measurements, or irregular measurement intervals, in both space (i.e., with depth) and time. The first stage of the thesis compared two spatial-gap-filling methods – linear and cubic spline interpolation – for measured water column profiles. In the end, the simplest method, linear interpolation, performed consistently better than cubic spline interpolation.

After proper data preparation, the impact of the now well documented late 1980s CRS on water temperatures in Swiss rivers and lakes was investigated. The analysis showed that the abrupt increase in air temperature across the Swiss Plateau was reflected in river and lake temperatures, although the effect diminished with lake depth. The largest increases in air temperature occurred in winter, spring and summer, while the largest increases in water temperature tended to occur in spring and summer. As a result of greater warming at the lake surface than in the hypolimnion, lake stability also increased abruptly.

The increase in thermal stability in turn led to either a reduction in the intensity or frequency of occurrence of annual deep water renewal. Reduced mixing in the Lower Lake of Zurich inhibited oxygen replenishment to the hypolimnion, resulting in an increase in the extent and duration of seasonal hypoxia. Furthermore, the increase in hypoxia appears to have resulted in an increase in the internal loading of phosphorus from the sediment, a potentially significant setback for a lake that had undergone nearly 30 years of decreasing total phosphorus concentration due to reduced external phosphorus loading.

Due to the scale and scope of global climate change, it can be assumed that many lakes will be affected by hypoxia. In fact, a recent study using satellite-derived water temperatures showed

that lake surface temperatures have been increasing globally (Schneider and Hook, 2010). A large-scale decline in lake oxygen concentrations resulting from increasing water temperature (e.g., Foley et al., 2012; Rösner et al., 2012), could have serious consequences for lake ecosystems (e.g., Carpenter et al., 1998; Evans, 2007; Nürnberg, 2009; Arend et al., 2010). An effort therefore needs to be made to adapt our water resource management practices to account for the effects of climate change. With this in mind, in the final stage of the thesis a simple modelling tool was developed that can accurately predict annual oxygen concentrations at the end of the summer stratification period. It is hoped that this tool, combined with a lake monitoring program, can help water resource managers account for increased variability in the duration and extent of hypoxia in lakes.

As is often the case, the conclusions reached in this thesis have led to more questions, specifically about the impact of climate change on lake processes. Several research questions and recommendations that may be applicable to future research projects are outlined below, with a particular focus on European lakes.

- In the late 1980s an abrupt increase in water temperature occurred simultaneously in several lakes. However, in this thesis, the influence of increasing water temperature on lake oxygen concentrations was only considered for one lake, the Lower Lake of Zurich. Therefore, it is not yet known whether a similar increase in the extent and duration of hypoxia has occurred in other Swiss lakes. Further investigations could consider the variability in lake hypoxia in multiple lakes, as well as compare lakes of differing morphometry and trophic state, located at different altitudes and latitudes, and subject to different local climates.

- A particularly interesting observation with regard to the Lower Lake of Zurich was that inhibited deep-water mixing by increasing thermal stability did not appear to affect the ability of SRP to mix annually between the hypolimnion and epilimnion. Further investigations into how lake mixing patterns are changing would be necessary to fully understand lake response to climate change. Mixing is clearly an important process, particularly with regard to the transport of oxygen and nutrients. Thus, an improved understanding of climate change impacts on lake mixing should improve our understanding of oxygen and nutrient dynamics.

- Another major conclusion of Chapter 5 was that internal phosphorus loading in the Lower Lake of Zurich had increased, most likely because of an increase in hypoxia. However, further analysis would be required to determine whether hypoxia is the sole cause of the increase in deep-water SRP concentration. Furthermore, it would be very interesting to see whether other lakes in Europe have experienced a similar increase in internal phosphorus loading.

- Unlike in the marine environment, research into the impact of climate change on hypoxia in freshwater systems is still in its infancy. Typically, lake research has focused on the impact of climate change on water temperature and thermal stability. Further research into how ecosystems are affected by hypoxia through the combined effect of eutrophication and climate change is therefore recommended.

- Finally, the most important recommendation that has resulted from the research conducted for this thesis is to ensure the continuation of long-term lake monitoring programs. Without the extensive data sets that exist for multiple Swiss lakes, the conclusions of this work would never have been reached. There is currently a disconcerting trend to reduce lake monitoring programs (e.g., the Lake of Walenstadt and Aegerisee) or to completely eliminate them (e.g., the closing of the Experimental Lakes Area in Canada). While in some cases a reduced

monitoring program may still be sufficient (see Chapter 6), any reduction in monitoring frequency nevertheless results in the loss of a great deal of data. With the impact of climate change becoming clearer with every study, the importance of long-term studies has never been more apparent. While modelling is able to fill in gaps in some cases (Chapters 5 and 6), only by observing change can truly concrete conclusions be drawn. Therefore, the strongest recommendation of this thesis is to continue, improve and expand existing lake monitoring programs.

Bibliography

Adrian, R., O'Reilly, C. M., Zagarese, H., Baines, S. B., Hessen, D. O., Keller, W., Livingstone, D. M., Sommaruga, R., Straile, D., Van Donk, E., Weyhenmeyer, G. A., and Winder, M. (2009). Lakes as sentinels of climate change. *Limnology and Oceanography*, 54(6):2283–2297.

Alheit, J., Mollmann, C., Dutz, J., Kornilovs, G., Löwe, P., Morholz, V., and Wasmund, N. (2005). Synchronous ecological regime shifts in the central Baltic and the North Sea in the late 1980s. *ICES Journal of Marine Science*, 62(7):1205–1215.

Amritkar, R. E. and Kumar, P. P. (1995). Interpolation of missing data using nonlinear and chaotic system analysis. *Journal of Geophysical Research*, 100(D2):3149–3154.

Anneville, O., Gammeter, S., and Straile, D. (2005). Phosphorus decrease and climate variability: mediators of synchrony in phytoplankton changes among European peri–alpine lakes. *Freshwater Biology*, 50(10):1731–1746.

Anneville, O., Souissi, S., Gammeter, S., and Straile, D. (2004). Seasonal and interannual scales of variability in phytoplankton assemblages: comparison of phytoplankton dynamics in three perialpine lakes over a period of 28 years. *Freshwater Biology*, 49(1):98–115.

Arend, K. K., Beletsky, D., DePinto, J. V., Ludsin, S. A., Roberts, J. J., Rucinski, D. K., Scavia, D., Schwab, D. J., and Höök, T. O. (2010). Seasonal and interannual effects of hypoxia on fish habitat quality in central Lake Erie. *Freshwater Biology*, 56(2):366–383.

Arlot, S. and Celisse, A. (2010). A survey of cross–validation procedures for model selection. *Statistics Surveys*, 4:40–79.

AWEL (2010). Kanton Zürich Abwasserreinigung in Zahlen. Technical report, Amt für Abfall, Wasser, Energie und Luft des Kantons Zürich. Zürich, Switzerland.

Baltazar, J.-C. and Claridge, D. E. (2002). Study of cubic splines and Fourier series as interpolation techniques for filling in short periods of missing building energy use and weather data. *ASME Conference Proceedings*, 2002(16893):15–21.

Beaugrand, G. (2004). The North Sea regime shift: evidence, causes, mechanisms and consequences. *Progress in Oceanography*, 60(2):245–262.

Benincà, E., Jöhnk, K. D., Heerkloss, R., and Huisman, J. (2009). Coupled predator–prey oscillations in a chaotic food web. *Ecology Letters*, 12(12):1367–1378.

Benson, A. J. and Trites, A. W. (2002). Ecological effects of regime shifts in the Bering Sea and eastern North Pacific Ocean. *Fish and Fisheries*, 3(2):95–113.

Beutel, M. W. (2003). Hypolimnetic anoxia and sediment oxygen demand in California drinking water reservoirs. *Lake and Reservoir Management*, 19(3):208–221.

Beutel, M. W., Horne, A. J., Roth, J. C., and Barratt, N. J. (2001). Limnological effects of anthropogenic desiccation of a large, saline lake, Walker Lake, Nevada. *Hydrobiologia*, 466(1):91–105.

Blenckner, T., Adrian, R., Livingstone, D. M., Jennings, E., Weyhenmeyer, G. A., George, D. G., Jankowski, T., Järvinen, M., Aonghusa, C. N., Nõges, T., Straile, D., and Teubner, K. (2007). Large–scale climatic signatures in lakes across Europe: A meta–analysis. *Global Change Biology*, 13(7):1314–1326.

Blenckner, T. and Chen, D. (2003). Comparison of the impact of regional and North Atlantic atmospheric circulation on an aquatic ecosystem. *Climate Research*, 23:131–136.

Blumberg, A. F. and Di Toro, D. M. (1990). Effects of climate warming on dissolved oxygen concentrations in Lake Erie. *Transactions of the American Fisheries Society*, 119(2):210–223.

Carpenter, S. R., Caraco, N. F., Correll, D. L., Howarth, R. W., Sharpley, A. N., and Smith, V. H. (1998). Nonpoint pollution of surface waters with phosphorus and nitrogen. *Ecological Applications*, 8(3):559–568.

Chen, H. and Claridge, D. E. (2000). Procedures for filling short gaps in energy use and weather data. *12th Symposium on Improving Building Systems in Hot and Humid Climates, San Antonio*, pages 314–326.

Claridge, D. E. and Chen, H. (2006). Missing data estimation for 1–6 h gaps in energy use and weather data using different statistical methods. *International Journal of Energy Research*, 30(13):1075–1091.

Clark, B. J., Dillon, P., Molot, L., and Evans, H. E. (2002). Application of a hypolimnetic oxygen profile model to lakes in Ontario. *Lake and Reservoir Management*, 18(1):32–43.

Coats, R., Perez-Losada, J., Schladow, G., Richards, R., and Goldman, C. (2006). The warming of Lake Tahoe. *Climatic Change*, 76(1):121–148.

Conversi, A., Fonda-Umani, S., Peluso, T., Molinero, J. C., Santojanni, A., and Edwards, M. (2010). The Mediterranean Sea regime shift at the end of the 1980s, and intriguing parallelisms with other European basins. *PLoS ONE*, 5(5):e10633.

Conversi, A., Peluso, T., and Fonda-Umani, S. (2009). Gulf of Trieste: A changing ecosystem. *Journal of Geophysical Research*, 114(C3):C03S90.

Cornett, R. J. and Rigler, F. H. (1979). Hypolimnetic oxygen deficits: Their prediction and interpretation. *Science*, 205(4406):580–581.

Coutant, C. (1985). Striped bass, temperature, and dissolved oxygen: a speculative hypothesis for environmental risk. *Transactions of the American Fisheries Society*, 114(1):31–61.

Davison, W. (1981). Supply of iron and manganese to an anoxic lake basin. *Nature*, 290(5803):241–243.

Deutsch, C., Brix, H., Ito, T., Frenzel, H., and Thompson, L. (2011). Climate–forced variability of ocean hypoxia. *Science*, 333(6040):336–339.

Diaz, R. J. (2001). Overview of hypoxia around the world. *Journal of Environmental Quality*, 30(2):275–281.

Diaz, R. J. and Rosenberg, R. (2008). Spreading dead zones and consequences for marine ecosystems. *Science*, 321(5891):926–929.

Eischeid, J. K., Pasteris, P. A., Diaz, H. F., Plantico, M. S., and Lott, N. J. (2000). Creating a serially complete, national daily time series of temperature and precipitation for the western United States. *Journal of Applied Meteorology*, 39(9):1580–1591.

Emery, W. J. (2001). *Data Analysis Methods in Physical Oceanography*. Elsevier Science Inc.

Evans, D. O. (2007). Effects of hypoxia on scope-for-activity and power capacity of lake trout (Salvelinus namaycush). *Canadian Journal of Fisheries and Aquatic Science*, 64(2):345–361.

Figura, S., Livingstone, D. M., Hoehn, E., and Kipfer, R. (2011). Regime shift in groundwater temperature triggered by the Arctic Oscillation. *Geophysical Research Letters*, 38(23):L23401. doi: 10.1029/2011GL049749.

Foley, B., Jones, I. D., Maberly, S. C., and Rippey, B. (2012). Long–term changes in oxygen depletion in a small temperate lake: effects of climate change and eutrophication. *Freshwater Biology*, 57(2):278–289.

Folke, C., Carpenter, S. R., Walker, B., Scheffer, M., Elmqvist, T., Gunderson, L., and Holling, C. (2004). Regime shifts, resilience, and biodiversity in ecosystem management. *Annual Review of Ecology, Evolution, and Systematics*, 35(1):557–581.

Gallina, N., Anneville, O., and Beniston, M. (2011). Impacts of extreme air temperatures on cyanobacteria in five deep peri-Alpine lakes. *Journal of Limnology*, 70(2):186–196.

Gammeter, S. and Forster, R. (1997). Limnologische Untersuchung des Zürichsees 1972–1996. Technical report, Zurich Water Supply. Zürich, Switzerland.

Gammeter, S. and Forster, R. (2002). Langzeituntersuchungen im Zürichobersee. Technical report, Zurich Water Supply. Zürich, Switzerland.

Gerdeaux, D., Anneville, O., and Hefti, D. (2006). Fishery changes during re–oligotrophication in 11 peri–alpine Swiss and French lakes over the past 30 years. *Acta Oecologica*, 30(2):161–167.

Gerten, D. and Adrian, R. (2000). Climate–driven changes in spring plankton dynamics and the sensitivity of shallow polymictic lakes to the North Atlantic Oscillation. *Limnology and Oceanography*, 45(5):1058–1066.

Ghil, M., Allen, M. R., Dettinger, M., Ide, K., Kondrashov, D., Mann, M., Robertson, A., Saunders, A., Tian, Y., and Varadi, F. (2002). Advanced spectral methods for climatic time series. *Reviews of Geophysics*, 40(1):1003.

Gray, J. S., Wu, R. S.-s., and Or, Y. Y. (2002). Effects of hypoxia and organic enrichment on the coastal marine environment. *Marine Ecology Progress Series*, 238:249–279.

Hare, S. R. and Mantua, N. J. (2000). Empirical evidence for North Pacific regime shifts in 1977 and 1989. *Progress in Oceanography*, 47(2):103–145.

Hari, R. E., Livingstone, D. M., Siber, R., Burkhardt-Holm, P., and Güttinger, H. (2006). Consequences of climatic change for water temperature and brown trout populations in Alpine rivers and streams. *Global Change Biology*, 12(1):10–26.

Hendricks Franssen, H. J. and Scherrer, S. C. (2008). Freezing of lakes on the Swiss plateau in the period 1901–2006. *International Journal of Climatology*, 28(4):421–433.

Holdaway, M. (1996). Spatial modeling and interpolation of monthly temperature using kriging. *Climate Research*, 6(3):215–225. doi: 10.3354/cr0006215.

Holzner, C. P., Aeschbach-Hertig, W., Simona, M., Veronesi, M., Imboden, D. M., and Kipfer, R. (2009). Exceptional mixing events in meromictic Lake Lugano (Switzerland/Italy), studied using environmental tracers. *Limnology and Oceanography*, 54(4):1113–1124.

Hupfer, M. and Lewandowski, J. (2008). Oxygen controls the phosphorus release from lake sediments – a long–lasting paradigm in limnology. *International Review of Hydrobiology*, 93(4-5):415–432.

Hurrell, J. W. (1995). Decadal trends in the North Atlantic Oscillation: regional temperatures and precipitation. *Science*, 269(5224):676–679.

Hurrell, J. W., Kushnir, Y., and Visbeck, M. (2001). The North Atlantic Oscillation. *Science*, 291(5504):603–605.

Hutchinson, G. E. (1957). *A Treatise on Limnology. Volume 1, Geography, Physics, and Chemistry*. Wiley, New York, USA.

Idso, S. B. (1973). On the concept of lake stability. *Limnology and Oceanography*, 18(4):681–683.

Imboden, D. M. and Emerson, S. (1978). Natural radon and phosphorus as limnologic tracers: Horizontal and vertical eddy diffusion in Greifensee. *Limnology and Oceanography*, 23(1):77–90.

Imboden, D. M. and Wüest, A. (1995). Mixing mechanisms in lakes. In Lerman, A., Imboden, D. M., and Gat, J. R., editors, *Physics and Chemistry of Lakes*, pages 83–138. Springer.

IPCC (2007a). *Climate Change 2007 – Impacts, Adaptation and Vulnerability: Working Group II contribution to the Fourth Assessment Report of the IPCC*. Cambridge University Press, Cambridge, UK and New York, NY, USA.

IPCC (2007b). *Climate Change 2007 – The Physical Science Basis: Working Group I contribution to the Fourth Assessment Report of the IPCC*. Cambridge University Press, Cambridge, UK and New York, NY, USA.

Jankowski, T., Livingstone, D. M., Bührer, H., Forster, R., and Niederhauser, P. (2006). Consequences of the 2003 European heat wave for lake temperature profiles, thermal stability, and hypolimnetic oxygen depletion: Implications for a warmer world. *Limnology and Oceanography*, 51(2):815–819.

Jochimsen, M. C., Kümmerlin, R., and Straile, D. (2012). Compensatory dynamics and the stability of phytoplankton biomass during four decades of eutrophication and oligotrophication. *Ecology Letters*. doi: 10.1111/ele.12018.

Keeling, R. F., Körtzinger, A., and Gruber, N. (2010). Ocean deoxygenation in a warming world. *Annual Review of Marine Science*, 2(1):199–229.

Kidokoro, H., Goto, T., Nagasawa, T., Nishida, H., Akamine, T., and Sakurai, Y. (2010). Impact of a climate regime shift on the migration of Japanese common squid (Todarodes pacificus) in the Sea of Japan. *ICES Journal of Marine Science*, 67(7):1314–1322.

Korobeynikov, A. (2010). Computation– and space–efficient implementation of SSA. *Statistics and its Interface*, 3(3):357–368. R package version 0.8.3.

Kratz, T. K., Soranno, P. A., Baines, S. B., Benson, B. J., Magnuson, J. J., Frost, T. M., and Lathrop, R. C. (1998). Interannual synchronous dynamics in north temperate lakes in Wisconsin, USA. In George, D. G., Jones, J. G., Puncochár, P., Reynolds, C. S., and Sutcliffe, D. W., editors, *Management of Lakes and Reservoirs During Global Climate Change*, pages 273–287. Kluwer Academic.

Lamont, G., Laval, B. E., Pawlowicz, R., Pieters, R., and Lawrence, G. A. (2004). Physical mechanisms leading to upwelling of anoxic bottom water in Nitinat Lake. In *17th ASCE Engineering Mechanics Conference*, June 13-16, 2004, University of Delaware, Newark, Delaware.

Levin, L. A., Ekau, W., Gooday, A. J., Jorissen, F., Middelburg, J. J., Naqvi, W., Neira, C., Rabalais, N. N., and Zhang, J. (2009). Effects of natural and human–induced hypoxia on coastal benthos. *Biogeosciences Discussions*, 6:3563–3654.

Lin, Z. H. (2010). Modelling hypolimnetic dissolved oxygen depletion in lakes. Master's thesis, Trent University, Peterborough, Canada.

Livingstone, D. M. (1993). Temporal structure in the deep–water temperature of four swiss lakes: A short–term climatic change indicator? *Verhandlungen der Internationalen Vereinigung für Limnologie*, 25:75–81.

Livingstone, D. M. (1997). An example of the simultaneous occurrence of climate–driven "sawtooth" deep–water warming/cooling episodes in several Swiss lakes. *Verhandlungen der Internationalen Vereinigung für Limnologie*, 26:822–826.

Livingstone, D. M. (2003). Impact of secular climate change on the thermal structure of a large temperate central European lake. *Climatic Change*, 57:205–225.

Livingstone, D. M. (2008). A change of climate provokes a change of paradigm: Taking leave of two tacit assumptions about physical lake forcing. *International Review of Hydrobiology*, 93(4-5):404–414.

Livingstone, D. M., Adrian, R., Arvola, L., Blenckner, T., Dokulil, M. T., Hari, R. E., George, G., Jankowski, T., Järvinen, M., Jennings, E., Nõges, P., Nõges, T., Straile, D., and Weyhenmeyer, G. A. (2010). Regional and supra–regional coherence in limnological variables. In George, D. G., editor, *The Impact of Climate Change on European Lakes. Aquatic Ecology Series 4*, pages 311–337. Springer, Dordrecht.

Livingstone, D. M. and Hari, R. E. (2008). Coherence in the response of river and lake temperatures in Switzerland to short–term climatic fluctuations in summer. *Verhandlungen der Internationalen Vereinigung für Limnologie*, 30(3):449–454.

Livingstone, D. M. and Imboden, D. M. (1996). The prediction of hypolimnetic oxygen profiles: a plea for a deductive approach. *Canadian Journal of Fisheries and Aquatic Science*, 53(4):924–932.

Livingstone, D. M. and Lotter, A. (1998). The relationship between air and water temperatures in lakes of the Swiss Plateau: a case study with palaeolimnological implications. *Journal of Paleolimnology*, 19(2):181–198.

Lo, T. T. and Hsu, H. H. (2010). Change in the dominant decadal patterns and the late 1980s abrupt warming in the extratropical Northern Hemisphere. *Atmospheric Science Letters*, 11(3):210–215.

Magnuson, J. J., Benson, B. J., and Kratz, T. K. (1990). Temporal coherence in the limnology of a suite of lakes in Wisconsin, U.S.A. *Freshwater Biology*, 23(1):145–159.

Magnuson, J. J. and Kratz, T. K. (2000). Lakes in the landscape: approaches to regional limnology. *Verhandlungen der Internationalen Vereinigung für Limnologie*, 27:74–87.

Martin-Creuzburg, D., von Elert, E., and Hoffmann, K. H. (2008). Nutritional constraints at the cyanobacteria–Daphnia magna interface: The role of sterols. *Limnology and Oceanography*, 53(2):456–468.

Massol, F., David, P., Gerdeaux, D., and Jarne, P. (2007). The influence of trophic status and large–scale climatic change on the structure of fish communities in Perialpine lakes. *Journal of Animal Ecology*, 76(3):538–551.

McCabe, G. J., Clark, M. P., and Serreze, M. C. (2001). Trends in Northern Hemisphere surface cyclone frequency and intensity. *Journal of Climate*, 14(12):2763–2768.

McLeod, A. I. (2011). Kendall: Kendall rank correlation and Mann–Kendall trend test. R package version 2.2.

Molot, L., Dillon, P., Clark, B. J., and Neary, B. (1992). Predicting end–of–summer oxygen profiles in stratified lakes. *Canadian Journal of Fisheries and Aquatic Science*, 49:2363–2372.

Neilsen, D., Duke, G., Taylor, B., Byrne, J., Kienzle, S., and der Gulik, T. V. (2010). Development and verification of daily gridded climate surfaces in the Okanagan Basin of British Columbia. *Canadian Water Resources Journal*, 35(2):131–154.

Nürnberg, G. K. (1995). Quantifying anoxia in lakes. *Limnology and Oceanography*, 40(6):1100–1111.

Nürnberg, G. K. (2002). Quantification of oxygen depletion in lakes and reservoirs with the hypoxic factor. *Lake and Reservoir Management*, 18(4):299–306.

Nürnberg, G. K. (2004). Quantified hypoxia and anoxia in lakes and reservoirs. *TheScientificWorldJOURNAL*, 4:42–54.

Nürnberg, G. K. (2009). Assessing internal phosphorus load – Problems to be solved. *Lake and Reservoir Management*, 25(4):419–432.

Omlin, M., Reichert, P., and Forster, R. (2001). Biogeochemical model of Lake Zürich: model equations and results. *Ecological Modelling*, 141(1-3):77–103.

Overland, J., Rodionov, S., Minobe, S., and Bond, N. (2008). North Pacific regime shifts: Definitions, issues and recent transitions. *Progress In Oceanography*, 77(2):92–102.

Paterson, A. M., Quinlan, R., Clark, B. J., and Smol, J. P. (2009). Assessing hypolimnetic oxygen concentrations in Canadian Shield lakes: Deriving management benchmarks using two methods. *Lake and Reservoir Management*, 25(3):313–322.

Peeters, F., Livingstone, D. M., Goudsmit, G., Kipfer, R., and Forster, R. (2002). Modeling 50 years of historical temperature profiles in a large central European lake. *Limnology and Oceanography*, 47(1):186–197.

Peña, M., Katsev, S., Oguz, T., and Gilbert, D. (2010). Modeling dissolved oxygen dynamics and hypoxia. *Biogeosciences*, 7(3):933–957.

Pomati, F., Matthews, B., Jokela, J., Schildknecht, A., and Ibelings, B. W. (2012). Effects of reoligotrophication and climate warming on plankton richness and community stability in a deep mesotrophic lake. *Oikos*, 121(8):1317–1327.

Posch, T., Köster, O., Salcher, M. M., and Pernthaler, J. (2012). Harmful filamentous cyanobacteria favoured by reduced water turnover with lake warming. *Nature Climate Change*, 2(11):809–813.

R Development Core Team (2011). *R: A Language and Environment for Statistical Computing*. R Foundation for Statistical Computing, Vienna, Austria.

Redfield, C. A., Ketchum, B. H., and Richards, F. A. (1963). The influence of organisms on the composition of seawater. In Hill, M. N., editor, *The Sea*, pages 26–77. Wiley–Interscience, New York.

Reid, P. C., Borges, M. F., and Svendsen, E. (2001). A regime shift in the North Sea circa 1988 linked to changes in the North Sea horse mackerel fishery. *Fisheries Research*, 50(1):163–171.

Rempfer, J., Livingstone, D. M., Blodau, C., Niederhauser, P., Forster, R., and Kipfer, R. (2010). The effect of the exceptionally mild European winter of 2006-2007 on temperature and oxygen profiles in lakes in Switzerland: a foretaste of the future? *Limnology and Oceanography*, 55(5):2170–2180.

Rempfer, J., Livingstone, D. M., Forster, R., and Blodau, C. (2009). Response of hypolimnetic oxygen concentrations in deep Swiss perialpine lakes to interannual variations in winter climate. *Verhandlungen der Internationalen Vereinigung für Limnologie*, 30:717–721.

Rippey, B. and McSorley, C. (2009). Oxygen depletion in lake hypolimnia. *Limnology and Oceanography*, 54(3):905–916.

Roberts, J. J., Höök, T. O., Ludsin, S. A., Pothoven, S. A., Vanderploeg, H. A., and Brandt, S. B. (2009). Effects of hypolimnetic hypoxia on foraging and distributions of Lake Erie yellow perch. *Journal of Experimental Marine Biology and Ecology*, 381:S132–S142.

Rodionov, S. N. (2006). Use of prewhitening in climate regime shift detection. *Geophysical Research Letters*, 33(12):L12707. doi: 10.1029/2006GL025904.

Rodionov, S. N. and Overland, J. E. (2005). Application of a sequential regime shift detection method to the Bering Sea ecosystem. *ICES Journal of Marine Science*, 62(3):328–332.

Rösner, R., Müller-Navarra, D. C., and Zorita, E. (2012). Trend analysis of weekly temperatures and oxygen concentrations during summer stratification in Lake Plußsee: A long–term study. *Limnology and Oceanography*, 57(5):1479–1491.

Rudnick, D. L. and Davis, R. E. (2003). Red noise and regime shifts. *Deep Sea Research Part I: Oceanographic Research Papers*, 50(6):691–699.

Scheffer, M., Carpenter, S. R., Foley, J. A., Folke, C., and Walker, B. (2001). Catastrophic shifts in ecosystems. *Nature*, 413(6856):591–596. doi: 10.1038/35098000.

Schindler, D. W. (2009). Lakes as sentinels and integrators for the effects of climate change on watersheds, airsheds, and landscapes. *Limnology and Oceanography*, 54(6):2349–2358.

Schindler, D. W., Hecky, R. E., Findlay, D. L., Stainton, M. P., Parker, B. R., Paterson, M. J., Beaty, K. G., Lyng, M., and Kasian, S. E. M. (2008). Eutrophication of lakes cannot be controlled by reducing nitrogen input: Results of a 37–year whole-ecosystem experiment. *Proceedings of the National Academy of Sciences*, 105(32):11254–11258.

Schmidt, W. (1928). Über die Temperatur– und Stabilitätsverhältnisse von Seen. *Geografiska Annaler*, 10:145–177.

Schneider, P. and Hook, S. J. (2010). Space observations of inland water bodies show rapid surface warming since 1985. *Geophysical Research Letters*, 37(22):L22405. doi: 10.1029/2010GL045059.

Scott, J. T. and McCarthy, M. J. (2010). Nitrogen fixation may not balance the nitrogen pool in lakes over timescales relevant to eutrophication management. *Limnology and Oceanography*, 55(3):1265–1270.

Shimoda, Y., Azim, M. E., Perhar, G., Ramin, M., Kenney, M. A., Sadraddini, S., Gudimov, A., and Arhonditsis, G. B. (2011). Our current understanding of lake ecosystem response to climate change: What have we really learned from the north temperate deep lakes? *Journal of Great Lakes Research*, 37(1):173–193.

Skaugen, T. and Andersen, J. (2010). Simulated precipitation fields with variance–consistent interpolation. *Hydrological Sciences Journal*, 55(5):676–686.

Snodgrass, W. (1987). Analysis of models and measurements for sediment oxygen demand in Lake Erie. *Journal of Great Lakes Research*, 13(4):738–756.

Stainsby, E. A., Winter, J. G., Jarjanazi, H., Paterson, A. M., Evans, D. O., and Young, J. D. (2011). Changes in the thermal stability of Lake Simcoe from 1980 to 2008. *Journal of Great Lakes Research*, 37(S3):55–62.

Stefan, H. G. and Fang, X. (1994a). Dissolved oxygen model for regional lake analysis. *Ecological Modelling*, 71(1–3):37–68.

Stefan, H. G. and Fang, X. (1994b). Model simulations of dissolved oxygen characteristics of Minnesota lakes: Past and future. *Environmental Management*, 18:73–92.

Stefan, H. G., Hondzo, M., Fang, X., Eaton, J. G., and McCormick, J. H. (1996). Simulated long–term temperature and dissolved oxygen characteristics of lakes in the north-central United States and associated fish habitat limits. *Limnology and Oceanography*, 41(5):1124–1135.

Straile, D. (2002). North Atlantic Oscillation synchronizes food–web interactions in central European lakes. *Proceedings of the Royal Society of London. Series B: Biological Sciences*, 269(1489):391–395.

Straile, D., Jöhnk, K. D., and Rossknecht, H. (2003). Complex effects of winter warming on the physicochemical characteristics of a deep lake. *Limnology and Oceanography*, 48(4):1432–1438.

Temnerud, J. and Weyhenmeyer, G. A. (2008). Abrupt changes in air temperature and precipitation: Do they matter for water chemistry? *Global Biogeochemical Cycles*, 22(2):GB2008.

Tian, Y., Kidokoro, H., Watanabe, T., and Iguchi, N. (2008). The late 1980s regime shift in the ecosystem of Tsushima warm current in the Japan/East Sea: Evidence from historical data and possible mechanisms. *Progress in Oceanography*, 77(2–3):127–145.

Tian, Y., Ueno, Y., Suda, M., and Akamine, T. (2004). Decadal variability in the abundance of Pacific saury and its response to climatic/oceanic regime shifts in the northwestern subtropical Pacific during the last half century. *Journal of Marine Systems*, 52(1):235–257.

Torrence, C. and Compo, G. P. (1998). A practical guide to wavelet analysis. *Bulletin of the American Meteorological Society*, 79(1):61–78.

Vaquer-Sunyer, R. and Duarte, C. M. (2008). Thresholds of hypoxia for marine biodiversity. *Proceedings of the National Academy of Sciences*, 105(40):15452–15457.

Verburg, P. and Hecky, R. E. (2009). The physics of the warming of Lake Tanganyika by climate change. *Limnology and Oceanography*, 54(6):2418–2430.

Verburg, P., Hecky, R. E., and Kling, H. (2003). Ecological consequences of a century of warming in Lake Tanganyika. *Science*, 301(5632):505–507.

Wetzel, R. (2001). *Limnology: lake and river ecosystems*. Academic Press, San Diego, U.S.A.

Yasunaka, S. and Hanawa, K. (2002). Regime shifts found in the Northern Hemisphere SST field. *Journal of the Meteorological Society of Japan*, 80(1):119–135.

Zhang, C. I., Yoon, S. C., and Lee, J. B. (2007). Effects of the 1988/89 climatic regime shift on the structure and function of the southwestern Japan/East Sea ecosystem. *Journal of Marine Systems*, 67(3):225–235.

Zimmermann, U., Forster, R., and Sontheimer, H. (1991). Langzeitveränderung der Wasserqualität im Zürich– Zürichober– und Walensee [Long–term change in the water quality of Lake Zurich, Upper Lake Zurich, and the Lake of Walenstadt]. Technical report, Zurich Water Supply. Zürich, Switzerland.